UNIVERSITY OF CALIFORNIA, MERCED

Caloric Restriction and/or SGLT2 Inhibition Improve Glucose Tolerance and Elicit Metabolic Adaptations in the OLETF Rat Model of Metabolic Syndrome

A dissertation submitted in partial satisfaction of the requirements for the degree

Doctor in Philosophy

In

Quantitative and Systems Biology

By

Manuel Alejandro Cornejo

Committee in charge:

Prof. Rudy M. Ortiz, Thesis Advisor
Prof. Frederick Wolf, Chair
Prof. Nestor Oviedo
Prof. Peter Havel

2021

The dissertation of Manuel Alejandro Cornejo is approved, and it is acceptable in quality and form for publication on microfilm and electronically.

Frederick Wolf, Chair

Nestor Oviedo

Peter Havel

Rudy M. Ortiz, Thesis Advisor

University of California, Merced

2021

Table of Contents

List of Tables

List of figures

List of abbreviations

AC, acylcarnitine
ACE, Angiotensin-converting enzyme
ADP, adenosine diphosphate
AgRP, agouti-related peptide
Akt, protein kinase B
AMPK, adenosine monophosphate-activated protein kinase
Ang II, Angiotensin II
ANOVA, Analysis of variance
AT, Adipose tissue
ATP, Adenosine triphosphate
AUC, Area under the curve
BCCA, Branched-chained amino acid
β-HAD, Beta-hydroxyacyl-coA dehydrogenase
BM, Body mass
BMI, Body mass index
BP, Blood pressure
CCK, cholecystokinin
Ccr, Creatinine clearance
CD36, Cluster of differentiation 36
CerS2, Ceramide Synthase 2
CR, caloric restriction
CV, Coefficient of variability
CVD, cardiovascular disease
DAG, diacylglycerol
DIO, Diet induced obesity
DPP4, Dipeptidyl-peptidase 4
EE, Energy expenditure
Epi, Epididymal
FAS, fatty acid synthase
FE, Fractional excretion
FFA, Free fatty acids
FFM, Fat-free mass
FM, Fat mass
FPG, Fasting plasma glucose
FPI, Fasting plasma insulin
G6Pase, Glucose 6-phosphatase
G6PC, glucose-6-phosphatase
Gastro, Gastrocnemius
GC, Gas chromatography
GLP-1, Glucagon-like peptide-1
GLUT2, Glucose transporter 2
GLUT4, Glucose transporter 4
HDL, High density lipoprotein
HFD, High fat diet
HOMA-IR, Homeostatic Model Assessment for Insulin Resistance
hsCRP, high sensitivity C-reactive protein
HSL, Hormone-sensitive lipase
IF, Intermittent fasting

IR, Insulin receptor
IRI, Insulin resistance index
Kpi, Potassium Phosphate Buffer
LCD, Low-calorie diet
LETO, Long-Evans Tokushima Otsuka
LNAPS, N-acyl-lysophosphatidylserine
MS, Metabolic Syndrome
MetS, Metabolic Syndrome
MUFA, mono unsaturated fatty acid
Na^+-K^+ATPase, Sodium–potassium adenosine triphosphatase
NEFA, Non-esterified fatty acids
Nox2, NADPH oxidase 2
oGTT, Oral glucose tolerance test
OLETF, Otsuka Long Evans Tokushima Fatty
PBS, Phosphate buffered saline
PA, Physical activity
PC, Principal Component
PC1, Principal Component 1
PC2, Principal Component 2
PCA, Principal Component Analysis
PCK1, Phosphoenolpyruvate carboxykinase 1
PE, phosphatidyl ethanolamines
PEPCK, Phosphoenolpyruvate carboxykinase 1
PIC, protease inhibitor
PPAR-γ, Peroxisome proliferator-activated receptor-γ
PPP, Pentose phosphate pathway
PR, Partial recovery
RAAS, Renin-angiotensin-aldosterone system
Retro, Retroperitoneal
REE, Resting energy expenditure
ROS, Reactive oxygen species
RQ, Respiratory quotient
SBP, Systolic blood pressure
SD, Sprague Dawley
SE, Standard error
SGLT1, Sodium-glucose linked transporter 1
SGLT2, Sodium-glucose linked transporter 2
SGLT2i, Sodium-glucose linked transporter 2 inhibitor
SHR, Spontaneously hypertensive rats
T2DM, Type 2 diabetes mellitus
TAG, Triglycerides, triacylglycerol
TCA, Tricarboxylic acid
TNF-α, Tumor necrosis factor-alpha
TOF, Time-of-flight
VLCD, Very low calorie diet

Acknowledgements

The text of chapter 2 of this dissertation is a reprint of the material as it appears in the publication specified at the beginning of the chapter. In addition, the text of chapters 3 and 4 is a reprint of material currently under external peer-review. This research was supported in part by doctoral fellowship UC MEXUS- CONACYT 440553 and by National Institute on Minority Health and Health Disparities grant 9T37-MD001480. In addition, Manuel Cornejo received the Quantitative and Systems Biology Top-off Fellowship (2017-2019), the School of Natural Sciences External Fellowship Top Off Award (2018), and the UC MEXUS exigency stipend funds (2021).

I am very grateful to my advisor, Prof. Rudy Ortiz for inviting me to join his lab and making sure I had all the resources available to help me grow as a scientist. I also want to thank my committee members, Prof Frederick Wolf, Prof. Nestor Oviedo and Prof. Peter Havel for their patience and helpful guidance on this work.

I want to thank Prof. Akira Nishiyama and Prof. Daisuke Nakano for hosting me in their lab during three summers in Japan, for their advice on designing the experiments, and for making sure we were well provided. My thanks to Dr. Yu Guan, Ningning Wan, Yumi Sakane, Yoko Ichihara and Yu Kusano for their valuable assistance during our experiments.

The research in this dissertation was possible thanks to the hard work of: Julie Nyugen, Benny Escobedo, Joshua Cazares, Asad Asghar, Iris Montes, Janna Emery, Megan Smith and Prof. Jaapna Dhillon. I also want to thank Dr. Ruben Rodriguez, Dr. Max Thorwald, Dr. Bridget Martinez and Jose Godoy-Lugo for their valuable mentorship and insight, and for their really useful feedback on research proposals, presentations and manuscripts.

I would like to acknowledge my parents Maria de Lourdes Blanco-Garcia and Jose Manuel Cornejo-Bravo, Aracely Serrano-Medina, David Macias-Sandoval, and my siblings: Natalia Cornejo-Blanco, Adrian Cornejo-Serrano and Lucia Cornejo-Serrano, for their love, patience, and invaluable support. Lastly, I would like to express my gratitude to Isaura Lara-Arenas and our daughter, Emily Cornejo-Lara, for their unconditional love and for inspiring me to finish this life chapter.

Research Experience

University of California Merced Merced, CA
PhD Research; Advisor: Rudy M. Ortiz 2015 – Present

- Continued collecting data the projects started at Kagawa University (listed below)
- Published one first-author paper and submitted three manuscripts for peer-review
- Performed metabolomics and lipidomics analyses on the acute caloric restriction and partial body mass recovery study
- Assisted fellow graduate students in dissections and data collection

Kagawa University Medical School Kagawa, Japan
PhD. Summer Research 2016, 2017 & 2019
Research advisors: Akira Nishiyama and Daisuke Nakano
• Conducted a study and collected preliminary data on the immediate and short term effects of visceral lipectomy in metabolic syndrome
• Examined the effect of moderate (30%) caloric restriction and SGLT2i in metabolic syndrome
• Examined the effect of acute (50%) caloric restriction and partial body mass recovery on metabolic syndrome

Universidad Autonoma de Baja California Tijuana, BC, Mexico
Bachelor in Science in Biopharmaceutical Chemistry 2015
Undergraduate Research; Advisor: Bertha Landeros 2013 – 2015

- Undergraduate Thesis "Expression of the Recombinant Protein HSP70 of Mycobacterium avium subsp. Paratuberculosis in the BL21(DE3) strain of Escherichia coli."
- Undergraduate Research Assistant at Biopharmacy laboratory 2011
    - Assisted on collection of data on pharmacokinetics of release of antihypertensive drug-polymer complexes in-vitro.

Publications

1. Cornejo M, Ortiz R. Body Mass Cycling and Predictors of Body Mass Regain during Impaired Metabolism. *Metabolism*. Under review.
2. Cornejo M, Emery J, Daisuke N, Nishiyama A, Ortiz R. Simultaneous SGLT2 Inhibition and Caloric Restriction Improves Insulin Resistance and Kidney Function in OLETF Rats. *Endocrinology*. Under review
3. Cornejo M, Jaapna D, Daisuke N, Nishiyama A, Ortiz R. Mass Recovery following Caloric Restriction Reverses Lipolysis and Proteolysis, but not Gluconeogenesis, in Insulin Resistant OLETF Rats. *PLOS One*. Under review.
4. Cornejo M, Nguyen J, Cazares, J, Escobedo B, Daisuke N, Nishiyama A, Ortiz R. Partial Body Mass Recovery After Caloric Restriction Abolishes Improved Glucose Tolerance in Obese, Insulin Resistant Rats. *Frontiers in Endocrinology, Obesity*, 2020, 11(363), 1-14.
5. Gomez-Resendiz V, Serrano-Medina A, Carrillo-Cedillo E, Cornejo M, Cornejo-Bravo J. 2014. Poly (metacriloiloxi-o-benzoic acid) as a carrier for controlled drug release. Journal of the Mexican Chemical Society, 2014, 58(4); 424-430.

Peer-Reviewed Abstract

Cornejo M, Nakano D, Nishiyama A, Ortiz R. Blood Pressure is Maintained Despite Varying Degrees of Acute Caloric Restriction and Sodium-Glucose Cotransporter-2 Inhibition in Obese, Insulin Resistant Rats. Hypertension. 74, A061, 2019

Awards

- Santiago Maza Award for the best paper contribution in the field of Biotechnology. XLVI Pharmaceutical Sciences National Meeting (Mexico).
- GSA Travel Award 2016, 2017

Fellowships

University of California, Merced

- UC MEXUS exigency stipend funds (2021).
- School of Natural Sciences External Fellowship Top Off Award 2018
- Quantitative and Systems Biology Top-off Fellowship 2017-2019
- UC MEXUS-CONACYT Doctoral Fellowship 2016-2020

University of California, Santa Cruz

Minority Health Disparities International Training Fellowship 2016, 2017 & 2020

Caloric Restriction and/or SGLT2 Inhibition Improve Glucose Tolerance and Elicit Metabolic Adaptations in the OLETF Rat Model of Metabolic Syndrome

Manuel Alejandro Cornejo
Doctor of Philosophy in Quantitative and Systems Biology
University of California, Merced, 2021
Chair: Dr. Rudy M. Ortiz

Abstract

Caloric restriction (CR) is an effective intervention to acutely reduce adiposity and total body mass (BM) to improve insulin resistance and ameliorate metabolic derangements. However, CR also results in metabolic adaptations, including increase expression of orexigenic hormones, decreased resting metabolic rate, and prioritization of gluconeogenesis and lipolysis as fuel sources, which in combination promote a higher caloric intake and facilitate the regain of body mass. In the first original study presented in this dissertation we demonstrated that acute, severe (50%) CR in the obese, insulin resistant OLETF rat, elicits improvements in insulin resistance and plasma lipid profiles. However, these improvements were accompanied by a large collateral loss of lean body mass, and were abrogated after partial recovery of body mass following CR. The next study showed, via assessment of plasma metabolomic profiles, that lipolysis and proteolysis, but not gluconeogenesis, reverted towards pre-caloric restriction levels following recovery of body mass, providing a partial explanation of why insulin resistance rapidly returned following mass recovery, and confirmed the presence of extensive lean tissue catabolism. In the third study, we showed that moderate (30%) CR improved insulin resistance and kidney function, albeit not as profoundly as 50% CR, while preserving body mass. However, when combined with administration of a SGLT2 inhibitor, 30% CR further improved insulin sensitivity via changes in muscle and liver metabolism, without causing hypoglycemia or lean tissue catabolism. Together these findings contribute to the current body of knowledge on the metabolic impact of caloric restriction via implementation of different degrees of CR in a rat model that recapitulates the progression of metabolic syndrome observed in humans. Moreover, this work contributes novel findings on the metabolic consequences of regaining fat mass, or “rebound effect”, along with results that support the potential of a simultaneous intervention of moderate CR and SGLT2 inhibition as a potential means to successfully improve glucose tolerance and lower blood pressure.

Chapter 1: Introduction

The following dissertation starts with a mini-review on the metabolic adaptations derived from caloric restriction (CR) in both clinical studies and rodent models, and how these adaptations translate into an increased risk of developing metabolic syndrome when body mass regain or cycling occurs (Chapter 1). It continues with a study on how acute, severe CR elicit transient improvements on insulin resistance on an animal model of metabolic syndrome, which are abrogated almost entirely by partial body mass recovery (Chapter 2). This study is further expanded in subsequent chapters with a metabolomics analysis in plasma, exploring changes in metabolic pathways and correlations to adipose mass and insulin resistance index (Chapter 3). The dissertation continues with an independent study on the same model on how mild CR, in combination with SGLT2 inhibition, improves insulin resistance while assessing potential changes in metabolic pathways by plasma metabolomics (Chapter 4). Chapter 6 closes this dissertation by summarizing the most important findings of the previous chapters, expands on the broader impact of the research presented, and finishes with future directions for this research.

1.1 Body Mass Cycling and Predictors of Body Mass Regain during Impaired Metabolism

1.1.1 Abstract

Caloric restriction (CR) is the first line intervention to reduce adiposity and total body mass (BM) to improve insulin resistance and ameliorate metabolic derangements. However, the lost adipose is difficult to maintain reduced in the long term due to several factors including compensatory changes in orexigenic hormones, adipokine release, pro-inflammatory state, adipose morphology, and resting metabolic rate as a consequence of the caloric deficit. Hence, most patients undergoing a BM reduction intervention ultimately regain the lost mass and too often additional adipose overtime, which is hypothesized to have increased deleterious effects chronically. In this mini-review we describe the effects of BM cycling (loss and regain) on insulin resistance and cardiometabolic health and factors that may predict BM regain in clinical studies. We also describe the factors that contribute to the chronic deleterious effects of BM cycling in rodent models of diet-induced obesity (DIO) and other metabolic defects. We conclude that most of the improvements in insulin resistance are observed after a profound loss in BM regardless of the diet and that BM cycling abrogates these beneficial effects. We also suggest that more BM cycling studies are needed in rodent models resembling the development of T2DM in humans.

1.1.2 Introduction

Caloric restriction (CR) is a first line intervention to reduce adiposity and total body mass (BM) during obesity, which is especially important for improving the factors of metabolic syndrome (MetS). Even a modest reduction in daily caloric intake (500-1000 kcal/day) can decrease fat mass (FM) and improve insulin sensitivity to a greater extent than 5 days/week of moderate exercise [1]. Moreover, remission of T2DM with sustained normalization of basal blood glucose and liver and pancreas triglycerides (TG) was observed in patients that lost 15 kg of BM via CR [2]. Additionally, a previous systematic review categorized the decrease in total caloric intake (specifically sugar-sweetened beverages) as a primary determinant of maintaining the lost BM, surpassing meal replacement and socioeconomic factors [3]. Moreover, the CR-induced decrease in visceral adipose improved cardiometabolic risk factors (increased serum HDL and decreased TG and VLDL concentrations) and decreased systemic inflammatory markers (high sensitivity C-reactive protein [hsCRP] and α1-acid glycoprotein) [4]. In addition to the aforementioned benefits, CR may

increase survival as observed in a DIO mouse model where 30% CR and BM cycling decreased mortality compared to ever-obese mice [5].

However, several factors make further loss of BM and maintenance a challenge, in particular energetic deficit, making CR a less effective BM loss strategy compared to other interventions (e.g. bariatric surgery) for chronic BM reduction and maintenance [6]. This is further explained by a disparity between decreased energy expenditure (EE) and increased appetite proportional to the lost BM, causing an average BM regain of 80% within 5 years after the intervention in patients undergoing long-term BM loss [7]. Additionally, total daily EE decreased in obese subjects, and more so when BM loss exceeded 10% of total mass, thus accentuating net-positive caloric intake [8], although the change in RMR correlated better with free-fat mass (FFM) than fat-mass (FM), which was shed in higher proportion [9]. For high BM loss (>5%), the amount and rate of BM loss had a strong, positive association ($P<0.001$ and $P=0.049$, respectively) with the amount of BM regain, whereas this relationship was not observed when the lost mass was lower [10]. This is particularly important to consider when a high amount of FM loss is desirable. Nonetheless, the potential detrimental effects of BM cycling on obesity (i.e. fat mass accumulation) and metabolic risk factors remain controversial and inconclusive as indicated by roughly half the studies previously reviewed from 1994 to 2015 [11].

1.1.3 Predictive Factors of Regain in BM Loss Interventions

Changes in basal fasting insulin and insulin sensitivity after BM loss have been suggested to be predictors of future BM regain. However, two independent studies, one with obese, non-diabetic patients and another with T2DM patients failed to find a correlation between decreased basal insulin (non-diabetic patients) or increased insulin sensitivity (diabetic patients) and BM regain after 30 and 24 months, respectively [12]. In contrast, fasting plasma glucose (FPG) has been suggested to predict BM regain. In a randomized diet (high MUFA) study in obese, non-hyperglycemic adults (FPG > 105 mg/dL), after losing >8% of BM on average, patients with FPG below 90 mg/dL and/or insulin below 50 pM regained BM to a lesser extent than the cohort with higher basal glucose and insulin [13]. However, the proportion of dietary fat was not found to have a significant impact on rate of regain, as supported by another study [14].

Fasting levels of orexigenic hormones such as leptin and ghrelin can discriminate between future BM regainers from non-regainers. In overweight and obese patients enrolled in a 2-month nutritional BM loss program, the leptin:ghrelin ratio was higher at baseline in patients that regained >10% of BM lost over the next 6 months [15], while in obese, T2DM patients, reduction of leptin after 6 months of BM reduction, but not basal leptin, strongly predicted the regain of BM in the following 18 months [16]. In addition, sex hormone-binding globulin (SHBG), adiponectin, and testosterone were inversely correlated with obesity and parameters of MetS and positively correlated with leptin, retinol-binding protein 4 (RBP4), luteinizing hormone (LH), and prolactin in obese males [17]. These observations are important to consider as they highlight the increase in risk of BM regain when low levels of FPG and leptin are not maintained prior to BM reduction. Furthermore, this risk is not corrected with short term leptin reduction following BM reduction whatsoever. Therefore, the advantage of monitoring FPG and hormonal profile well before the onset of obesity for securing the success of future BM loss interventions is made evident.

1.1.4 Long-Term Re-examination of Biomarkers after BM Loss and Their Correlation with Regain

Recent follow-up studies have tried to identify associations between basal levels of adipokines and other biomarkers before BM loss intervention with the rate of BM regain, with a focus on circulating leptin due to its effects on increasing EE and insulin sensitivity [18]. This is of particular interest to identify potential pharmaceutical targets to prevent regain [19]. In a study of morbidly obese patients participating in a 2 month BM loss intervention with a daily intake of 20-25 kcal/kg of ideal BM, a re-examination 3 months after the intervention showed that BM was maintained, while after 12 months excess BM was only partially recovered (17.7% of the 35.5% lost on average) and did not correlate to the rate of excess mass loss or the presence of diabetes [20]. In overweight, non-diabetic women with an 800 kcal/day diet intended to reduce BMI below 25 kg/m2, re-examination after 2 years revealed that 80% of BM was recovered, which had no correlation to basal insulin sensitivity, serum leptin concentrations, or RMR [21].

Fasting active ghrelin was increased and RMR decreased in non-diabetic, overweight subjects undergoing an 8-week, 550-660 kcal/day diet followed by 4 weeks of BM maintenance [22] and in diabetic subjects undergoing 10% BM loss without reversal after a 1 year follow-up [23]. Additionally, a >10% BM loss decreased circulating leptin, peptide YY, cholecystokinin (CCK), and insulin [24]. This is important to consider because these hormones regulate appetite and are key to helping to regulate BM maintenance.

In addition to the associations between adipokines and appetite regulation with BM regain, higher circulating levels of long-chain acyl carnitines (AC) (particularly C18:1, C20:1 and C20:2), higher free fatty acids (FFA), and lower respiratory quotient (RQ) predicted the maintenance of BM after >8% diet-induced BM loss [25]. Moreover, higher subcutaneous adipose mitochondrial capacity was associated with BM loss without regain. Basal expression of important mitochondrial pathway genes (TCA cycle, oxidative phosphorylation, β-oxidation, and branched-chained amino acid (BCCA) catabolism) was lower in the group that partially regained BM (11% to 5% BM loss) compared to the non-regain group 12 months after the start of BM loss [26]. Collectively, these studies demonstrate that profound reductions in BM elicit adaptations on appetite regulating hormones, both orexigenic and anorexigenic, in response to a proportionally lower FM, which may help explain why it is difficult to maintain BM loss chronically. Conversely, efficient mitochondrial activity and a successful shift toward greater lipid metabolism after BM loss are influential factors that may prevent regain.

1.1.5 BM Loss and Regain in Insulin Resistance

The CR-induced reduction in BM may improve markers of MetS, especially insulin resistance and SBP. This was observed in a cohort of obese, pre-diabetic patients, which had an average reduction in BM of 8.7-10.2% after 6 months of a lifestyle intervention associated with reduced FPG, insulin, and HOMA-IR [27]. However, 18 months after BM reduction, these parameters increased in the loss-regain group compared to the loss-maintain group, to the point where FPG was higher in the loss-regain group compared to the group that did not experience an initial loss in BM [28]. Additionally, a short-term intervention with healthy, non-overweight patients subjected to 1 week of overfeeding (50% above daily caloric requirements) followed by 3 weeks of 50% CR, then 2 weeks of refeeding, increased fasting insulin and HOMA-IR after overfeeding that were corrected after CR and increased again after refeeding. Moreover, the transient improvement in insulin sensitivity was correlated with increased ghrelin and decreased leptin, TSH, and fT3 [29]. An

analysis of the Look AHEAD (Action for Health in Diabetes) trial, comprised of diabetic patients with ≥3% BM loss after a 1-year intervention, demonstrated that patients with ≥10% BM loss had lower basal HbA1c and diastolic BP, and more favorable cardiovascular risk factors. Moreover, patients who regained >75% of their lost BM during the 1-year intervention had higher HbA1c, SBP, and TG concentrations 3 years after, even when BM was maintained after the intervention [30]. Nonetheless, the improvement in HbA1c after 4 years was more profound in patients with higher BM loss compared to those with small or no BM loss, even with full regain [31].

Different degrees of CR (500 kcal/d [VLCD] and 1250 kcal/d [LCD]) with equivalent BM loss did not induce differential effects between groups (including regain) except for a greater decrease in ACE activity. However, at 9 months re-examination, the post-oGTT glucose was lower in VLCD group, while glucose returned to basal levels in LCD [19] suggesting that the degree of CR and not absolute BM loss had a greater effect on improving insulin resistance. Nonetheless, a high-saturated-fat meal test in a pooled sample did not alter fatty acid uptake in subcutaneous adipose before or after BM loss [32]. Additionally, expression of several leucocyte integrin genes following BM loss correlated positively with the percentage of BM regain suggesting that residual inflammation is present following BM loss, increasing the risk of BM regain and the metabolic risks associated with BM cycling [33]. CR-induced BM loss may reverse β-cell functionality in early onset T2DM. Several patients undergoing a CR for 16 weeks and achieving an average loss of 16.4 kg of BM achieved non-diabetic HbA1c and FPG without needing antidiabetic drugs, and half of these patients maintained normoglycemia after re-examination at 2 years [34]. In short, a higher degree of CR confers more profound benefits to improving insulin sensitivity and has the potential to delay the onset of T2DM in healthy subjects, while a profound reduction of BM via CR reduces cardio metabolic risk factors in diabetic patients. However, the degree of CR may not be sustainable chronically due to the metabolic adaptations summarized previously, and even partial BM recovery (>70%) [19, 28] is enough to abolish these benefits ultimately.

1.1.6 BM Cycling and Intermittent Fasting in Clinical Studies

BM cycling (a.k.a. yo-yo dieting) is driven by an absence of compensatory changes in hunger and satiety in response to overfeeding and impairs the ability of subjects to sustain BM loss chronically [35]. Studies have suggested that BM cycling may be more deleterious than simply maintaining BM and may increase the risk of T2DM and CVD. For example, in obese, non-diabetic patients with MetS, BM regain after 60 months increased pulse wave velocity (PWV), a measure of arterial stiffness [36]. Additionally, follow-up studies after 4 [37], 10 [38] and 16 years [39] showed that higher BM fluctuations increased HOMA-IR and mortality [39], with the added detriments of increased SBP, total cholesterol, and TG [38] or higher risk for T2DM [37]. Conversely, the incidence of T2DM decreased with higher fluctuations in BM (protective effect) in overweight subjects [39] demonstrating the inconsistency in the BM cycling effects. Nonetheless, patients with an average loss of 16.7 kg after a 21-day intervention regained 15.1 kg after discharge but did not report differences in resting EE (REE), SBP, glucose, or insulin before CR and after BM regain [40].

Despite the potential deleterious effects of BM cycling, intermittent cycles of energy restriction (ER) of 2 weeks, due to the bi-phasic nature of adaptation to BM loss, has been recommended to trigger the acute alterations in cellular metabolism without reaching the later phase of REE reduction. BM loss and attenuation of REE was greater with intermittent ER compared to 33% CR after 16 weeks [41]. A similar trend in BM loss and REE attenuation was observed in healthy, lean subjects, albeit to a lower magnitude [42], potentially due to higher proportion FFM in these

subjects. A short-term intervention consisting of 5 days ad libitum intake followed by 2 days of absolute restriction achieved short-term improvements in BM, FM, and hs-CRP but not lipid profiles [43]. In general, these studies suggest that multiple BM cycling events may increase the risk factors for metabolic syndrome, and that intermittent fasting without cycling could be a viable alternative to avoid BM cycling by preventing the undesired metabolic adaptations caused by sustained CR.

1.1.7 BM Cycling and Insulin Resistance in Rodents

Several studies on BM cycling have been performed in rodent models to elucidate the mechanisms contributing to metabolic derangements after BM regain. We have shown that partial BM regain following 50% CR abolished the acute improvements in insulin resistance independent of a regain in FM with further derangement in gluconeogenesis in OLETF rats [44]. These results are consistent with others in Wistar rats, which were subjected to 4 BM loss-regain cycles via 50% CR and had lower FM compared to control; however, the expected increases in ghrelin, leptin, or insulin after BM regain were not observed [45]. Furthermore, 4 bouts of diet-induced (high fat-low fat) BM cycling decreased basal EE and glucose tolerance compared to obese controls in C57Bl/6J mice [46].

The effects of BM regain associated with HFD in C57Bl/6J mice on mediators of insulin resistance depend on diet duration. The BM regain following a 4-wk HFD intervention increased the accumulation of TG and of lysophosphatidic acid (LPC), an important lipid effector of fatty acid-induced insulin resistance, in the gastrocnemius and soleus muscles, respectively [47]. The improvements in fasting glucose and insulin induced by approximately 25% loss in BM with a control diet were abolished by 6 weeks of HFD with visceral adiposity increasing above HFD only mice [48]. Additionally, mice regaining BM had hepatic TG similar to HFD only mice, and higher basal insulin compared to mice that did not experience BM cycling [49]. After 8 weeks of BM cycling, relative mRNA and protein expressions of CTRP3, an anti-inflammatory and hypoglycemic adipokine, decreased and adipocyte volume increased [50]. Alternating low-high fat diet cycles for 9 weeks increased adipose CD4+ and CD8+ T-cells despite similar BM to the obese, non-cycling mice suggesting that BM cycling may be more detrimental than BM maintenance even if in an obese condition. Furthermore, BM cycling decreased adipose pAKT, a measure of insulin sensitivity, and increased both fasting glucose and glucose AUC after GTT [51]. However, BM cycling induced by 80% CR reduced adipocyte size after two cycles without changing food efficiency or fasting glucose, leptin, and adiponectin [52]. Intermittent fasting (IF) cycles with a 2:1 ratio (2 days of ad libitum feeding and 1 day of fasting) decreased FM in both obese and lean mice, without any change in FFM unlike previous studies with 1:1 IF cycles. Moreover, IF reduced glucose AUC after intraperitoneal GTT in both DIO mice (C57BL/6J) and leptin impaired ob/ob mice [53]. These results are important to consider, as BM cycling reduces EE and insulin sensitivity regardless of the duration of CR. Moreover, BM cycling promotes accumulation of TG in the muscle and liver, and activated T-cell accumulation in adipose tissue, which further promotes insulin resistance.

1.1.8 BM Cycling, Blood Pressure, and RAAS in Rodents

BM loss, especially in the form of FM, is suggested to improve CV health. A 9% reduction in BM in obese subjects improved the recovery of heart rate after a maximal aerobic capacity test compared to baseline [54]. The changes in SBP paralleled the BM loss and regain achieved by alternating an obesity diet with 50% CR every 2 wks in normotensive Sprague-Dawley rats;

however, the BM cycling per se did not elicit a net change in SBP at the end of the study [55]. The BM regain following severe CR increased the sensitivity of the RAAS. In female Fischer rats, 60% CR for 2 weeks, reduced MAP by 20 mmHg after BM decreased 15%. However, 3 months after refeeding and complete BM regain, MAP reverted to basal levels. Furthermore, angiotensin converting enzyme (ACE) activity and angiotensin II (Ang II) were increased, and MAP was more sensitive to exogenous Ang II in the regain group [56].

In SHRs, 50% CR increased cardiac atrophy and sarcoplasmic remodeling of myofibrils and mitochondria, and decreased the ionotropic effect when stimulated with Ca2+ and isoproterenol compared to ad libitum fed rats. However, these differences were absent in the cycling group (weekly between 50% CR and ad libitum refeeding) compared to non-cycling group [57]. These results support the notion that the improvements in blood pressure are related to BM reduction. However, they also demonstrate the loss of these improvements with BM cycling. Moreover, the cardiac remodeling after severe CR may potentiate adverse effects on CV health.

1.1.9 Potential Regulators of BM Regain in Rodents

In the agouti-related peptide (AgRP)-carnitine acyltransferase (Crat) KO mouse, 9 days of 60% CR decreased RQ, FM, and plasma leptin without changing basal glucose; however, FM regain was greater after 11 days of ad libitum refeeding [58]. In C57/BL6 mice, 9 weeks of HFD-induced obesity was not reverted by a subsequent low fat diet (LFD) for 9 weeks. However, glucose tolerance was improved with LFD but adipose and prostaglandin signaling were maintained, while most of the liver metabolome was reverted to basal levels [59]. Conversely, BM regain induced by 4 weeks of HFD decreased several liver amino acids and lactate, a gluconeogenic intermediate, and increased the gluconeogenic enzymes, glucose-6-phosphatase (G6Pase) and pyruvate carboxylase (PC), which translated into higher fasting glucose [60]. In mice, 40% CR with LFD after 8 weeks of HFD, increased RER compared to the LFD controls suggesting that the transition from glucose to fatty acid oxidation was delayed, a sign of obesity-induced metabolic dysregulation. Furthermore, when re-challenged with HFD, adipose hormone-sensitive lipase (HSL) phosphorylation was lower translating into reduced lipolysis compared to lean mice [61].

The BM loss achieved by LFD following an obesity-inducing diet increased feeding motivation compared to non-cycling mice without changing physical activity. Additionally, the rate of BM loss was positively correlated with rate of regain [62]. Suppressed thermogenesis may also increase BM regain especially when disproportionate FM recovery is associated. In SD rats, BM cycling (50% CR for 2 weeks followed by 16 days of ad libitum refeeding) reduced mean core body temperature during CR and BM regain, and increased the rate of FM regain, compared to age- and mass-matched controls [63].

Activated CD4+ cells have also been suggested to determine BM regain because of their contributions to chronic inflammation and accumulation in adipose. Activation of CD4+ cells were increased in DIO C57BL/6J mice experiencing 1 month of HFD followed by BM normalization. In these mice, the rate of BM regain and adipose T-cell abundance increased compared to non-cycling mice, whereas these differences where abrogated with administration of dexamethasone, a T-cell and pro-inflammatory cytokine inhibitor. Moreover, mice experiencing BM cycling had a lower RER even after normalization of BM suggesting that “memory” adaptation to acquire most of the lost energy via fatty acid oxidation may exist [64]. While there is a general consensus of the metabolic shift from lipid oxidation to gluconeogenesis and FA mobilization to the liver and muscle after substantial BM loss, it is of interest that suppressed thermogenesis and maintained

inflammation in adipose, even after BM loss, are factors that may facilitate BM regain. It may be of interest to further investigate the extent to which altered diets influence adipose and systemic inflammation as these relate to the successful maintenance of BM following loss.

1.1.10 Limitations and Future Directions

The focus of this review was the evaluation of studies that perform intentional, controlled interventions to reduce BM and achieve BM cycling. We recognize that a significant body of literature exists from clinical data for T2DM patients in which collateral BM regain was due to unsuccessful maintenance regiments rather than an intentional BM regain. Thus, this review did not include or account for these studies. However, clinical studies of intentional BM regain are scarce and challenging especially in already compromised individuals because of ethical considerations. Therefore, further BM cycling studies in rodents, especially those that model metabolic defects in humans, will be of great importance for the advancement of the field.

1.1.11 Concluding Remarks

While the benefits of CR-induced BM loss are established in rodents and humans, the effects of BM regain and cycling are not well defined. Furthermore, biomarkers to predict the potential severity of the BM regain on health are lacking and inconsistent. From our review, we conclude that: (1) the CR benefits are proportional to the extent of the BM loss, especially in the form of FM, but can be abrogated by partial or complete BM regain, (2) multiple (>1) cycles of BM loss-regain are associated with worse metabolic outcomes, and (3) the metabolic adaptations related to BM cycling have a strong hormonal and pro-inflammatory component, especially adipokines, orexigenic hormones, and activated T-cells. A diagram summarizing the adaptations that lead to BM regain can be found in Figure 1.

Chapter 2. Partial Body Mass Recovery after Caloric Restriction Abolishes Improved Glucose Tolerance in Obese, Insulin Resistant Rats

2.1 Abstract

Caloric restriction, among other behavioral interventions, has demonstrated benefits on improving glycemic control in obesity-associated diabetic subjects. However, an acute and severe intervention without proper maintenance could reverse the initial benefits, with additional metabolic derangements. To assess the effects of an acute caloric restriction in a metabolic syndrome model, a cohort of 15-week old Long Evans Tokushima Otsuka (LETO) and Otsuka Long Evans Tokushima Fatty (OLETF) rats were calorie restricted (CR: 50% × 10 days) with or without a 10-day body mass (BM) recovery period, along with their respective ad libitum controls. An oral glucose tolerance test (oGTT) was performed after CR and BM recovery. Both strains had higher rates of mass gain during recovery vs. ad lib controls; however, the regain was partial (ca. 50% of ad lib controls) over the measurement period. Retroperitoneal and epididymal adipose masses decreased 30% (8.8 g, $P < 0.001$) in OLETF; however, this loss only accounted for 11.5% of the total BM loss. CR decreased blood glucose AUC 16% in LETO and 19% in OLETF, without significant decreases in insulin. Following CR, hepatic expression of the gluconeogenic enzyme, PEPCK, was reduced 55% in OLETF compared to LETO, and plasma triglycerides (TG) decreased 86%. Acute CR induced improvements in glucose tolerance and TG suggestive of improvements in metabolism; however, partial recovery of BM following CR abolished the improvement in glucose tolerance. The present study highlights the importance of proper maintenance of BM after CR as only partial recovery of the lost BM reversed benefits of the initial mass loss.

2.2 Introduction

Obesity and its associated metabolic disorders are significant health problems that have sustained global attention and concern for over the past 3 decades, with an alarming, increasing trend (1, 2). Unfortunately, obesity is related to 300,000 deaths per year in the United States alone (3), most of them attributed to class II/III obesity (3.8% excess deaths for females, 2.5% males compared to a cohort with normal BMI) (4) and type 2 diabetes mellitus (T2DM) was the underlying cause of death of 75,486 adults in the U.S. in 2013 (5). The adult, obese U.S. population increased from 30.5% in 1999 to 39.6% in 2016 (1). Excess body mass (BM) and obesity increase morbidity and mortality associated with numerous complications, including T2DM, dyslipidemia, hypertension, and atherosclerosis (6, 7). Behavioral interventions such as a low-carbohydrate diet (8), caloric restriction (CR) (9), vigorous physical activity (PA), or some combination (10) have demonstrated benefits for improving glycemic control and adiposity in obesity-associated diabetic subjects. However, rapid loss of BM can be associated with adipose mass regain and an increase of HOMA-IR over time if vigorous PA or CR is not maintained (11). The detriments (increased adiposity, insulin resistance, adipokines, and triglycerides) observed following the regain of the lost BM is known as the "rebound effect" (11, 12). Furthermore, CR alone may be associated with increased loss of lean tissue (fat-free mass) and the associated water vs. adipose mass loss (70% of total mass loss derived from water and 5% from lean tissue, vs. 25% from adipose) (13), especially during prolonged semi-starvation conditions where lean tissue loss can account for up to 41% of the BM loss (14), which may minimize greater potential benefits. However, the metabolic adjustments associated with CR during metabolic syndrome and following a subsequent regain in BM are not well-elucidated.

Caloric restriction leads to glycogen depletion in muscle and liver, leading to increased lipolysis and formation of ketone bodies, while decreasing glucose output via inhibition of gluconeogenesis and glycogenolysis (15). However, increased utilization of lipids as a consequence of CR can lead to insulin resistance (IR) (16).

Adipose tissue secretes many biologically active proteins including leptin and adiponectin (17). Decreased leptin during adipose mass loss can contribute to increased hunger, lower metabolic rate and mass regain (18). Conversely, increased leptin decreases insulin sensitivity, contributing to systemic hyperinsulinemia and T2DM (19). Adiponectin has protective effects against cardiovascular disease, is negatively correlated to triglyceride levels, is positively correlated to HDL levels (20), and enhances insulin action when administered to animals during conditions of increased fat oxidation (21).

The goal of this study was to assess the benefits of acute CR on glycemic control and lipid metabolism in a model of metabolic syndrome and comparing these effects to those induced by subsequent regain in BM in the form of adipose tissue, or "rebound effect." Previous studies found an increase in fatty acid synthesis and liver lipid accumulation to be principal consequences of the rebound effect after a moderate (30%) CR in OLETF (22), and increased leptin and peripheral glucose resistance after fat mass recovery following a 40–50% CR in obesity-prone Wistar rats (23). However, other aspects of this phenomenon are yet to be elucidated such as humoral factors driving the change in glucose tolerance, adiposity, and arterial pressure.

The OLETF model resembles the pathological features of human metabolic syndrome including late onset hyperglycemia, mild obesity (24, 25), insulin resistance, hyperlipidemia, and hypertension (26–28). We hypothesized that: (1) CR will improve systemic insulin sensitivity and adipokine profile while decreasing hepatic gluconeogenesis and increasing lipolysis and NEFA uptake, and (2) mass recovery will reverse the improvements realized by CR-induced BM.

2.3 Materials and Methods

All experimental procedures were reviewed and approved by the institutional animal care and use committee of Kagawa Medical University (Kagawa, Japan).

2.3.1 Animals

Male, lean strain-control, Long Evans Tokushima Otsuka (LETO) (n = 29) and obese, insulin resistant Otsuka Long Evans Tokushima Fatty (OLETF) (n = 29) rats (Otsuka Pharmaceutical Co., Ltd., Tokushima, Japan) of 11 weeks of age were fed ad libitum with standard laboratory rat chow (MF; Oriental Yeast Corp., Tokyo, Japan) for 4 weeks. At 15 weeks, rats were randomly assigned to one of the following groups: (1) LETO ad libitum control for CR (n = 8), (2) LETO ad libitum control for partial recovery of BM (n = 7), (3) LETO with 50% caloric restriction (LETO CR) (n = 7), (4) LETO with 50% CR followed by ad libitum feeding, resulting in partial recovery of BM (LETO PR; 73% recovery of mass loss) (n = 7), (5) OLETF ad libitum control for CR (n = 7), (6) OLETF ad libitum control for PR (n = 8), (7) OLETF 50% CR (n = 7), and (8) OLETF PR (n = 7; 59% recovery of mass loss) (Figure 2). Total mass recovery was not achieved purposefully to best assess the impacts of partial recovery. The LETO strain was restricted as well to be able to discriminate between physiological CR- driven changes and the changes related to metabolic syndrome, as well as to contrast with the baseline levels in the OLETF animals. All animals were maintained in groups of two animals per cage at the start of the study to minimize stress (29) and

one per cage during the CR phase. Ad libitum food intake per rat was calculated as the mean intake for double occupancy cages. Animals were maintained in a specific pathogen-free facility under controlled temperature (23◦C) and humidity (55%) with a 12-h light, 12-h dark cycle. All animals were given free access to water for the entire study.

2.3.2 Blood Pressure

Systolic blood pressure (SBP) was consistently measured in triplicate in conscious rats by tail-cuff plethysmography (BP98A; Softron Co., Tokyo, Japan) (n = 6/group) as previously described (26, 30, 31). Rats were acclimated to the tube restraints prior to measurements. Measurements were taken after feeding once a week during the first 4 weeks of the study (LETO vs. OLETF before start of CR), every other day until 16 weeks for CR vs. control and 17 weeks for PR vs. control groups. Repeated measures with a percent coefficient of variability (CV) >15% were excluded.

2.3.3 Body Mass (BM) and Food Intake

BM and food intake were measured daily to calculate the appropriate amount of chow to be given to CR and PR groups. At 15 weeks, all groups except LETO and OLETF ad lib controls were given 50% of mean food intake of control group for the next 10 days resulting in mean decreases in BM of 12 and 14% for LETO and OLETF, respectively. Immediately following this 10-day CR phase, a subset of the remaining animals (n = 7– 8) (from the CR cohorts) were fed ad libitum again for 1 week, representing the PR phase.

2.3.4 Oral Glucose Tolerance Test (oGTT)

After the 10 days of CR, oGTTs were performed in half of the ad lib control groups (LETO and OLETF, n = 7/group) and in all the CR groups (LETO and OLETF, n = 7/group). oGTTs were performed in the remaining animals representing the PR groups 7 days later. oGTTs were performed as previously detailed in our hands (26). Briefly, a 2 g/kg glucose bolus was given by gavage to overnight-fasted (14+ h) rats. Blood was collected via the caudal vein before gavage and 15, 30, 60, and 120 min after. Dissections Three days after oGTTs, animals were fasted overnight and tissues collected the subsequent morning. After BM measurements were obtained, animals were anesthetized with 100 mg/kg i.p. pentobarbital injection and arterial blood was collected via the abdominal aorta into chilled vials containing a cocktail of 50 mmol/L EDTA, 5000 KIU aprotinin, and 0.1 mmol sitagliptin phosphate (DPP4 inhibitor). Vials were kept on ice until they could be centrifuged. Systemic perfusion with chilled PBS was performed via the same artery with an incision in the inferior vena cava as the exit point and proceeded until no blood was present. Thereafter, organs and fat depots were rapidly removed, weighed, and snap frozen in liquid nitrogen. Frozen samples were kept at −80◦C until analyzed. Blood samples were centrifuged (3,000 g, 15 min at 4◦C), and the plasma was transferred to cryo-vials and immediately stored at −80◦C.

2.3.5 Biochemical Analyses

Plasma triglycerides (TG) was measured using a Hitachi 7020 chemistry analyzer (Diamond Diagnostics, Massachusetts, USA), and total protein content was measured by the Bradford assay (Bio-Rad Laboratories, CA, USA). Plasma and liver nonesterified fatty acids (NEFA), and liver diacylglycerol (DAG) were measured using commercially available kits (Wako, Osaka, Japan; MyBioSource, San Diego, USA). Hepatic NEFA and DAG measurements were performed

following whole lipid extraction from an aliquot of liver (20–30 mg) by the method described previously (32) and later modified (18). Lipase activity was measured in plasma as previously described (33). Plasma insulin (Wako, Osaka, Japan), total GLP-1 (Millipore, Burlington, USA), plasma aldosterone, and serum leptin and adiponectin (R&D Systems, Minneapolis, USA) were measured using commercially available ELISA kits (34, 35). All samples were analyzed in duplicate and run in a single assay with intra-assay and percent CV of <10% for all assays. Amino acids were measured by GCTOF MS (West Coast Metabolomic Center, University of California Davis, CA, USA). Creatinine and urea were measured by colorimetric method (QuantiChrom, Bioassay Systems, CA, USA) to better assess changes in lean mass [i.e., catabolism; (8)]. Serum electrolytes were measured by ISE (EasyLyte, MA, USA).

2.3.6 Protein Expression by Western Blot

Frozen kidney cortex was homogenized in 200 µl RIPA buffer (Thermo Fisher Scientific, NY, USA) and frozen liver was homogenized in either 200 µl RIPA (for G6Pc) or 150 µl STM buffer (250 mM sucrose, 50 mM Tris–HCl pH 7.4, and 5 mM MgCl2) containing 1% protease and 3% phosphatase inhibitor cocktail (Sigma-Aldrich, St. Louis, USA). Tissue homogenate was then sonicated for 20 s, centrifuged (15,120 g × 15 min for kidney and 800 g × 15 min for liver), and the supernatant total protein content was measured by the Bradford assay (Bio-Rad Laboratories, Hercules, CA). Predetermined amounts of total protein (TP) for kidney (40 µg) and liver homogenate (20 µg) were resolved in a 10% Tris-HCl SDS gel. Proteins were electroblotted using the BioRad Trans Blot onto a 0.45µm Inmovilon-FL polyvinylidene difluoride (PVDF) membrane for 2 h at 100 V. Membranes were blocked with 25% Odissey Blocking Buffer (PBS) and incubated 16 h at 4◦C with primary antibody against SGLT2 (1:200 dilution), PEPCK-C (1:200 dilution), G6Pc (1:500 dilution) (Santa Cruz Biotechnology, Dallas, USA). Membranes were washed with TBS 1% Tween-20 and incubated for 1 h with a secondary antibody (LI-COR Biosciences, Lincoln, USA) diluted 1:10,000, rewashed and visualized using a Li-Cor Odissey Imaging System. Densitometry values were quantified by ImageJ. software (NIH) and further normalized by correcting for densitometry values of a representative protein band stained with Ponceau S. Results are reported as percentage of expression compared to LETO baseline (CR control) unless stated otherwise.

2.3.7 Statistics

Means (±SE) were compared by two-way ANOVA for strain x treatment and interaction, with the Holm-Sidak method for post-hoc multiple comparison after excluding outliers by extreme studentized deviate test with $\alpha = 0.05$. Level of significance is considered for age-paired groups only, except for CR vs. PR. Glucose tolerance was assessed by comparing mean AUC values obtained from the glucose profiles during the oGTT. The AUC values were also compared by twoway ANOVA. SBP measurements were compared per day by one-way (before CR) or two-way (during CR and PR) ANOVA. Mass increment and food intake per day were also compared by one-way ANOVA before intervention and two-way ANOVA during CR and PR. Repeated measures ANOVA was performed in glucose and insulin data, but avoided for SBP analysis as samples were randomized and measures with >15% CV were excluded. Relationships between dependent and independent variables were evaluated by simple regression (except for insulin and DAG analysis, where a 4th order regression and power regression were used, respectively). Correlations were evaluated using Pearson correlation coefficients. Means, regression, and correlations were considered significantly different at $P < 0.05$. Statistical analyses were performed with SigmaPlot 12.5 software (Systat Software Inc., San Jose, CA).

2.4. Results

2.4.1 Increased ad lib Refeeding After CR Increases the Rate of Mass Gain

Slope analysis was performed to better appreciate the impacts of the treatments (CR and PR) on the changes in BM (Figure 3). Mean mass increment per day decreased in LETO ad lib control from 3.0 ± 0.4.g/day ($r^2 = 1$) before CR to 0.4 ± 1.4 g/day ($r^2 = 0.63$; $P < 0.001$) during recovery period, and decreased from 4.7 ± 0.5 ($r^2 = 1$) to 1.2 ± 1.3 g/day ($r^2 = 0.55$; $P < 0.001$) in OLETF. Mean mass decrease during CR was −4.8 ± 1.3 g/day ($r^2 = 0.96$) and −7.1 ± 2.1 g/day ($r^2 = 0.93$) for LETO and OLETF, respectively ($P = 0.392$ LETO vs. OLETF). During partial recovery, mean mass increase was 5.6 ± 4.3 g/day ($r^2 = 0.73$) for LETO and 6.9 ± 4.9 g/day ($r^2 = 0.75$) for OLETF ($P = 0.847$ LETO vs. OLETF). During the regain phase, animals in both strains regained ∼50% of the lost BM in 7 days, and the rates of regain were not different between the two strains, despite ad lib food intake increase in LETO during PR, compared to before CR (19.6 ± 0.6 vs. 23.7 ± 1.1 g/day; $P = 0.004$ in LETO and 24.4 ± 1.8 vs. 29.0 ± 2.0 g/day; $P = 0.100$ in OLETF).

2.4.2 CR Decreased Fat Depots, but Did Not Increase With Partial Recovery

The principal intraperitoneal fat depots were measured to better ascertain the degree to which the treatments (CR and PR) altered adiposity. Mean retroperitoneal adipose mass decreased after CR in both strains; by half in LETO ($P = 0.037$) and by 32% in OLETF ($P < 0.001$; Figure 4A). Retroperitoneal mass did not significantly increase after PR in OLETF (17% above CR; $P = 0.121$), but recovered to basal levels in LETO (10% below CR Control; $P = 0.841$; Figure 4A). In LETO, mean epididymal fat mass remained unchanged after CR ($P = 0.999$) and did not significantly increase with PR (25%: $P = 0.751$). Conversely, in OLETF, epididymal fat decreased 27% ($P = 0.009$) after CR and remained reduced after PR (23% below PR Control; $P = 0.018$; Figure 4B). Similar changes were observed after calculating the relative masses (Table 1). There were no significant changes in the relative masses of heart, kidney or liver in any of the strains following CR (Table 1). However, there was an increase in plasma amino acids independent of decreased protein intake during CR suggesting that lean tissue catabolism was primarily from skeletal muscle (Table 2).

2.4.3 CR Did Not Ameliorate the Increase in SBP Associated With the Metabolic Syndrome in OLETF

Mean SBP for both LETO and OLETF was similar before CR (129 ± 4 vs. 126 ± 4 mmHg; $P = 0.631$, respectively). SBP increased in OLETF compared to LETO 2 days after starting CR (121 ± 2 vs. 146 ± 3 mmHg; $P < 0.001$), and this difference was maintained through the rest of the study. However, there was not a significant difference between control groups and CR or PR in either of the strains, with the exception for LETO Control vs. CR at the end of the CR period (124 ± 4 vs. 137 ± 3 mmHg; $P = 0.026$, respectively; Figure 5). Serum Na^+ and Cl^- were unaltered between strains or after CR; however, K^+ was 30% higher ($P = 0.045$) in OLETF PR control (7.9 ± 0.2 mmol/L) compared to LETO (6.1 ± 0.3 mmol/L). Basal serum aldosterone was 2-fold higher ($P = 0.024$) in OLETF compared to LETO (10.4 ± 2.6 vs. 4.8 ± 0.9 mmol/L × 10−9). However, CR did not change aldosterone concentration in any of the strains.

2.4.5. CR Improves Glucose Tolerance and Insulin Resistance, but PR Completely Negates These Improvements

Glucose tolerance tests with corresponding insulin measurements and subsequent insulin resistance index (IRI) calculations were performed to quantify the functional metabolic effects of the treatment-induced alterations in BM (IRI = Glucose AUC × Insulin AUC/100). Mean blood glucose AUC was 2.4-fold higher in OLETF compared to LETO at baseline ($P < 0.001$). OLETF had a more pronounced decrease in glucose (19%, $P = 0.010$) compared to a non-significant decrease in LETO (16%, $P = 0.758$) after CR. However, LETO mean AUC increased 7% above control ($P = 0.948$), while OLETF maintained 5% below control after PR ($P = 0.827$), with a minimal 1% reduction vs. CR ($P = 0.882$). Blood glucose concentration peaked at 60 min for OLETF and 15 min for LETO after CR, and peaked at 30 min in OLETF after the recovery period (Figures 6A, B).

Mean plasma insulin AUC was 8% higher in LETO at 16 weeks, but 35% higher ($P = 0.035$) in OLETF at 17 weeks. Mean plasma insulin in LETO was lower, and higher in OLETF, for PR Ctrl compared to CR control, however this differences were non-significant and could be attributed to intra-subject variability rather than age effect. Plasma insulin AUC had a nonsignificant decrease in both strains after CR (25% in LETO and 31% in OLETF). Plasma insulin concentration peaked at 15 min for all groups except for OLETF CR, which peaked at 30 min (Figures 6C,D). Mean baseline IRI was 128% higher in OLETF compared to LETO ($P < 0.001$), and decreased 44% ($P = 0.015$) in OLETF after CR. However, IRI returned to baseline levels after PR (Figure 6E). It is important to consider that glucose AUC influenced the IRI calculations more profoundly than the insulin AUC, suggesting that impaired glucose handling/metabolism (most likely at the cellular level) is the primary factor contributing to the metabolic derangement associated with the condition as opposed to impaired glucose-stimulated insulin secretion (i.e., insulin response) in untreated OLETF.

2.4.6 Basal Expression of Gluconeogenic Enzymes Is Higher in OLETF

To further help elucidate potential mechanisms that contribute to the changes in glucose tolerance induced by the treatments, the protein expressions of hepatic PEPCK and G6Pc were quantified as markers of hepatic gluconeogenesis. Decrease in expression of these enzymes after CR was not significant; however, basal expression of cytosolic phosphoenolpyruvate carboxykinase (PEPCK-C) in OLETF was 113% higher than LETO ($P = 0.007$; Figure 7A) and mean basal expression of the downstream gluconeogenic enzyme, glucose-6- phosphatase (G6Pc) was 4.6-fold higher ($P < 0.001$) in OLETF control compared to LETO control (Figure 7B). CR and PR had no detectable effects on protein expressions of either enzyme.

2.4.7 Kidney SGLT2 Expression Increases in OLETF With Partial Recovery of BM

Given the benefits of CR on glucose tolerance and IRI, kidney SGLT2 was measured to assess the potential of its contribution to the improvements in glucose metabolism. CR did not significantly change the mean relative expression of SGLT2 in either strain (Figure 7C). Regardless of the treatment, the expression remained relatively constant in LETO. However, there was a significant increase in OLETF PR control compared to OLETF CR control (183 vs. 97%; $P = 0.015$) and LETO PR control (98%; $P = 0.006$), which likely reflects the progression of the metabolic syndrome in this strain (Figure 7C).

2.4.8 The CR-Induced Decrease in Adipose in OLETF Is Associated With a Concomitant Decrease in Serum Leptin and Increased Adiponectin After PR

Given the changes in the principal i.p. adipose depots with the treatments, the adipose-derived hormones, leptin and adiponectin, were measured to gain insights on the sensitivity of adipose to the treatment's effects and their potential to contribute to the metabolic effects observed. Mean serum leptin was higher in OLETF control ($P = 0.038$) than LETO control, representative of the increased adiposity associated with the model, and decreased 3.1-fold after CR without reaching significance (CR Control: 3.9 ± 0.3 vs. CR: 1.3 ± 0.1 mmol/L; $P = 0.177$). However, in OLETF mean serum leptin was maintained below control after partial recovery (PR Control: 8.2 ± 2.4 vs. PR: 4.5 ± 0.6 mmol/L; $P = 0.028$; Figure 8A). Regardless of treatment, plasma leptin remained constant in LETO throughout the study. Serum adiponectin remained unchanged in both strains at baseline and after CR, but increased 61% ($P < 0.001$) after PR in LETO and 18% ($P = 0.05$) in OLETF (Figure 8B). Baseline leptin: adiponectin ratio was 3-fold higher in OLETF vs. LETO; however, the ratio decreased 2-fold in LETO and 3-fold in OLETF ($P < 0.001$) after CR (Figure 8C).

2.4.9 Strain-Effect on Plasma GLP-1 Remains Despite CR

Mean plasma GLP-1 concentrations were greater in OLETF compared to LETO at baseline and following CR ($P < 0.05$), despite substantial, however non-significant decreases in both strains with CR (Figure 8D). Significant differences in mean GLP-1 concentrations following PR were not detected. The reduction of circulating GLP-1 in OLETF after CR and the greater basal levers in OLETF compared to LETO suggests that, although GLP-1 improves glucose tolerance by augmenting peripheral insulin action (16, 36), it may not be a key factor in improving glucose tolerance in this study.

2.4.10 CR-Induced Decrease in Plasma TG Is Abolished With PR

Mean plasma TGs were nearly 2-fold ($P < 0.05$) greater in OLETF compared to LETO at baseline, and levels decreased ($P < 0.001$) 86% in OLETF with CR compared to control (Figure 9A). After PR, levels in OLETF returned to baseline concentrations ($P = 0.941$; Figure 8A). Liver TGs were higher in OLETF compared to LETO throughout the study, but hepatic levels were not altered by either treatment in OLETF (Figure 9B). In LETO, liver TGs were lower ($P = 0.002$) in PR controls than CR controls, which maybe a reflection of a time (age effect), and levels were not significantly altered with either treatment (Figure 9B). Plasma NEFA concentration were higher in OLETF following PR compared to the levels following CR ($P = 0.002$; Figure 9C). Otherwise, plasma NEFA levels remained constant in LETO regardless of treatment. CR did not induce a significant effect in either strain on hepatic NEFA concentrations, but because levels remained constant in OLETF and decreased in LETO, a strain effect ($P < 0.05$) was detected during the PR phase (Figure 9D). Mean plasma lipase activity was nearly 3-fold higher ($P = 0.003$) in OLETF at baseline, but otherwise levels were stable within strain and were not altered by treatment (Figure 9E). CR did not alter mean hepatic diacylglycerol (DAG) content in either strain, but levels remained higher ($P = 0.009$) in LETO than OLETF (Figure 9F). PR had no effect on levels in in either strain, but were reduced ($P < 0.05$) in both control and PR LETO compared to values following CR (Figure 9F). The lack of DAG accumulation in liver, particularly in OLETF after CR, suggests that lipolysis of TGs remained static. This is particularly beneficial as hepatic DAG accumulation is associated with increased insulin resistance more so than NEFA accumulation (37, 38).

2.4.11 CR Increased Relative Plasma Creatinine in LETO, but Not in OLETF, While It Decreased Urea in OLETF

Mean relative plasma creatinine in LETO increased 75% ($P < 0.001$) after CR compared to control, but the effect of PR was not significant. Treatment effects in OLETF were not detected for creatinine, but plasma urea decreased 46% ($P < 0.001$), and by consequence urea: creatinine ratio (49%, $P = 0.016$), after CR, returning to basal levels after PR compared to PR control. Mean relative plasma urea did not exhibit a treatment effect in LETO (Table 2). We hypothesized that the transient decrease urea in the OLETF without increase in creatinine concentration can be attributed to protein depletion (39) rather than diabetic nephropathy, as the latter develops later in the OLETF (34).

2.5 Discussion

Caloric restriction ameliorates metabolic syndrome in obese individuals (40), even in the presence of T2DM (13, 41). However, only a few studies have demonstrated the consequences of interrupting caloric restriction (42) without providing sufficient insight on the molecular mechanisms involved. The aim of this study was to provide further insights into how CR ameliorates metabolic syndrome, and how recovery of BM due to CR interruption abolishes these benefits.

2.5.1 Caloric Restriction Promotes Loss of Lean Tissue and Water Rather Than Adipose

BM gain and food intake were consistently higher in OLETF compared to LETO, which is consistent for this model of diet induced obesity (24, 25). The acute phase of severe CR resulted in nearly a 30% greater rate of mass loss in OLETF compared to LETO yet the loss of epididymal and retroperitoneal mass accounted for only about 5% of the total mass loss in OLETF suggesting that there was significant loss of lean tissue and the associated water. The loss of the primary adipose depots in the relatively lean LETO accounted for closer to 10% of the total BM loss suggesting that acute, severe CR in the healthier strain was less detrimental with respect to preserving lean tissue and total body water. Thus, these data suggest that during a diabetic condition that presents with metabolic syndrome, acute, severe CR may result in a disproportionate loss of lean tissue and water over the desired effect of preferential loss of excess fat mass (43). The loss of intracellular water derived from muscle catabolism may be a significant contribution to the total BM loss as has been observed in malnourished populations (44). In perspective, an extended bout of CR during a condition of metabolic syndrome has the potential to induce more severe cachexia and loss of total body water although the benefit of improved glucose tolerance could still be present. Thus, an appropriate balance between benefits in glucose tolerance and perseverance of lean tissue would need to be struck if this degree of CR was to be implemented as a treatment modality.

For both strains, the rate of mass recovery was greater than the normal growth rate for ad libitum control rats suggesting that the CR animals compensated for the rapid loss of mass by disproportionately increasing their food intake during the PR phase. This PR phase may have been associated with a decrease in basal metabolism to facilitate the rapid mass gain (45), consistent with lower BM (i.e., lower caloric balance) without obvious change in physical activity, which further widens the energy gap (energy intake vs. expenditure) (46). Interestingly, although mass loss and regain trends were similar for both strains, only OLETF rats had significant fat mass loss, which was not completely recovered after the PR phase. These observations suggest that the

recovery of BM, most likely lean tissue, is prioritized in diabetic OLETF animals, more so than in lean, LETO.

2.5.2 Caloric Restriction Did Not Ameliorate the Elevated SBP Despite Reductions in Adipose Mass

Differences in SBP between strains were detected 2 days after starting the caloric restriction (at 15 weeks) consistent with the hypertension in OLETF at 14 weeks (47). Obesity, especially visceral adiposity, is a known independent risk factor for hypertension, although several studies suggest that insulin sensitization induced by CR are also associated with a decrease in SBP (48). Even a modest decrease in BM (5– 10%) can normalize blood pressure in obese patients (10). Metformin-induced increase in glucose tolerance elicited a BM-independent reduction in SBP of more than 10 mmHg in hypertensive OLETF rats (49) suggesting that an improvement in glucose tolerance may alter arterial pressure independent of reducing BM. Despite the profound reductions in adiposity and improvements in glucose tolerance in OLETF, these benefits did not translate into sustained or modest reductions in SBP. However, the reductions in SBP with metformin not observed here with CR may reflect off-target effects of metformin (i.e., pharmaceutical vs. behavioral interventions). Paradoxically, CR increased SBP in LETOs, which was normalized to control LETO levels after partial mass recovery suggesting that during nondiabetic conditions, potential stress, independent of the reninangiotensin-aldosterone system (RAAS), during CR may have been sufficient to induce an increase in SBP.

The exact mechanisms promoting the strain-associated hypertension are not well-defined in OLETF; however, elevated RAAS is a likely contributing factor (26, 28, 50). The nearly 2-fold greater plasma aldosterone levels at baseline in OLETF compared to LETO substantiate the previous studies that increased RAAS is a contributing factor in the strain-associated hypertension. However, in the present study, the substantial reductions in BM with CR and the reciprocal increases in BM in the regain (PR) phase did not alter SBP or plasma aldosterone despite improvements in glucose tolerance suggesting that the benefits of acute, severe CR do not translate into amelioration of the hypertension and that the elevated RAAS is resistant to changes in BM and/or adiposity.

2.5.3 SGLT2 Expression Is Sensitive to Perturbations During Metabolic Syndrome

In order to assess the contributions of renal glucose absorption via SGLT2, its expression was measured. The lack of changes in SGLT2 expression in LETO regardless of perturbation suggests that renal glucose handling in healthy animals is constant and robustly regulated. However, the changes in expression in OLETF following the perturbations suggest that the regulation of SGLT2 expression is more sensitive to variable aspects associated with mass loss and regain during diabetic conditions. Nonetheless, these differences in expression were not significant nor translate into robust biological effects.

Aside from the potential contributions of renal glucose handling, we can’t discount the potential contributions of intestinal reabsorption on improving glucose tolerance. Unfortunately, we were not able to measure SLGT1 and GLUT2, the primary monosaccharide transporters in the intestine. However, these transporters are upregulated after feeding, especially after a glucose challenge (51). Therefore, we suspect they would be downregulated with CR and, at least, partially rebound during the regain phase.

2.5.4 Despite Basal Differences in Gluconeogenic Enzymes, CR, and PR Did Not Induce Changes in Gluconeogenesis

Binding of insulin to its hepatic receptor activates a signaling cascade that inhibits the expression of the gluconeogenic enzymes, G6Pc, and PEPCK, in favor of increasing glucokinase expression and hepatic sequestration of glucose (52). However, the increased expression of the basal levels of both enzymes in the OLETF compared to LETO rats in the presence of similar insulin levels for both strains suggests that the liver is resistant to insulin. Moreover, the increased levels of basal glucose in the OLETF rats without significant changes in the potential for increased kidney glucose reabsorption (assessed via SGLT2) suggests that hepatic glucose production could be a major contributor in the systemic hyperglycemia during diabetic conditions that is not profoundly altered with CR nor PR. This is especially alarming if severe CR fails to suppress the relatively elevated expression of hepatic gluconeogenesis, even in the presence of a potential increase in insulin-stimulated glucose uptake in muscle via Akt2 activation after acute (53) and prolonged (54) CR. The combination of these factors could impair further potential benefits of CR, reflected by an improvement in IRI in the present study.

2.5.5 Increased Adiponectin May Contribute to Amelioration of Peripheral IR

CR did not statistically alter adiponectin, an insulin-sensitizing adipokine (55), but levels increased after partial recovery in both strains. Moreover, leptin and leptin: adiponectin ratio decreased after CR, while leptin remained below basal levels after PR. These data suggest that the modest increase in adiponectin, however statistically insignificant, in the presence of suppressed leptin, reflected in the decreased leptin: adiponectin ratio, may be a more critical marker of the potential insulin sensitizing phenomenon in peripheral tissues than the changes in adiponectin levels alone following a bout of CR. Moreover, the decrease in leptin paired with loss of adipose tissue after CR in OLETF suggests that the hyperleptinemia present in the OLETF is a consequence of greater adipose mass rather than a derangement in leptin sensitivity and/or secretion (56). The increase in adiponectin following PR may be a compensatory response to protect against leptin-induced inflammation (19). Interestingly, this increase in adiponectin following PR was not sufficient to maintain the improvements in glucose tolerance because only partial recovery of the lost BM induced by CR was enough to abolish them. Thus, other aspects associated with the partial recovery of BM, which was not primarily adipose, contributed to the reversal of the CR-induced benefits on glucose tolerance.

2.5.6 Few Metabolic Improvements Are Maintained After Only Partial Recovery of BM in a Model of Metabolic Syndrome

Acute CR improved glucose tolerance and reduced IRI in a model of metabolic syndrome likely through a reduction in hepatic gluconeogenesis, increased peripheral tissue glucose utilization induced via enhanced insulin sensitization, and increased NEFA uptake most likely by muscle. These improvements were accomplished despite minimal reductions in intraperitoneal adipose mass and significant reductions in lean tissue. Upon partial recovery of BM, the only metabolic change of note that we observed with some potential benefit was increased adiponectin; however, this change was not sufficient to maintain the benefit in glucose tolerance and reduced IRI despite only modest recovery in adipose mass suggesting that the very modest changes in adipose mass likely had minimal effects on the observed metabolic alterations.

Chapter 3 Mass Recovery following Caloric Restriction Reverses Lipolysis and Proteolysis, but not Gluconeogenesis, in Insulin Resistant OLETF Rats

3.1 Abstract

Caloric restriction (CR) is one of the most important behavioral interventions to reduce excessive abdominal adiposity, which is a risk factor for the development of insulin resistance. Previous metabolomics studies have characterized substrate metabolism during healthy conditions; however, the effects of CR and subsequent mass recovery on shifts in substrate metabolism during insulin resistance (IR) have not been widely investigated. To assess the effects of acute CR and the subsequent mass recovery on shifts in substrate metabolism, a cohort of 15-week old Long Evans Tokushima Otsuka (LETO) and Otsuka Long Evans Tokushima Fatty (OLETF) rats were calorie restricted (CR: 50% × 10 days) with or without partial body mass recovery (PR; 73% x 7 days), along with their respective *ad libitum* controls. End-of-study plasma samples were analyzed for primary carbon metabolites by gas chromatography (GC) time-of-flight (TOF) mass spectrometry (MS) data acquisition. Data analysis included PCA, Pearson correlation vs previously reported variables (adipose and body masses, and insulin resistance index, IRI), and metabolomics maps (MetaMapp) generated for the most significant group comparisons. All treatments elicited a significant group differentiation in at least one principal component. CR improved TCA cycle in OLETF, and increased lipolysis and proteolysis. These changes were reversed after PR except for gluconeogenesis. Plasma lipid concentrations were inversely correlated to IRI in LETO, but not OLETF. These shifts in substrate metabolism suggest that the CR-induced decreases in adipose may not be sufficient to more permanently alter substrate metabolism to improve IR status during metabolic syndrome.

3.2 Introduction

Abdominal adiposity, concomitant with increased plasma leptin and branched chain amino acids (BCAA), and lower adiponectin, are risk factors for insulin resistance (IR) independent of higher protein intake and body mass index (BMI) [1, 2]. Also, obesity leads to excessive β-oxidation (e.g. mitochondrial overload) in skeletal muscle concomitant with decreased fatty acid oxidation in liver, which in turn may be responsible for muscle insulin resistance [3]. Excessive β-oxidation is also associated with an increase of glucose-6-phosphate dehydrogenase (G6PD), the rate limiting enzyme in the pentose phosphate pathway (PPP), which in turn increases circulating triglyceride (TG), non-esterified fatty acids (NEFA), and pro inflammatory cytokines [4]. Moreover, increased BCAA, and glucuronic and hexuronic acids are correlated with the progression of type 2 diabetes mellitus (T2DM) in rats [5].

Caloric restriction (CR), especially when associated with a decrease in carbohydrate intake [6, 7], is an important behavioral intervention to reduce excess adipose mass [8]. In healthy mice, short term CR (30% for 16 days) increased the hepatic glycogenic amino acid, valine (a BCAA), and lean tissue turnover, and decreased fasting glucose and VLDL [9]. In healthy humans, acute, severe CR (90%, 48 hrs) decreased glucose and pyruvate, and increased glucogenic amino acids, ketone bodies, and lipolysis products, but these changes were reversed after a 48-h *ad libitum* refeeding [10] demonstrating the shifts in critical metabolic pathways to acute alterations in caloric intake. In elderly patients, enteral refeeding after 10 days of food deprivation resulted in a decrease in acylcarnitines concomitant with an increase of free amino acids and higher urea cycle activity [11]. However, to the best of our knowledge there is still little information on the shifts in biochemical processes (assessed via metabolomics) in response to CR and the subsequent mass recovery from refeeding during metabolic syndrome.

The OLETF rat develops early onset hyperglycemia, obesity, insulin resistance, hyperlipidemia, and hypertension, all components of the metabolic syndrome [12-15]. Moreover, OLETF rats develop an age-associated reduction in hepatic beta-hydroxyacyl-coA dehydrogenase (β-HAD) and citrate synthase, which are rate limiting steps of β-oxidation and tricarboxylic acid cycle (TCA) cycle, respectively [16]. In addition, OLETF rats present with lower plasma levels of tryptophan and its metabolite, kynurenine, compared with their healthy, lean strain control Long-Evans Tokushima Otsuka (LETO). These variables may be predictive markers for the development of T2DM [17]. We hypothesized that reducing abdominal adiposity (i.e. visceral adipose) during metabolic syndrome via an acute CR without a modification in the macronutrient proportion, reduces gluconeogenesis, the pentose phosphate pathway (PPP), and plasma BCAA concentrations, with the advantage of increasing the rate of TCA cycle, lipolysis, and β-oxidation, without compromising lean tissue catabolism (lean tissue proteolysis). However, based on our previous results, we also hypothesized that partial recovery of body mass, even without full adipose recovery, is sufficient to fully revert these changes.

3.3 Method

Details of the current study have been published previously [18] and summarized in **Figure 10**. The current study complements the previous data by using metabolomics approaches to examine the shifts in metabolism associated with changes in body mass induced by CR and refeeding. The study was approved by IACUC of Kagawa Medical University.

3.3.1 Caloric Restriction (CR) and Partial Recovery (PR)

Briefly, lean strain control LETO (n=29) and obese, insulin resistant OLETF rats (n=29) were fed *ad libitum* with standard laboratory rat chow (MF; Oriental Yeast Corp., Tokyo, Japan) for 4 weeks. At 15 weeks of age, rats were separated in two *ad libitum* food control groups (n=8/group/strain), two CR groups (n=7/group/strain), and two partial recovery (PR) groups (n=7/group/strain). Both CR and PR groups were subjected to 50% CR (compared to *ad libitum* control) for 10 days. CR groups were subjected to an oral glucose tolerance test (oGTT) and dissected three days later along with their respective *ad libitum* controls (CR Ctrl, n=8/group/strain). Meanwhile, PR groups were fed *ad libitum* for 7 days, achieving partial body mass recovery (73% recovery of mass loss) before an oGTT and dissection paired with their PR control groups (n=7/group/strain). Both CR and PR control groups were fed *ad libitum* for the entire study. However, they were considered independent groups to avoid the confounding factor of age as they were dissected 1 week apart; however, no significant differences were detected between CR and PR control groups despite the slight difference in age suggesting that age was not a confounding factor here. Animals were maintained in a specific pathogen-free facility under controlled temperature (23◦C) and humidity (55%) with a 12-h light, 12-h dark cycle. All animals were given free access to water for the entire study.

3.3.2 Oral Glucose Tolerance Test (oGTT)

Oral glucose tolerance tests (oGTT) were performed as previously reported [18] and insulin resistance index (IRI) was calculated as previously described [13] and reported [18]. Data were used here to correlate the shifts in metabolites with IRI.

3.3.3 Blood Sample and Tissue Collection

Details of blood sample and tissue collections have been previously reported [18]. Briefly, animals were anesthetized after an overnight fasting with a 100 mg/kg i.p. pentobarbital injection and retroperitoneal and epididymal fat depots were dissected, weighed, and collected for other analyses. Arterial blood was collected via the abdominal aorta into chilled vials containing a cocktail of 50

mmol/L EDTA, 5000 KIU aprotinin, and 0.1 mmol sitagliptin phosphate (DPP4 inhibitor). Blood samples were centrifuged (3,000 g, 15min at 4°C), and the plasma was transferred to cryo-vials and immediately stored at −80°C. Aliquots of plasma (n=5 per group/strain) were analyzed for primary carbon metabolites by gas chromatography (GC) time-of-flight (TOF) mass spectrometry (MS) data acquisition and processing at the West Coast Metabolomics Center as previously described [19], generating a dataset of 143 consistently identified metabolites.

3.4 Data Analysis

3.4.1 Data Normalization and Transformation

Data were reported as quantitative ion peak heights and were normalized by the sum peak height of all structurally annotated compounds (mTIC normalization) [20]. Transformations were done using Johnson's family of transformation, depending on data normality, as described in other studies [21]. Student's t-test was performed in 10 previously selected pairwise comparisons (**Table 3**) and Benjamini-Hochberg False Discovery Rate (FDR) correction [22] q values were calculated for each metabolite per comparison.

3.4.2 Metabolic Mapping

Fold changes were calculated as mean condition B / mean condition A, after mTIC normalization. The conditions are described in **Table 3**. Metabolic maps were plotted per comparison only for metabolites with $p<0.05$ after Student's t-test using MetaMapp [23] and visualized in Cytoscape 3.7.1 with organic layout. Nodes with significant difference after FDR correction ($q<0.2$) were highlighted for fold-change and direction of change. Metabolites were classified into either primary or secondary metabolism pathways based on their entry on the Kyoto Encyclopedia of Genes and Genomes (KEGG) database [24], where secondary metabolism encompasses either cofactor, vitamin or xenobiotic metabolism. The maps with the most significant differences are shown in **Figure 11** and further discussed.

3.4.3 Correlations with Body Mass, Insulin Resistance Index, and Adipose Depots

Pearson correlations were calculated for parameters previously reported [18]. Johnson transformed body mass, IRI, and retroperitoneal and epididymal adipose masses were treated as independent variables and Johnson transformed metabolites were treated as dependent variables. Correlations were considered strong at $r<-0.8$ or $r>0.8$ and $q<0.2$. Statistical analyses were performed in JMP pro (version 14, SAS Institute Inc., Cary, NC, USA).

3.4.4 Partial Least Squares-Discriminant Analysis (PLS-DA) and Principal Component Analysis (PCA)

PLS-DA was run on all metabolites for all 10 comparisons (**Table 3**) by nonlinear iterative partial least squares (NIPALS), with leave-one-out validation, four (n-1) factors and variable importance in the projection (VIP) score threshold (alpha) of 0.1. The metabolites above the threshold were used further for PCA for correlation analyses. The scripts showing the metabolites considered for each PCA analysis can be found in the online repository. The rationale behind using PCA after PLS-DA was to avoid the increased group separation due to artifacts inherent to PLS-DA, and instead visually reflect the variability that distinguishes the groups [25]. For each PCA, mean of scores for PC1 and PC2, and standard deviations were calculated, and a t-test performed for both PC for significant difference ($P<0.05$) (**Table 4**). For each comparison, the metabolites with the five highest positive and 5 highest negative loadings are shown in **Table 5**.

3.4.5 Availability of Data and Material

The datasets generated for this study are available on request to the corresponding author. Raw and normalized metabolomics files can be found in the following repository: https://doi.org/10.6084/m9.figshare.12831005

3.5 Results

3.5.1 *Ad libitum* fed OLETF rats had lower glycolysis and TCA variables, and higher PPP compared to LETO

OLETF rats had lower basal levels of the glycolysis intermediates, 3-phosphoglycerate (10.9- fold, q<0.001), glyceric acid (2.4-fold, q<0.001), and glycerol-alpha-phosphate (2.5-fold, q=0.001). Moreover, the basal concentrations of citric acid and isocitric acid, the first intermediates of the TCA, were reduced in OLETF compared to LETO (1.9-fold, q=0.032 and 2.0-fold, q=0.061 respectively). Conversely, basal glucose was higher in OLETF (1.3-fold, q=0.020), and ribitol and ribose concentrations were increased in OLETF compared to LETO (2.2-fold, q=0.009 and 1.4-fold, q<0.001, respectively) (**Figure 11A**). These data suggest that during normo-caloric conditions, PPP may contribute significantly to energy production during an insulin resistant condition.

3.5.2 CR induced higher lipolysis intermediates in OLETF compared to LETO

Compared to LETO after CR, OLETF had higher plasma concentrations of the long-chain fatty acids (LCFA) lignoceric acid (3.1-fold, q=0.087), myristic acid (1.8-fold, q=0.125), and palmitoleic acid (2.6-fold, q=0.038), and the medium-chain saturated fatty acid (MCFA) caprylic acid (2.9-fold, q=0.103), which could reflect a higher rate of lipolysis in OLETF. Moreover, there is an even more pronounced difference between strains in uracil and uric acid concentration (5.3-fold, q=0.041 and 4.9-fold, q=0.021 higher, respectively) (**Figure 11B**), which suggest either an increase in lean tissue catabolism and/or a deficit in kidney function in the insulin resistant strain.

3.5.3 CR increased intermediates in PPP and TCA, and amino acid concentration, while reducing fasting glucose in OLETF

CR in OLETF increased the concentration of the pentoses ribose (2.5-fold, q=0.002) and xylulose (11.6-fold, q=0.003), which are intermediates in the PPP. Moreover, 3-phosphoglycerate, a product of both PPP and glycolysis, increased by 5.6-fold (q=0.009), as well as several intermediates of the TCA cycle: citric acid (2.2-fold, q=0.004), aconitic acid (1.9-fold, q=0.005), isocitric acid (2.2-fold, q=0.008), fumaric acid (5.6-fold, q=0.001), and malic acid (7.2-fold, q=0.001). Furthermore, an increase in the concentration of the amino acids, alanine (1.7-fold, q=0.011), beta-alanine (2.4-fold, q=0.041), cysteine (2.2-fold, q=0.010), serine (1.3-fold, q=0.011), and threonine (1.3-fold, q=0.078), was observed. This translated into a decrease in circulating glucose by 2.6-fold (q<0.001), while increasing adenosine 5-monophosphate (AMP) by 5.2-fold (q=0.005). However, these changes were not observed in LETO after CR. In addition, 5-methoxytrypamine, a metabolite closely related to serotonin, increased 22.3-fold (q=0.038) (**Figure 11C**). The significant increase in plasma AMP and TCA cycle intermediates may reflect an increase in ATP utilization during CR.

3.5.4 Partial mass recovery increased fasting glucose and decreased TCA, pyrimidine catabolism and lipolysis in OLETF

Partial recovery did not change fasting glucose in LETO, but increased glucose in OLETF by 2.5-fold (q=0.001). Conversely, pyrophosphate, a product of ATP hydrolysis, decreased by 2.3-fold (q=0.007) with an even more pronounced changes in the TCA cycle intermediates, fumaric acid

(3.5-fold, q=0.015), malic acid (4.0-fold, q=0.019), and succinic acid (19-fold, q=0.010). Moreover, lignoceric acid (4.4-fold, q=0.010), palmitic acid (2.1-fold, q=0.028), stearic acid (2.5-fold, q=0.017), and caprylic acid (3.7-fold, q=0.006) decreased, along with the pyrimidines, thymine (1.8-fold, q=0.098) and uracil (6.2-fold, q=0.007), its catabolic products, beta-alanine (3.7-fold, q=0.003) and uric acid (4.4-fold, q=0.025), and the glucogenic amino acids, alanine (1.6-fold, q=0.045), cysteine (2.2-fold, q=0.013), glycine (2.5-fold, q<0.001), and aspartic acid (2.0-fold, q=0.016). Interestingly, the concentration of 5-methoxytrypamine was reduced (24.5-fold, q=0.032) after mass recovery in a similar degree as it was increased after CR (**Figure 11D**). Collectively, these changes suggest that, after one week of *ad libitum* diet: **1)** the ATP: ADP ratio is recovered, **2)** hyperglycemia is maintained in OLETF even with decreased endogenous glucose production, and **3)** the reliance on lipid and protein catabolism for energy during insulin resistance is decreased (**Table 6**).

3.5.5 Lipid metabolism was inversely correlated to IRI after PR in LETO, but not OLETF

Stearic acid (r=-0.95, q=0.097), palmitoleic acid (r=-0.90, q=0.159), palmitic acid (r=-0.95, q=0.097), myristic acid (r=-0.87, q=0.159), linoleic acid (r=-0.82, q=0.159), glycerol alpha-phosphate (r=-0.94, q=0.097), docohexaenoic acid (r=-0.96, q=0.097), dihydrocholesterol (r=-0.88, q=0.159), cholesterol (r=-0.85, q=0.159), capric acid (r=-0.83, q=0.159), beta-sitosterol (r=-0.83, q=0.159), and arachidonic acid (r=-0.86, q=0.159) had strong, inverse correlations with IRI after PR in LETO. However, no metabolite had a strong, inverse correlation (r<-0.8 and P<0.05) with IRI after CR in LETO nor OLETF, neither after PR in OLETF. (**Figure 12B**). These results suggest that reductions in plasma lipids induced by CR may help maintain normal insulin signaling in LETO, while this protective effect was not observed in the insulin resistant state, and may contribute to the condition.

3.5.6 Amino acid metabolism was more closely correlated with visceral adiposity than total body mass in OLETF after PR

We previously showed that visceral adipose (retroperitoneal and epididymal) depots were reduced with CR, but depots did not recovered after PR in OLETF suggesting that lean tissue accounted for most of the mass recovery. Moreover, total amino acids increased exclusively in OLETF after CR. Thus, we expected that plasma amino acids would be directly correlated to body mass, rather than adipose, after mass recovery in OLETF. However, contrary to our hypothesis, no amino acid had a strong, positive correlation with body mass, while 4-hydroxyphenylacetic acid (r=0.99, q=0.068) was directly correlated with retroperitoneal fat mass, and tryptophan (r=0.95, q=0.128), phenylethylamine (r=0.91, q=0.172), methionine (r=0.90, q=0.172), histidine (r=0.91, q=0.172), glutamine (r=0.96, q=0.128), glutamic acid (r=0.99, q=0.051), and cystine (r=0.95, q=0.128) were directly correlated with epididymal fat mass in OLETF after PR (**Figure 12C**).

3.5.7 PLS-DA with subsequent PCA successfully separated each pair of groups at PC1 except for LETO CR vs OLETF CR

PLS-DA was performed for each significant pairwise comparison before performing pairwise PCA analyses (**Figure 13**). Each pairwise comparison had significantly different ($P < 0.05$) PC1 score means, while none of the PC2 score means were significantly different in any of the comparisons. The only exception was comparison C (LETO CR vs OLETF CR) where PC1 scores were not significantly different (**Table 4**). Moreover, this comparison had the closest PC1 score means compared to the rest. This could be explained by the relatively higher variability between samples in the OLETF CR group (SD of 5.80 for PC1). In contrast, LETO CR had relatively much smaller variability, (SD of 0.76 for PC1). Based on these observations, and the fact that PC1 accounted for at least 40% of the variation in all comparisons, further PCA analyses focused on PC1.

3.5.8 Carbohydrate metabolism contributed to the distinction between LETO and OLETF *ad libitum* controls

The monosaccharides, glucose and ribitol, were among the top 5 metabolites that contributed to differentiation between OLETF and LETO (strain effect) on *ad libitum* diet on PC1 at 16 weeks of age (**Table 5, Comparison A**), while hexitol and ribose were added to the list at 17 weeks of age (**Table 5, Comparison B**). Conversely, the metabolites that contributed to the differentiation between the LETO and OLETF CR control groups were involved in lipid, amino acid, and secondary metabolism, with the exception of 3-phosphoglycerate, which is involved in glycolysis. (**Table 5, Comparison A**). These changes could imply a higher reliance in glucose metabolism from the OLETF rats or an impairment in lipid or amino acid metabolism during the insulin resistant state.

3.5.9 Amino acid metabolism contributed to the distinction between LETO and OLETF after CR, but not after PR

From the top five absolute loadings, 2 metabolites involved in amino acid metabolism (putrescine and pantothenic acid), and beta-alanine, involved in nucleotide metabolism, contributed to the distinction of OLETF from LETO after CR, while the amino acids, tryptophan, lysine, and oxoproline, as well as arachidonic acid (involved in lipid metabolism), contributed to distinguish LETO from OLETF after CR (**Table 5, Comparison C**). This suggests that OLETF rats may rely on protein catabolism in order to synthetize coenzyme A, in contrast to LETO rats that use lipids primarily as a source of energy when carbohydrates are depleted. Conversely, after PR, the metabolites that contributed the most to the distinction between the strains were associated with either lipid metabolism (glycerol-alpha-phosphate for LETO and cholesterol for OLETF) or carbohydrate metabolism (3-phosphoglycerate for LETO, and ribitol and ribose for OLETF) (**Table 5, Comparison D**).

3.6 Discussion

The previous results show that CR elicited more profound metabolic changes in the insulin resistant state compared to the healthy state. Several of the changes observed in glucose metabolism were expected based on previous findings. However, it was rather surprising that these metabolic shifts were not sufficient to spare the utilization of proteins for fuel in the insulin resistant rats, and even more, that mass recovery did not reverted gluconeogenesis to its basal levels, as we will further discuss.

3.6.1 Carbohydrate metabolism prevailed with an improvement in the TCA cycle, without affecting the oxidative phase of the PPP, after a week of CR in OLETF

A reduction in caloric intake is usually associated with a shift toward increased lipid metabolism because of the reduction in glucose [26-28]. Thus, after 7 days of 50% CR in OLETF rats, we expected to observe a shift toward a greater reliance on lipid metabolism [29]. However, the increases in 3-phosphoglycerate, a by-product of glycolysis, several TCA intermediates, and two intermediates from the non-oxidative phase of the PPP, independent of any detectable changes in oxidative phase intermediates suggest that glucose metabolism is increased with CR during insulin resistance. This highlights the clear benefit of CR to improving glucose metabolism and ameliorating the hyperglycemia during insulin resistance. The increase in plasma ribose likely indicates an increase in PPP concomitant with a decrease on nucleotide synthesis in peripheral tissue [30]. The increase in TCA intermediates suggests that CR even during an insulin resistant state may improve the strain-associated impairment in the TCA cycle. This impairment has been previously described in obese, diabetic rats secondary to hyperphagia and an impairment in the

leptin receptor [3], and in T2D patients compared to healthy subjects [31]. The improvement in IRI in OLETF with CR [18] substantiates this data suggesting that CR improves glucose metabolism via enhanced TCA cycle activity. However, in the OLETF the impairment in basal glucose metabolism is likely induced by impaired glycolysis because basal levels of 3-phosphoglycerate were lower in OLETF compared to LETO.

3.6.2 Partial mass recovery reverted lipolysis, rather than gluconeogenesis, to basal levels

The decrease in glycerol after PR compared to CR suggests that either lipolysis and/or gluconeogenesis is decreased after mass recovery [32], and demonstrates that seven days of partial recovery were sufficient to reverse the limited reliance in lipids in OLETF during an insulin resistant state. This result is consistent with our previous finding where triglyceride levels returned to basal levels following PR [18]. Furthermore, the decrease in the glucogenic amino acids, alanine, cysteine, glycine, and aspartic acid after refeeding (PR), is consistent with the metabolomics data from humans following starvation and refeeding [33]. However, we previously showed strain-dependent changes in the expressions of glucogenic enzymes, although we did not detect consistent changes in these enzymes with CR and PR in OLETF [18] suggesting that the rate of lipolysis, but not gluconeogenesis, is reverted to basal levels in OLETF after PR, Furthermore, comparing our previous measures of hepatic glucogenic enzyme expressions with the current metabolomics data suggests that the lack of detectable changes in protein expression do not accurately reflect the dynamic changes in gluconeogenesis, which puts more of an onus on metabolomics analyses such as these to better complement the molecular data. Additionally, these shifts in lipolysis and gluconeogenesis following PR may highlight the potential detriment of mass recovery, even if only partial as demonstrated here, after CR in an insulin resistant state, as the amelioration of the hyperglycemia with CR may be re-established from the combination of *de novo* glucose synthesis in the liver [34] and impaired glucose uptake from peripheral tissues [35, 36]. If so, this emphasizes the importance of maintaining the reduced body mass after CR as even partial recovery of body mass independent of adiposity has the potential to induce detrimental shifts in glucose metabolism that revert to an insulin resistant, hyperglycemic condition.

3.6.3 Plasma lipids are better correlated to IRI in a non-insulin resistant state than glucose metabolism intermediates

The lack of an inverse correlation between IR and circulating fatty acids (i.e. products of lipolysis) in an insulin resistant state in the present study may be explained by previous findings where insulin was unable to suppress lipolysis in an insulin resistant state compared to an insulin sensitive condition [37]. This is supported by the lack of changes in plasma lipids in OLETF after CR, even though we previously showed that CR improved IRI in OLETF suggesting that this improvement is largely driven by improvements in glucose metabolism independent of improved lipid metabolism. While an association between long-chain fatty acids and insulin sensitivity in obese, insulin resistant patients has been shown [38] that does not seem to apply during the early onset of insulin resistance in our model.

3.6.4 Proteolysis is more profound in OLETF than LETO, and is reversed after mass recovery

Normally, during negative caloric imbalance (i.e. CR) most of the amino acids generated after CR are either used by the liver for gluconeogenesis or by the muscle for energy production [39]. Consistent with these findings, we observed small but significant increases in several glucogenic amino acids, which translated into an overall increase in total amino acid concentration after CR in OLETF that returned to baseline levels after PR, but not in LETO. This increase in total amino acids suggests that lean tissue catabolism was increased and that these amino acids may be shuttled into gluconeogenesis to help support the changes in energetic demands. One advantage of this level

of CR, however, is that the increased availability of cysteine may increase the production of glutathione [40], thus reducing the overall oxidative damage caused by the insulin resistant state. The potential benefit of PR during an insulin resistant condition is that carbohydrates and lipids return as the primary sources of energy, sparing lean tissue via a reduction in proteolysis. However, the potential detriment of the shift in metabolism is the partial reversal of gluconeogenesis, which could translate into exacerbation of the hyperglycemia in insulin resistant OLETF demonstrating the risk of mass recovery after an acute caloric restriction independent of recovery of visceral adiposity. Furthermore, this highlights the importance of properly managing a caloric restriction regiment following the onset of insulin resistance to ameliorate inappropriately elevated lean tissue catabolism and the potential consequences of this shift in metabolism including an increase nitrogen load on the kidneys [41] and inappropriate muscle loss. These data suggest that a reduction in adipose *per se* may not be sufficient in the long term to improve IRI in an insulin resistant state when gluconeogenesis is inappropriately elevated.

In summary, severe acute caloric restriction was sufficient to elicit significant changes in several metabolic pathways in OLETF but not LETO, and a partial mass recovery comprised mostly by lean tissue reverted most of these changes to baseline levels with the exception of increased gluconeogenesis, and decreased lipolysis and amino acid catabolism. These shifts in substrate metabolism suggest that failure to adhere to this regiment could be detrimental in the long term due to the ability of metabolic shifts to adapt to changes in caloric intake.

Chapter 4. Simultaneous SGLT2 Inhibition and Caloric Restriction Improves Insulin Resistance and Kidney Function in OLETF Rats

4.1 Abstract

SGLT2 inhibitors (SGLT2i) are emerging as a novel therapy for T2DM due to its effective hypoglycemic and potential cardio- and nephron-protective effects, while caloric restriction (CR) is the first line of treatment to improve adiposity and insulin resistance. Previous data suggest that the simultaneous use of both treatments can further improve metabolic syndrome due to the suggested effect of SGLT2i on carbohydrate metabolism. In order to test this hypothesis, we subjected a cohort of 10-week old male Long Evans Tokushima Otsuka (LETO) and Otsuka Long Evans Tokushima Fatty (OLETF) rats to 4 weeks of 10 mg Luseoglifozin /kg/day (OLETF only) and/or 2 weeks of 30% CR at 12 weeks of age. CR maintained body mass in both strains while SGLT2i did not have any effect on body mass. Simultaneous treatment decreased SBP in OLETF vs SGLT2i alone, decreased insulin resistance index (IRI), and increased creatinine clearance vs OLETF Control. Conversely, CR decreased albuminuria independent of SGLT2i. In conclusion, SGLT2i treatment by itself did not elicit significant improvements in insulin resistance, kidney function or blood pressure. However, when combined with CR, these changes where more profound than with CR alone.

4.2 Introduction:

Sodium-glucose cotransporter 2 (SGLT2) is highly expressed in the renal proximal tubule and inhibition of SGLT2 decreases plasma glucose by increasing urinary excretion. For this reason, SGLT2 inhibitors (SGLT2i) are rapidly emerging as a novel therapy for T2DM **(1)**. When used in monotherapy, these inhibitors present low risk for hypoglycemia, preserved islet mass, and improved insulin sensitivity **(2).** Current data suggest that cardiovascular health is improved as well; however, the use of this drug is not advised in the event of low-carbohydrate diets, extreme insulin deficiency, or cachexia **(3).** However, it is also suggested that chronic SGLT2 inhibition can cause metabolic adaptations similar to those observed in aestivation, which is characterized by increased amino and fatty acid utilization as sources of energy while reducing metabolic rate **(4).**

A low carbohydrate diet (LCHD) with simultaneous SGLT2i in non-diabetic rats resulted in a reduction in HOMA-IR, but not LCHD alone, suggesting that a compensatory increase in liver (and potentially kidney) gluconeogenesis induced by chronically reduced dietary carbohydrate may have masked the effects. Moreover, treatment with a SGLT1/2i reduced hepatic glycogen content and glucose production independent of changes in gluconeogenic enzymes or GLUT2 abundance in T2D mice **(5)** suggesting that inhibition of SGLT2 may alter hepatic glucose metabolism and glucose homeostasis via multiple pathways, some of which have not been identified to date. Additionally, reduction in carbohydrate consumption further reduced the SGLT2i-induced glycosuria **(6)** suggesting that simultaneous nutritional intervention and SGLT2i could potentially alter glucose homeostasis. However, the effects of chronic SGLT2i on gluconeogenesis are not well-described especially in relation to altered nutritional intake.

Moreover, 30% caloric restriction (CR) or SGLT2i resulted in a similar decrease in fasting blood glucose and albuminuria over time compared to untreated, strain controls and correction of the overexpression of tricarboxylic acid (TCA) intermediates in BTBR ob/ob mice **(7);** however, the effects of combined treatments were not examined. SGLT2i treatment in diet-induced obesity increased muscle AMPK phosphorylation in a dose-dependent manner, which may facilitate increased fatty acid oxidation in muscle **(8).** These findings are consistent with a reduction in carbohydrate oxidation and an increase in lipolysis and ketogenesis found in T2DM patients on

SGLT2i therapy that was proportional to the duration of the therapy **(9).** Collectively, these studies suggest that altered glucose metabolism during treatment with SGLT2i during conditions of metabolic derangement may alter lipid and protein metabolism as well.

Furthermore, applying metabolomic analyses demonstrated that 12 weeks of SGLT2i treatment in patients with T2DM or non-alcoholic liver disease improved metabolic pathways related to energy metabolism, and mitochondrial and endothelial function suggesting that impaired SGLT2 activity associated with metabolic defects contributes to a decline in kidney function **(10).**

Severe (70%), long-term (7 wks) caloric restriction **(11)** and chronic SGLT2i treatment (3 mo) **(12)** improved glucose tolerance and reduced proteinuria and glomerular damage in rat models of metabolic derangement (OLETF and T2DN, respectively); however, the potential benefits following more acute interventions of either or combined have not been examined during similar conditions. Therefore, we hypothesized that acute (10 d), mild caloric restriction (30%) combined with SGLT2i treatment will improve insulin resistance and kidney function and injury associated with improved glucose metabolism without inducing hypoglycemia. Furthermore, studies of the potential benefits of SGLT2i and/or CR in a model of metabolic syndrome (MetS), which is more complicated than T2D alone, are scarce, and those examining the combined effects are unrealized.

4.3 Methods

The Animal Experimentation Ethics Committee at Kagawa University, Kagawa, Japan approved the experimental protocols (ID: 21614). All experimental procedures were conducted in accordance with the guidelines for care and use of animals established by Kagawa University.

4.3.1 Animals

Male, lean strain-control, Long Evans Tokushima Otsuka (LETO) (n = 15) and obese, insulin resistant Otsuka Long Evans Tokushima Fatty (OLETF) (n = 29) rats (Otsuka Pharmaceutical Co., Ltd., Tokushima, Japan) were fed *ad libitum* with standard laboratory rat chow (MF; Oriental Yeast Corp., Tokyo, Japan) until 10 weeks of age. Both strains of rats were matched for age throughout the study. OLETF rats were then randomly assigned to either (1) untreated (n=14; equivalent volume of saline solution (0.9%) x 4 wks) or (2) SGLT2i treated (n=15; 10 mg luseogliflozin/kg/d x 4 wks by gavage) groups. Luseogliflozin was dissolved in deionized water (0.25% w/v) prior to dosing. At 12 wks of age, LETO rats were randomly assigned to either (1) untreated, *ad libitum*-fed, strain controls (LETO Ctrl; n=8) or (2) untreated, calorie restricted (LETO CR; n=7; 30% CR x 2 wks) groups. Likewise, both OLETF groups were randomly assigned to (1) untreated, *ad libitum*-fed, within-strain controls (OLETF Ctrl; n=8), (2) SGLT2i treated, *ad libitum*-fed (OLETF SGLT2i; n=7), (3) untreated, 30% CR (OLETF CR; n=7), or (4) SGLT2i treated + 30% CR (OLETF SGLT2i CR; n=7). SGLT2 inhibitors were developed to ameliorate the consequences of T2D, thus there is no expectation that SGLT2i would be prescribed to healthy, non-diabetic individuals. Therefore, providing SGLT2i to the healthy LETO rats would not provide further insights to the undiscovered, biomedical benefits of such a treatment during metabolic derangement, which is a principal outcome of the present study. Although we recognize the potential to enhance our knowledge of the basic biology of the SGLT2 transporter by providing the inhibitor to healthy animals, the focus of the present study was on the biomedical implications during a condition of impaired glucose metabolism, which is associated with metabolic syndrome, for which the drug was produced. Thus, our study design controls for both the CR and SGLT2i during the metabolic syndrome. All animals were maintained in groups of two animals per cage for the entire study to minimize stress **(13)** except during CR, which was necessary to ensure the appropriate degree of CR. *Ad libitum* food intake per rat was calculated as the mean intake for double occupancy cages. Two days before oral glucose tolerance test (oGTT), all animals were

transferred to metabolic cages for 24 h to collect urine for further biochemical analyses, while maintaining their previous level of food intake. Animals were maintained in a specific pathogen-free facility under controlled temperature (23◦C) and humidity (55%) with a 12:12 light-dark cycle. All animals were given free access to water for the entire study.

4.3.2 Blood Pressure.

Systolic blood pressure (SBP) was routinely measured in triplicate in conscious rats by tail-cuff plethysmography (BP- 98A; Softron Co., Tokyo, Japan) (n = 6/group) as previously described **(14-16)**. Rats were acclimated to the restraint tube prior to measurements. Measurements were made every other day after treatment for the entire study. Repeated measures with a percent coefficient of variability (CV) >15% were excluded. Measurements were averaged by week and analyzed by one-way ANOVA.

4.3.3 oGTT.

oGTTs were performed in all animals at 14 wks of age as previously detailed in our hands **(14).** Briefly, a 2 g/kg glucose bolus was given by gavage to overnight-fasted (14+ h) rats. Blood was collected via the caudal vein before gavage and at 5, 10, 30, 60, and 120 min.

4.3.4 Dissections.

Three days after oGTTs, animals were fasted overnight, and tissues collected the subsequent morning. After body mass (BM) measurements were obtained, animals were anesthetized with 100 mg pentobarbital/kg i.p. and arterial blood was collected via the abdominal aorta into chilled vials containing 500 mM EDTA and 1600 KIU aprotinin. Vials were kept on ice until centrifuged (3,000*g* x 15min at 4°C), and the plasma was transferred to cryo-vials and immediately stored at −80°C. Systemic perfusion with chilled PBS was performed via the same artery with an incision in the inferior vena cava as the exit point and proceeded until no blood was present. Thereafter, liver, heart, pancreas, kidneys, gastrocnemius muscle, and epididymal and retroperitoneal fat depots were rapidly removed, weighed, and snap frozen in liquid nitrogen. Frozen samples were kept at −80°C until analyzed.

4.3.5 Biochemical Analyses.

Plasma creatinine, and urine glucose, creatinine, albumin, Na^+ and K^+, were measured using a Hitachi 7020 chemistry analyzer (Diamond Diagnostics, Massachusetts, USA). Serum Na^+ and K^+ measurements were outsourced to a local commercial lab (Central Valley Diagnostic Lab, Merced, CA, USA). Plasma insulin was measured using commercially available ELISA kits (Wako, Osaka, Japan). Liver glucose (Wako, Osaka, Japan), glycogen (Cell Biolabs, San Diego, USA), and glucose-6-phosphate (G6P) content, and hexokinase (HK) activity (Sigma-Aldrich, St. Louis, USA) were measured by commercially available colorimetric kits, with values normalized to total protein (TP) content. All samples were analyzed in duplicate and run in a single assay with intra-assay percent CV of <10% for all assays. Creatinine clearance (C_{cr}) was calculated to estimate glomerular filtration rate (GFR) as:

C_{cr} (mL/min) = urine creatinine (mg/dL) x urine flow (mL/min)/plasma creatinine (mg/dL) **(17).** Fractional excretion of Na^+ and K^+ ($FE_{[x]}$) was calculated as:

FE (%) = (urinary excretion of [x] (mEq/min)/C_{cr} (ml/min) x serum [x] (mEq/ml)) * 100

4.3.6 Protein Expression by Western Blot.

Homogenates of gastrocnemius muscle and liver were separated into cytosolic and plasma membrane fractions. The cytosolic fraction was obtained by homogenizing 15-25 mg of tissue in 200 µl KPi buffer containing 1% protease and 3% phosphatase inhibitor cocktail (Sigma-Aldrich, St. Louis, USA) and centrifuging (15,000 rpm x 15 min) to separate. The pellet was then homogenized and sonicated (20 s) in 150 µl KPi buffer with 1% Tween-20, 1% protease and 3% phosphatase inhibitor cocktail, and centrifuged in the same conditions to extract the membrane fraction. The purity of the fractions was assessed by measuring fraction-specific proteins (α-tubulin for cytosol and Na^+-K^+ATPase for membrane). Supernatant total protein content was measured by Bradford assay (Bio-Rad Laboratories, Hercules, CA).

Predetermined amounts of total protein (TP) were resolved in a 10% Tris-HCl SDS gel. Proteins were electroblotted using the Invitrogen™ Mini Blot module onto a 0.45µm Inmovilon-FL polyvinylidene difluoride (PVDF) membrane for 1 h at 20V. Membranes were blocked 1 h with Odissey blocking buffer (TBS) and incubated 16 h at 4°C with primary antibodies diluted in TBS with 0.2% Tween-20 targeted against GLUT2 **(18)** (1:1000 dilution, 20 µg TP) , G6Pc **(19)** (1:500 dilution, 40 µg TP) , PCK1 **(20)** (1:4000 dilution, 6 µg TP) , AMPK **(21)** and p-AMPK **(22)** (1:1000 dilution, 40 µg TP), Akt **(23)** and p-Akt **(24)** (1:1000 dilution, 30 µg TP), IR **(25)** (1:1000 dilution, 12.5 µg TP), GLUT4 **(26)** and p-GLUT4 **(27)** (1:1000 dilution, 8 µg TP), α-tubulin **(28)** (1:40,000 dilution, 5-20 µg TP), and Na^+-K^+ATPase **(29)** (1:40,000 dilution, 5-20 µg TP). Membranes were washed with TBS with 1% Tween-20 and incubated for 1 h with a secondary antibody (LI-COR Biosciences, Lincoln, USA) diluted 1:20,000 in TBS with 0.2% Tween-20 and 0.1% SDS, rewashed and visualized using a Li-Cor Odissey Imaging System.

4.3.7 Metabolomic Analysis.

Aliquots of plasma (n=6-7/group) were analyzed for primary carbon metabolites by gas chromatography (GC) time-of-flight (TOF) mass spectrometry (MS) data acquisition and processed at the NIH West Coast Metabolomics Center at UC Davis as previously described **(30)**, generating a dataset of 136 consistently identified metabolites. Data were reported as the mTIC normalized **(31)** quantitative ion peak heights of all structurally annotated compounds. Data was rank transformed **(32)** as previously described **(33).** Student's t-test was performed in 9 previously selected pairwise comparisons (**Table 9)** and Benjamini-Hochberg False Discovery Rate (FDR) correction **(34)** q-values were calculated for each metabolite per comparison. Fold changes were calculated per comparison as mean group B / mean group A, after mTIC normalization. Network maps were plotted per comparison using MetaMapp **(35)** and visualized in Cytoscape 3.7.1. Raw and transformed data can be found in the following repository: https://doi.org/10.6084/m9.figshare.14403935.v1

4.3.8 Statistics.

Means (±SE) were compared by one-way ANOVA, with the Holm-Sidak method for post-hoc multiple comparison after excluding outliers by extreme studentized deviate test with $\alpha = 0.05$. Glucose tolerance was assessed by comparing mean AUC values obtained from the glucose profiles during the oGTT. The accompanying AUCs of the insulin response during the GTT were also calculated. The AUC values were also compared by one-way ANOVA. The insulin resistance index (IRI) was calculated as the product of $AUC_{glucose}$ and $AUC_{insulin}$ divided by 100 as previously described **(14, 36)** and used to assess the effects on MetS-associated insulin resistance observed in OLETF. Relationships between dependent and independent variables were evaluated by simple regression, except for insulin, where a 4th order regression was used. Correlations were evaluated using Pearson correlation coefficients. Means, regression, and correlations were considered

significantly different at $p < 0.05$. Statistical analyses were performed with JMP 15 software (Cary, USA).

4.4 Results

4.4.1 CR Blunts the Incremental Increase in BM and Is Not Altered Further with SGLT2i

Slope analysis was performed to better appreciate the impacts of all the treatments on the changes in BM **(Figure 14).** Between 7 and 10 wks of age (before starting treatments), the incremental increase in BM was significantly greater ($p = 0.031$) in OLETF (8.8 ± 0.8 g/d, $r^2 = 0.99$) compared to LETO (5.8 ± 1.0 g/d, $r^2 = 0.99$). After 10 wks of age, mean incremental increase was not significantly different ($p = 0.962$) between LETO control (3.8 ± 0.3 g/d, $r^2 = 0.98$) and OLETF control (4.6 ± 0.9 g/d, $r^2 = 0.98$). The incremental change in BM in LETO CR (-1.1 ± 0.9 g/d, $r^2 = 0.60$) was lower ($p = 0.003$) compared to LETO control. CR in OLETF without (-0.1 ± 1.1 g/d, $r^2 = 0.04$) and with SGLT2i (-0.9 ± 1.5 g/d, $r^2 = 0.16$) decreased ($p < 0.001$) the incremental change in BM compared to OLETF control, and the slopes between the two CR groups were not different ($p = 0.995$). In *ad lib*-fed OLETF, the incremental increases in BM without SGLT2i (4.6 ± 0.9 g/d, $r^2 = 0.98$) was the same ($p = 1$) compared to OLETF SGLT2i (4.6 ± 0.7 g/d, $r^2 = 0.98$). The relatively low coefficients of determination (r^2) and shallower slopes in all the CR groups suggest that BM was maintained relatively constant (incremental increase blunted) rather than reduced over time.

4.4.2 Simultaneous SGLT2i and CR Reduced MetS-induced Increase in SBP

Before the SGLT2i treatment at 9 wks of age, SBP was higher ($p < 0.001$) in OLETF (140 ± 3 mmHg) compared to LETO (118 ± 5 mmHg) confirming the MetS-induced increase in SBP **(Figure 15)**. At the end of the study, CR did not change SBP in either LETO ($p = 0.995$) or OLETF ($p = 0.985$). Moreover, SGLT2i without CR did not alter SBP in OLETF ($p = 0.931$). However, the simultaneous treatment of SGLT2i and CR decreased ($p = 0.038$) SBP compared to OLETF SGLT2i without CR by the end of the study.

4.4.3 Simultaneous SGLT2i and CR Improved MetS-associated Insulin Resistance Index

Glucose tolerance tests with corresponding insulin measurements and subsequent IRI calculations were performed to quantify the functional metabolic effects of both treatments alone and in combination. Mean glucose peak during oGTT (at 30 min) was reduced by 27% in OLETF SGLT2i CR rats compared to OLETF CR ($p = 0.022$) **(Figure 16A).** Mean $AUC_{glucose}$ was 97% higher ($p < 0.001$) in OLETF compared to LETO and was not reduced by either SGLT2i or CR alone; however, the OLETF SGLT2i CR group was not different from LETO CR suggesting that the simultaneous treatment tended to decrease $AUC_{glucose}$ **(Figure 16B).** There were no significant differences in basal insulin between strains. However, mean basal insulin was 44% lower in OLETF SLGT2i CR compared to OLETF CR ($p = 0.018$) and OLETF SGLT2i control ($p = 0.008$) **(Figure 16C)**. Moreover, neither of the treatments elicited a change in $AUC_{insulin}$ in OLETF. $AUC_{insulin}$ was 33% lower in LETO CR compared to OLETF CR ($p = 0.041$) **(Figure 16D).** Mean IRI was 98% greater ($p < 0.001$) in OLETF vs LETO and was nor reduced by SGLT2i or CR alone. However, the combined treatments reduced ($p = 0.019$) mean IRI in OLETF by 33% compared to CR alone **(Figure 16E).** At 14 wks of age, basal fasting blood glucose concentrations were 35% greater ($p < 0.001$) in *ad lib*-fed OLETF compared to *ad lib*-fed LETO. Neither treatments reduced basal fasting blood glucose concentrations in either strain. SGLT2i treatments in OLETF did not reduce static fasting blood glucose concentrations. However, CR in LETO increased ($p = 0.024$) basal glucose:insulin ratio by 66% **(Table 7).**

4.4.4 CR Reduced SGLT2i-induced Glycosuria

Urinary glucose excretion was minimally detectable (< 2 mg/d) in all non-SGLT2i-groups without significant differences between strains. CR reduced ($p < 0.001$) the SGLT2i-induced glycosuria by 64% in OLETF **(Figure 17)**. The robust glycosuria observed in the SGLT2i groups provides evidence of the drug's effectiveness.

4.4.5 CR Increased Urinary Na^+:K^+ Ratio and Decreased Fractional Excretion of K^+ (FE_{K+}) in OLETF

LETO CR had increased serum Na+ concentration compared to OLETF CR ($p = 0.021$), without significant changes with either CR or SGLT2i. Neither treatment alone or in combination changed urinary electrolyte excretion; however, CR increased ($p < 0.001$) urinary Na^+/K^+ ratio by 90% in OLETF. LETO control had higher FE_{Na+} compared to OLETF CR ($p = 0.029$) and OLETF SGLT2i CR ($p < 0.001$). Moreover, FE_{Na+} decreased in OLETF CR ($p = 0.003$) and OLETF SGLT2i CR ($p = 0.008$) compared to OLETF SGLT2i control. **(Table 8).**

4.4.6 CR Improved Albuminuria ($U_{alb}V$) and CR with SGLT2i Increased Creatinine Clearance (C_{cr}) in OLETF

Albuminuria was 15.6-fold greater ($p < 0.001$) in OLETF compared to LETO characteristic of the renal injury associated with the strain **(Figure 18).** Although SGLT2i alone did not reduce the albuminuria in OLETF, CR reduced mean $U_{alb}V$ by 74% ($p = 0.003$) and by 61% ($p = 0.009$) with SGLT2i **(Figure 18).** No profound changes in plasma creatinine were detected among the groups although levels tended to decrease ($p = 0.062$) with the combined treatment compared to OLETF SGLT2i. (**Figure 19A**). Urinary creatinine excretion ($U_{crt}V$) was 31% greater (P=0.001) in OLETF compared to LETO, and levels were similarly elevated with CR and/or SGLT2i **(Figure 19B).** Combined treatment in OLETF increased ($p = 0.015$) C_{cr} by 71% compared to LETO CR (**Figure 19C**), which is reflective of the trending decrease in plasma creatinine in this group.

4.4.7 CR and SGLT2i Increased Liver Gluconeogenesis in OLETF, while CR Reduced Glycolysis in LETO, and SGLT2i in OLETF.

We measured glucose and glucose-6-phosphate (G6P) content in the liver, calculated the glucose:G6P ratio, and measured the cytosol content of the gluconeogenic enzymes G6Pc and PCK1, and GLUT2 translocation for hepatic glucose release. Conversely, we measured hexokinase (HK) activity, as this is the first committed step in glycolysis. Mean hepatic glucose content was similar between *ad libitum* fed groups. However, glucose content increased by 102% in OLETF SGLT2i CR vs OLETF SGLT2i (P=0.007) **(Figure 20A)**. Mean hepatic G6P was two-fold higher in OLETF vs LETO with *ad libitum* diet (P=0.016), and 146% higher with CR (P=0.022). However, OLETF treated with SGLT2i had similar hepatic G6P content compared to LETO, independent of CR **(Figure 20B)**. This translated into an increased glucose:G6P ratio of 1.1±0.2 in OLETF SGLT2i CR vs 0.4±0.1 in OLETF control (P=0.007) and 0.6±0.2 in OLETF SGLT2i (P=0.042) **(Figure 20C)**. Nonetheless, there was no significant difference in hepatic glycogen content in any of the groups (**Figure 20D).** Mean hexokinase activity decreased 45% in OLETF control (P=0.019) and 48% in OLETF SGLT2i control (P=0.008) compared to LETO control. Moreover, CR decreased hexokinase activity by 68% in LETO (P<0.001) and OLETF SGLT2i CR had a 68% lower activity compared to OLETF CR (P=0.004) **(Figure 20E).** Although mean G6Pc was higher in OLETF vs LETO, this difference was not significant ($p = 0.628$). Neither CR nor SGLT2i changed G6Pc expression in OLETF; however, CR increased expression by over 5.5-fold in LETO (P=0.01) **(Figure 20F)**. On the other hand, PCK1 expression increased in OLETF CR vs OLETF control (107% vs 81%, P=0.048) **(Figure 20G).** GLUT2 translocation to the membrane did not

change between strains or with CR or SGLT2i alone. However, membrane GLUT2 translocation increased to 173% in OLETF SGLT2i CR vs 83% in OLETF SGLT2i control (P<0.001) and 87% in OLETF CR (P<0.001) **(Figure 20H).**

4.4.8 SGLT2i Decreased Insulin Receptor Expression and Increased Akt Phosphorylation in OLETF Independent of Changes in GLUT4 Translocation or Phosphorylation in Gastrocnemius Muscle

Given that skeletal muscle is the primary site of glucose clearance and could partially explain the increase in glucose tolerance, we measured insulin receptor (IR) expression as increased translocation is inversely correlated to receptor phosphorylation, and thus, linked to insulin resistance. In addition, we measured the phosphorylation of AMPK (pAMPK) and Akt (pAkt) as these are downstream events of IR activation. We also measured GLUT4 translocation, correlated to higher glucose absorption, and GLUT4 phosphorylation, which facilitates the receptor endocytosis. Relative IR expression was increased by over 2.3-fold (P=0.011) in OLETF control compared to LETO control; however, SGLT2i treatment reduced IR by 104% (P=0.029). CR increased IR in LETO and OLETF SGLT2i; however, these changes were not significant **(Figure 21A)**. AMPK expression was consistent among groups **(Figure 21B)** and SGLT2i did not significantly alter pAMPK. However, pAMPK increased by 56% (P=0.002) in OLETF CR and 44% (P=0.019) in OLETF SGLT2i CR compared to OLETF control **(Figure 21C)**. Despite these changes, the p-AMPK:AMPK ratio did not change significantly amongst groups **(Figure 21D).** Relative Akt expression increased by 54% (P=0.022) in OLETF CR compared to control without basal changes between strains **(Figure 21E)**. On the other hand, pAkt doubled (P=0.026) in OLETF SGLT2i compared to LETO control **(Figure 21F)** This difference was more pronounced after calculating the p-Akt:Akt ratio, also showing a significant difference vs OLETF control (2.3 ± 0.4 vs 1.0 ± 0.0, P=0.022) **(Figure 21G)**. These changes were not observed with CR. No significant differences in GLUT4 translocation nor phosphorylation were detected among the groups **(Figure 21H-J).**

4.4.9 CR Increased Primary Carbon Metabolite Differences between Strains while CR and SGLT2i Treatments Combined Increased Different Carboxylic Acids in OLETF compared to SGLT2i

CR did not induce significant shifts in the metabolome in LETO or OLETF **(Figure 22A and D)**, with SGLT2i alone in OLETF **(Figure 22E)** or CR alone **(Figure 22G),** except for a decrease in glyceric acid with CR (1.9-fold, q=0.027) and CR + SGLT2i (1.6-fold, q=0.159) in OLETF. However, at basal levels, OLETF had a higher plasma concentration of oleic acid (4.8-fold, q=0.102), ribitol (2.2-fold, q=0.005) and ribose (1.9-fold, q=0.031) compared to LETO. **(Figure 22B)**. This difference was accentuated when comparing both strains after CR, where OLETF had higher concentrations of the carbohydrates glucose (1.3-fold, q=0.158), ribitol (3.1-fold, q<0.001), ribose (2.4-fold, q<0.001), xylulose (1.2-fold, q=0.138), and sorbitol (1.7-fold, q=0.126), the fatty acids, oleic (2.2-fold, q=0.091) and palmitoleic (1.9-fold, q=0.049), and phenylethylamine (2.4-fold, q=0.126) and tyrosine (6.5-fold, q=0.010). On the other hand, OLETF CR had lower concentrations of compounds related to amino acid metabolism including putrescine (22.2-fold, q=0.153), glycine (2.1-fold, q<0.001) and urea (1.3-fold, q=0.072), and the fatty acids, azelaic acid (2-fold, q=0.091), heptadecanoic acid (1.5-fold, q<0.001), octadecanol (1.6-fold, q=0.126), and stearic acid (1.4-fold, q=0.060), and cholesterol (1.2-fold, q=0.111) compared to LETO CR **(Figure 22C)**. Moreover, combined treatments in OLETF increased the carboxylic acids, cinnamic (4.8-fold, q=0.106), nicotinic (3.5-fold, q=0.155), and salicylic (4.4-fold, q=0.129), and levoglucosan (1.5-fold, q=0.147) and succinate semialdehyde (3-fold, q=0.122), precursors of glucose and succinic acid, respectively, compared to OLETF SGLT2i. Conversely, the concentrations of oleic

(6-fold, q=0.155) glucuronic (1.7-fold, q=0.155), and glutaric acids (1.6-fold, q=0.155), and phenylalanine (1.7-fold, q=0.182), putrescine (1.6-fold, q=0.155), and valine (1.3-fold, q=0.155) were lower in OLETF SGLT2i CR vs OLETF SGLT2i alone **(Figure 22I)**.

4.5 Discussion

4.5.1 SGTL2i therapy does not further improve CR mediated body mass

Slope analysis of body mass changes over time revealed that SGLT2i did not significantly alter CR-induced decrease in BM in the OLETF animals. Previous studies have suggested that SGTL2i may decrease BM initially due to increased diuresis, which we did not observe in our study. If so, we calculated that it would take months for the glycosuria-mediated caloric deficit to actually reduce body mass **(37).** Other studies suggest that SGLT2i either increased fatty acid metabolism and/or reduced lipogenesis in diet-induced obese rats, decreasing liver and adipose mass **(38),** which could ultimately reduce BM but likely beyond the duration of the time frame of our study duration**.** However, the maintenance of body mass despite the combined treatments suggests that, at least in our model, there are other mechanisms balancing the caloric deficit caused by the glycosuria.

4.5.2 Combined SGLT2i and CR treatment has potential anti-hypertensive and nephroprotective effects

Several clinical trials have shown a modest but consistent reduction of SBP in SGLT2i treated patients compared to other antidiabetic drugs after one to two weeks of treatment. However, this reduction is attributed to an osmotic diuresis rather than natriuresis **(39).** This is confirmed by our urinary results, where FE_{Na+} and $U_{Na+}V$ were unaffected by SGLT2i. In our study, SLGT2i or CR alone did not reduce SBP significantly. Additionally, FE_{K+} tended to increase with SGLT2i alone suggesting that a potential downstream effect on Na^+-K^+ exchange in the distal tubule was induced but minimally **(40)**. However, when comparing exclusively the combined treatment in OLETF to the untreated control group at the end of the study, we observed a significant reduction in SBP comparable to that previously reported in the literature **(41)** suggesting that longer duration treatments could have had a more robust effect on SBP**.**

In this study we also assessed basal renal function between strains, as the OLETF model develops nephropathy over time **(42),** with marked proteinuria after 25 weeks of age **(43)**, and impaired function may diminish the benefits of SGLT2i inhibition. Moreover, previous clinical studies revealed that SGLT2i decreased urinary albumin-to-creatinine ratio, a marker of diabetic nephropathy (DN) **(44).** In our study, we observed increased albuminuria in the OLETF compared to the LETO, which was ameliorated with CR, independent of treatment with SGLT2i. The maintenance of plasma creatinine concentration across groups suggests that, at this stage of the MetS, the renal injury was not sufficient to reduce kidney function. These observations reinforce the notion that CR has potential nephroprotective effects, especially when accompanied by a net decrease in protein intake **(45),** which would be associated with the CR in the present study**.** However, independent of the CR-associated benefits on glomerular injury **(46, 47)**, the nephron-protective effects were not further enhanced with SGLT2i in our model suggesting that the suite of defects associated with MetS prohibit further improvements in the condition with the combined treatments. This is significant because it re-enforces the idea that early detection and intervention are critical to maximize the effectiveness of treatments when combating the multitude of defects that are associated with MetS.

4.5.3 Urinary glucose excretion was proportional to caloric intake and independent of fasting glucose

We measured 24 h glucose excretion to assess the efficacy of the SGLT2i treatment. Although fasting glucose concentration was not different between the untreated OLETF and SGLT2i treated rats, excreted glucose was several magnitudes higher in the SGLT2i treated groups compared to the others, clearly indicating the effectiveness of the drug. A negligible amount of excreted glucose was detected in the other groups, consistent with our previous results from similarly aged rats **(48),** demonstrating that the severity of the glomerular injury at this stage of the disease is not sufficient to induce robust glycosuria. Interestingly, the reductions in excreted glucose with CR did not translate to detectable changes in fasting glucose. These data may seem to conflict with previous findings where fasting serum glucose in dapagliflozin-treated patients was positively correlated with cumulative urine glucose **(49).** Moreover, results from SGLT2-deficient mice suggest that an increase in caloric intake and/or a potential increase in glucose absorption via SGLT1 would be sufficient to normalize blood glucose and maintain body mass similar to wild type mice, without changes in electrolytes, blood pressure, or GFR **(50)**. Furthermore, OLETF rats have an increased intestinal expression of SGLT1 compared to LETO rats **(51)**, which may partially explain the differential responses and lack of glycosuria-induced decrease in fasting blood glucose**.** We propose that compensatory mechanisms including an increase in SGLT1-mediated systemic absorption and release of hepatic glucose stores were sufficient to maintain circulating levels. Ironically, intact and fully functional compensatory mechanisms despite the insulin resistant condition may prohibit the combined therapies from ameliorating the strain-associated hyperglycemia.

4.5.4 Combined treatments improved the insulin resistance independent of IR or Akt activation in skeletal muscle

Insulin resistance index, a surrogate measure for systemic insulin resistance in the pre-diabetic state, was reduced by the combined treatments. We measured IR expression as well as AMPK and Akt phosphorylation in skeletal muscle to help elucidate mechanisms associated with insulin signaling **(52).** Moreover, impaired IR, and by consequence, Akt activation, decrease glucose infusion rate (a measure of insulin sensitivity) and endogenous glucose production **(53).** Although we measured insulin receptor expression (specifically in the membrane) rather than phosphorylation, previous studies with 30% CR in Fischer 344 x Brown Norway showed that glucose uptake was increased in slow and fast twitch muscle via increased Akt phosphorylation independent of insulin receptor (IR) phosphorylation **(54).**

However, the increase in insulin sensitivity could not be completely explained by the decrease in insulin receptor expression or Akt activation in the muscle, as these changes paradoxically occurred only after treatment with SGLT2i alone, but not with the combined treatment. Although Akt phosphorylation was not increased in the CR groups, 40% CR stimulated Akt2 phosphorylation, thus was isoform specific **(55),** which was associated with increased GLUT4 translocation (**56, 57**). Nevertheless, our results suggest that SGLT2i, rather than CR, may be more beneficial in activating total Akt.

A previous study with 30% CR in OLETF showed stable levels of fasting glucose and circulating glucose over time, even after 42 weeks of age, reportedly due to a higher expression and translocation of adipocyte GLUT4 in the CR group **(58).** In our study, however, GLUT4 translocation in the muscle was not different across groups. One distinction of our study, however, is that we measured GLUT4 in the fasted state when adaptation to the perturbation may have already occurred and not post-prandially, which would have stimulated a potential response. The potential changes in postprandial GLUT4 translocation are dependent of acute insulin stimulation

and at baseline (i.e. fasted state) the rate of GLUT4 endocytosis may exceed exocytosis **(59).** Nonetheless, our data confirms that the rate of GLUT4 translocation is similar in both strains regardless of treatment in the fasted state. Furthermore, the improvements in insulin resistance index observed with CR and SGLT2i as calculated from the oGTT data suggest that insulin signaling and GLUT4 translocation (and potentially GLUT2 in those tissues) at the time of the GTT were enhanced and that these changes were not captured by the end of study analyses.

4.5.5 30% CR did not induce proteolysis and elicited more changes in the metabolome compared to SGLT2i alone

In our previous study, a 50% CR increased the concentration of several plasma amino acids along with an acute reduction in BM that could not be completely accounted for by the reductions in adipose and organ mass losses suggesting that lean BM loss and proteolysis where sufficient to contribute to total BM loss **(36).** In contrast, 30% CR with or without SGLT2i did not significantly increase plasma amino acid concentrations in OLETF but rather a modest decrease in glyceric acid, a product of glycogenolysis was detected suggesting that glycogen stores may have been depleted at this stage of the CR. Moreover, body mass was maintained during the entire CR intervention, regardless of treatment with SGLT2i. These changes suggest that the degree of CR was not sufficient to induce significant proteolysis in OLETF rats. Furthermore, the decrease in total adipose with CR suggests that lipolysis was increased and was sufficient to ameliorate the potential for promoting proteolysis (and thus lean tissue catabolism), which is beneficial to maintain lean tissue and ameliorate the nitrogen load on the kidneys especially in the presence of existing glomerular injury.

The present study demonstrates that the combined treatment of 30% CR with SGLT2i ameliorated insulin resistance and provided modest nephron-protective and anti-hypertensive benefits without the deleterious effects of sustained hypoglycemia and lean tissue catabolism.

Chapter 5. Conclusions and Future Directions

Caloric restriction, and by consequence, body mass loss, mostly in the form of adipose tissue, is one of the first lines interventions to improve insulin resistance and ameliorate metabolic derangements. However, despite the beneficial effects achieved by this intervention, several metabolic adaptations will arise including 1) decrease of RMR, 2) prioritization of lipolysis and gluconeogenesis, and 3) change in hormonal profile in order to increase caloric intake. These changes would thus facilitate the regain of body mass even with reduced caloric intake while abrogating any beneficial effect on insulin resistance.

Our data showed that severe caloric restriction (50%), even when maintained for a short period of time, can induce transient improvements in glucose tolerance and adiposity, however coupled with unintended lean tissue catabolism. These improvements were abrogated almost entirely even with partial body mass recovery, the majority of it being fat-free mass. Further metabolomics analysis confirmed an extensive lean catabolism and revealed that gluconeogenesis was reverted in the healthy condition, but not in the insulin resistant one, contributing to the reappearance of hyperglycemia after partial mass recovery. In contrast, a moderate caloric restriction (30%) by itself did not show a profound effect in glucose tolerance as 50%. Moreover, metabolomics analyses did not show metabolic shifts as profound as the observed with 50% CR. However body mass was maintained, with the added benefit of potential nephroprotective effects. It should be noted that the majority of CR studies in the literature report profound beneficial effects with prolonged, moderate (15-30%) CR.

Nonetheless, when SGLT2i was used in combination with CR, improvements in glucose tolerance and blood pressure were enhanced, while preserving a stable body mass. Although we described in this work the changes in glucose metabolism occurring in the liver and muscle after CR with SGLT2i, we were not able to pinpoint the exact mechanism that drives the improvements in blood pressure, which is an important question left open for future studies. Another limitation of this study is that we did not exanimated metabolic changes derived from body mass recovery. It would be interesting to explore this further in a future study.

Based on the findings presented in this work we can conclude that 1) even short term CR can elicit important metabolic changes that are proportional to the degree of CR, 2) CR has to be maintained in order to keep this improvements long term and 3) SGLT2i inhibition, though it does not improve glucose tolerance by itself, proved to be a great aid when used in combination with moderate CR without the risk of exacerbated lean tissue catabolism nor hypoglycemia. The latter point is important to consider, as it suggests that combining CR (up to a certain degree) with SGLT2 inhibition could have a higher therapeutical value than implementing both interventions as mutually exclusive.

Future directions

Lipid accumulation in the liver is linked to insulin resistance, especially TAG accumulation. However, there are several other classes of lipids that could potentially be linked to insulin resistance as well. We are currently analyzing preliminary data on how the hepatic lipid profile is different in the LETO compared to the OLETF rats, and how it changes after CR and PR. It will also be of interest to find any correlation between length of fatty acid chains and insulin resistance in this model, as long-chain fatty acids are a sign of incomplete β-oxidation and thus mitochondrial impairment.

In addition, we also performed a visceral lipectomy study in OLETF rats. The rationale behind this study was that excess visceral fat is linked with insulin resistance, in part due to hepatic lipotoxicity, and that by partially removing visceral fat depots, we would facilitate improvements in insulin sensitivity akin of those observed in CR, without the collateral loss of lean mass or profound metabolic adaptations. On this study we excised fat mass equivalent to the fat mass lost via 50% CR. The preliminary data showed that the improvement of insulin sensitivity does not develop immediately (2 days after, Lpx), but rather short term (10 days, Rec) after surgery, and that this improvement is similar to the one elicited by CR **(Figure 23)**. Therefore, it would be of interest to further examine the metabolic shifts that drive this improvement, and to contrast them with the ones shown previously to be caused by CR.

References

Chapter 1:

1. Menshikova E V., Ritov VB, Dube JJ, et al. Calorie Restriction-induced Weight Loss and Exercise Have Differential Effects on Skeletal Muscle Mitochondria Despite Similar Effects on Insulin Sensitivity. J Gerontol A Biol Sci Med Sci. 2017;73(1):81-87. doi:10.1093/gerona/glw328
2. Taylor R. Calorie restriction for long-term remission of type 2 diabetes. Clin Med J R Coll Physicians London. 2019;19(1):37-42. doi:10.7861/clinmedicine.19-1-37
3. Varkevisser RDM, van Stralen MM, Kroeze W, Ket JCF, Steenhuis IHM. Determinants of Weight Loss Maintenance: A Systematic Review. Vol 20.; 2019. doi:10.1111/obr.12772
4. Sarin H V., Lee JH, Jauhiainen M, et al. Substantial fat mass loss reduces low-grade inflammation and induces positive alteration in cardiometabolic factors in normal-weight individuals. Sci Rep. 2019;9(1):1-14. doi:10.1038/s41598-019-40107-6
5. Smith DL, Yang Y, Nagy TR, et al. Weight Cycling Increases Longevity Compared with Sustained Obesity in Mice. Obesity. 2018;26(11):1733-1739. doi:10.1002/oby.22290
6. Rogge MM, Gautam B. Biology of obesity and weight regain: Implications for clinical practice. J Am Assoc Nurse Pract. 2017;29:S15-S29. doi:10.1002/2327-6924.12504
7. Hall KD, Kahan S. Maintenance of lost weight and long-term management of obesity. Med Clin North Am. 2018;102(1):183-197. doi:10.1016/j.mcna.2017.08.012.Maintenance
8. Melby CL, Paris HL, Foright RM, Peth J. Attenuating the biologic drive for weight regain following weight loss: Must what goes down always go back up? Nutrients. 2017;9(5). doi:10.3390/nu9050468
9. Stubbs RJ, Hopkins M, Finlayson GS, Duarte C, Gibbons C, Blundell JE. Potential effects of fat mass and fat-free mass on energy intake in different states of energy balance. Eur J Clin Nutr. 2018;72(5):698-709. doi:10.1038/s41430-018-0146-6
10. Turicchi J, O'Driscoll R, Finlayson G, Beaulieu K, Deighton K, Stubbs RJ. Associations between the rate, amount, and composition of weight loss as predictors of spontaneous weight regain in adults achieving clinically significant weight loss: A systematic review and meta-regression. Obes Rev. 2019;(February):1-12. doi:10.1111/obr.12849
11. Mackie GM, Samocha-Bonet D, Tam CS. Does weight cycling promote obesity and metabolic risk factors? Obes Res Clin Pract. 2017;11(2):131-139. doi:10.1016/j.orcp.2016.10.284
12. Wing RR. Insulin sensitivity as a predictor of weight regain. Obes Res. 1997;5(1):24-29. doi:10.1002/j.1550-8528.1997.tb00279.x
13. Hjorth MF, Due A, Larsen TM, Astrup A. Pretreatment Fasting Plasma Glucose Modifies Dietary Weight Loss Maintenance Success: Results from a Stratified RCT. Obesity. 2017;25(12):2045-2048. doi:10.1002/oby.22004
14. Due A, Larsen TM, Mu H, et al. The effect of three different ad libitum diets for weight loss maintenance: a randomized 18-month trial. Eur J Nutr. 2017;56(2):727-738. doi:10.1007/s00394-015-1116-6
15. Crujeiras AB, Díaz-Lagares A, Abete I, et al. Pre-treatment circulating leptin/ghrelin ratio as a non-invasive marker to identify patients likely to regain the lost weight after an energy restriction treatment. J Endocrinol Invest. 2014;37(2):119-126. doi:10.1007/s40618-013-0004-2
16. Erez G, Tirosh A, Rudich A, et al. Phenotypic and genetic variation in leptin as determinants of weight regain. Int J Obes. 2014;35(6):785-792. doi:10.1038/ijo.2010.217

17. Wang P, Menheere PPCA, Astrup A, et al. Metabolic syndrome, circulating RBP4, testosterone, and SHBG predict weight regain at 6 months after weight loss in men. Obesity. 2013;21(10):1997-2006. doi:10.1002/oby.20311
18. Andreoli MF, Donato J, Cakir I, Perello M. Leptin resensitisation: A reversion of leptin-resistant states. J Endocrinol. 2019;241(3):R81-R96. doi:10.1530/JOE-18-0606
19. Vink RG, Roumans NJ, Mariman EC, Van Baak MA. Dietary weight loss-induced changes in RBP4, FFa, and ACE predict weight regain in people with overweight and obesity. Physiol Rep. 2017;5(21):1-11. doi:10.14814/phy2.13450
20. Tadokoro R, Iida T, Mikura K, et al. Factors involved in body weight loss and its maintenance in morbidly obese inpatients. Diabetol Int. 2020;11(1):41-48. doi:10.1007/s13340-019-00403-y
21. Martins C, Gower BA, Hunter GR. Baseline Metabolic Variables Do Not Predict Weight Regain in Premenopausal Women. Obesity. 2020;28(5):902-906. doi:10.1002/oby.22780
22. Nymo S, Coutinho SR, Rehfeld JF, Truby H, Kulseng B, Martins C. Physiological Predictors of Weight Regain at 1-Year Follow-Up in Weight-Reduced Adults with Obesity. Obesity. 2019;27(6):925-931. doi:10.1002/oby.22476
23. Thom G, McIntosh A, Messow CM, et al. Weight loss-induced increase in fasting ghrelin concentration is a predictor of weight regain: Evidence from the Diabetes Remission Clinical Trial (DiRECT). Diabetes, Obes Metab. 2020:1-23. doi:10.1111/dom.14274
24. Sumithran P, Prendergast LA, Delbridge E, et al. Long-Term Persistence of Hormonal Adaptations to Weight Loss. Obstet Gynecol Surv. 2012;67(2):91-92. doi:10.1097/ogx.0b013e318247c6f7
25. Mai K, Li L, Wiegand S, et al. An integrated understanding of the molecular mechanisms of how adipose tissue metabolism affects long-term body weight maintenance. Diabetes. 2019;68(1):57-65. doi:10.2337/db18-0440
26. Jokinen R, Rinnankoski-Tuikka R, Kaye S, et al. Adipose tissue mitochondrial capacity associates with long-Term weight loss success. Int J Obes. 2018;42(4):817-825. doi:10.1038/ijo.2017.299
27. Katula JA, Vitolins MZ, Rosenberger EL, et al. One-year results of a community-based translation of the diabetes prevention program: Healthy-Living Partnerships to Prevent Diabetes (HELP PD) project. Diabetes Care. 2011;34(7):1451-1457. doi:10.2337/dc10-2115
28. Beavers KM, Case LD, Blackwell CS, Katula JA, Goff DC, Vitolins MZ. Effects of weight regain following intentional weight loss on glucoregulatory function in overweight and obese adults with pre-diabetes. Obes Res Clin Pract. 2015;9(3):266-273. doi:10.1016/j.orcp.2014.09.003
29. Karschin J, Lagerpusch M, Enderle J, Eggeling B, Müller MJ, Bosy-Westphal A. Endocrine determinants of changes in insulin sensitivity and insulin secretion during a weight cycle in healthy men. PLoS One. 2015;10(2):1-17. doi:10.1371/journal.pone.0117865
30. Berger SE, Huggins GS, McCaffery JM, Jacques PF, Lichtenstein AH. Change in Cardiometabolic Risk Factors Associated With Magnitude of Weight Regain 3 Years After a 1-Year Intensive Lifestyle Intervention in Type 2 Diabetes Mellitus: The Look AHEAD Trial. J Am Heart Assoc. 2019;8(20):1-15. doi:10.1161/JAHA.118.010951
31. Wing RR, Espeland MA, Clark JM, et al. Association of weight loss maintenance and weight regain on 4-year changes in CVD risk factors: The action for health in diabetes (Look AHEAD) clinical trial. Diabetes Care. 2016;39(8):1345-1355. doi:10.2337/dc16-0509
32. Vink RG, Roumans NJ, van der Kolk BW, et al. Adipose Tissue Meal-Derived Fatty Acid Uptake Before and After Diet-Induced Weight Loss in Adults with Overweight and Obesity. Obesity. 2017;25(8):1391-1399. doi:10.1002/oby.21903

33. Roumans NJT, Vink RG, Fazelzadeh P, Van Baak MA, Mariman ECM. A role for leukocyte integrins and extracellular matrix remodeling of adipose tissue in the risk of weight regain after weight loss. Am J Clin Nutr. 2017;105(5):1054-1062. doi:10.3945/ajcn.116.148874
34. Zhyzhneuskaya S V., Al-Mrabeh A, Peters C, et al. Time course of normalization of functional β-cell capacity in the diabetes remission clinical trial after weight loss in type 2 diabetes. Diabetes Care. 2020;43(4):813-820. doi:10.2337/dc19-0371
35. Contreras RE, Schriever SC, Pfluger PT. Physiological and Epigenetic Features of Yoyo Dieting and Weight Control. Front Genet. 2019;10(December):1-12. doi:10.3389/fgene.2019.01015
36. Liang KW, Lee WJ, Lee I Te, et al. Regaining body weight after weight reduction further increases pulse wave velocity in obese men with metabolic syndrome. Med (United States). 2018;97(40). doi:10.1097/MD.0000000000012730
37. Rhee EJ, Cho JH, Kwon H, et al. Increased risk of diabetes development in individuals with weight cycling over 4 years: The Kangbuk Samsung Health study. Diabetes Res Clin Pract. 2018;139:230-238. doi:10.1016/j.diabres.2018.03.018
38. Kakinami L, Knaüper B, Brunet J. Weight cycling is associated with adverse cardiometabolic markers in a cross-sectional representative US sample. J Epidemiol Community Health. 2020;74(8):662-667. doi:10.1136/jech-2019-213419
39. Oh TJ, Moon JH, Choi SH, et al. Body-Weight Fluctuation and Incident Diabetes Mellitus, Cardiovascular Disease, and Mortality: A 16-Year Prospective Cohort Study. J Clin Endocrinol Metab. 2018;104(3):639-646. doi:10.1210/jc.2018-01239
40. El Ghoch M, Calugi S, Dalle Grave R. Weight cycling in adults with severe obesity: A longitudinal study. Nutr Diet. 2018;75(3):256-262. doi:10.1111/1747-0080.12387
41. Byrne NM, Sainsbury A, King NA, Hills AP, Wood RE. Intermittent energy restriction improves weight loss efficiency in obese men: The MATADOR study. Int J Obes. 2018;42:129-138. doi:10.1038/ijo.2017.206
42. Campbell BI, Aguilar D, Colenso-Semple LM, et al. Intermittent energy restriction attenuates the loss of fat free mass in resistance trained individuals. A randomized controlled trial. J Funct Morphol Kinesiol. 2020;5(1):1-12. doi:10.3390/jfmk5010019
43. Ooi SL, Pak S. Short-term Intermittent Fasting for Weight Loss: A Case Report. Cureus. 2019;11(January). doi:10.7759/cureus.4482
44. Cornejo MA, Nguyen J, Cazares J, et al. Partial Body Mass Recovery After Caloric Restriction Abolishes Improved Glucose Tolerance in Obese, Insulin Resistant Rats. Front Endocrinol (Lausanne). 2020;11(363):1-14. doi:10.3389/fendo.2020.00363
45. Rosenbaum JL, Frayo RS, Melhorn SJ, Cummings DE, Schur EA. Effects of multiple cycles of weight loss and regain on the body weight regulatory system in rats. Am J Physiol Endocrinol Metab. 2019;317(5):E863-E870. doi:10.1152/ajpendo.00110.2019
46. Simonds SE, Pryor JT, Cowley MA. Repeated weight cycling in obese mice causes increased appetite and glucose intolerance. Physiol Behav. 2018;194(2017):184-190. doi:10.1016/j.physbeh.2018.05.026
47. Eum JY, Lee G Bin, Yi SS, Kim IY, Seong JK, Moon MH. Lipid alterations in the skeletal muscle tissues of mice after weight regain by feeding a high-fat diet using nanoflow ultrahigh performance liquid chromatography-tandem mass spectrometry. J Chromatogr B Anal Technol Biomed Life Sci. 2020;1141(January):1-8. doi:10.1016/j.jchromb.2020.122022
48. Schofield SE, Parkinson JRC, Henley AB, Sahuri-Arisoylu M, Sanchez-Canon GJ, Bell JD. Metabolic dysfunction following weight cycling in male mice. Int J Obes. 2017;41(3):402-411. doi:10.1038/ijo.2016.193

49. Zamarron BF, Porsche CE, Luan D, et al. Weight Regain in Formerly Obese Mice Hastens Development of Hepatic Steatosis Due to Impaired Adipose Tissue Function. Obesity. 2020;28(6):1086-1097. doi:10.1002/oby.22788
50. Li X, Jiang L, Yang M, Wu YW, Sun JZ. Impact of weight cycling on CTRP3 expression, adipose tissue inflammation and insulin sensitivity in C57BL/6J mice. Exp Ther Med. 2018;16(3):2052-2059. doi:10.3892/etm.2018.6399
51. Anderson EK, Gutierrez DA, Kennedy A, Hasty AH. Weight cycling increases T-cell accumulation in adipose tissue and impairs systemic glucose tolerance. Diabetes. 2013;62(9):3180-3188. doi:10.2337/db12-1076
52. Palm IF, Schram RGAE, Swarts HJM, van Schothorst EM, Keijer J. Body weight cycling with identical diet composition does not affect energy balance and has no adverse effect on metabolic health parameters. Nutrients. 2017;9(10). doi:10.3390/nu9101149
53. Kim RY, Lee JH, Oh Y, Sung HK, Kim KH. Assessment of the metabolic effects of isocaloric 2:1 intermittent fasting in mice. J Vis Exp. 2019;2019(153):1-9. doi:10.3791/60174
54. Brinkworth GD, Noakes M, Buckley JD, Clifton PM. Weight loss improves heart rate recovery in overweight and obese men with features of the metabolic syndrome. Am Heart J. 2006;152(4):693.e1-693.e6. doi:10.1016/j.ahj.2006.07.019
55. Contreras RJ, Williams VL. Dietary obesity and weight cycling: Effects on blood pressure and heart rate in rats. Am J Physiol - Regul Integr Comp Physiol. 1989;256(6). doi:10.1152/ajpregu.1989.256.6.r1209
56. de Souza AMA, Ji H, Wu X, Sandberg K, West CA. Persistent Renin-Angiotensin System Sensitization Months After Body Weight Recovery From Severe Food Restriction in Female Fischer Rats. J Am Heart Assoc. 2020;9(14):e017246. doi:10.1161/JAHA.120.017246
57. Pinotti MF, Matias AM, Sugizaki MM, et al. Fasting/refeeding cycles prevent myocardial dysfunction and morphology damage in the spontaneously hypertensive rats. Arq Bras Cardiol. 2018;111(3):400-409. doi:10.5935/abc.20180152
58. Reichenbach A, Stark R, Mequinion M, et al. Carnitine acetyltransferase (Crat) in hunger-sensing AgRP neurons permits adaptation to calorie restriction. FASEB J. 2018;32(12):6923-6933. doi:10.1096/fj.201800634R
59. Hernandez-Carretero A, Weber N, La Frano MR, et al. Obesity-induced changes in lipid mediators persist after weight loss. Int J Obes. 2018;42(4):728-736. doi:10.1038/ijo.2017.266
60. Kim MS, Kim IY, Sung HR, et al. Metabolic dysfunction following weight regain compared to initial weight gain in a high-fat diet-induced obese mouse model. J Nutr Biochem. 2019;69:44-52. doi:10.1016/j.jnutbio.2019.02.011
61. Kasher-Meron M, Youn DY, Zong H, Pessin JE. Lipolysis defect in white adipose tissue and rapid weight regain. Am J Physiol - Endocrinol Metab. 2019;317(2):E185-E193. doi:10.1152/ajpendo.00542.2018
62. Matikainen-Ankney BA, Ali MA, Miyazaki NL, Fry SA, Licholai JA, Kravitz A V. Weight Loss After Obesity is Associated with Increased Food Motivation and Faster Weight Regain in Mice. Obesity. 2020;28(5):851-856. doi:10.1002/oby.22758
63. Calonne J, Arsenijevic D, Scerri I, Miles-Chan JL, Montani JP, Dulloo AG. Low 24-hour core body temperature as a thrifty metabolic trait driving catch-up fat during weight regain after caloric restriction. Am J Physiol Endocrinol Metab. 2019;317(4):E699-E709. doi:10.1152/ajpendo.00092.2019
64. Zou J, Lai B, Zheng M, et al. CD4+ T cells memorize obesity and promote weight regain. Cell Mol Immunol. 2018;15(6):630-639. doi:10.1038/cmi.2017.36

Chapter 2:

1. Fryar CD, Carroll MD, Ogden CL. Prevalence of overweight, obesity, andextreme obesity among adults: United States, 1960–1962 through 2011–2012. Natl Health Nutr Exam Survey. (2014) 1–6. Available online at: https://www.cdc.gov/nchs/data/hestat/obesity_adult_11_12/obesity_adult_11_12.pdf
2. Ogden CL, Carroll MD, Kit BK, Flegal KM. Prevalence of childhood andadult obesity in the United States, 2011–2012. J Am Med Assoc. (2014) 311:806–14. doi: 10.1001/jama.2014.732
3. Allison DB, Fontaine KR, Manson JE, Stevens J, VanItallie TB. Annual deaths attributable to obesity in the United States. J AmMed Assoc. (1999) 282:1530–8. doi:10.1001/jama.282.16.1530
4. Mehta NK, Chang VW. Mortality attributable to obesity amongmiddle-aged adults in the United States. Demography. (2009) 46:851–72. doi: 10.1353/dem.0.0077
5. Alva ML, Hoerger TJ, Zhang P, Cheng YJ. State-level diabetes-attributable mortality and years of life lost in the United States. Ann Epidemiol. (2018) 28:790–5. doi: 10.1016/j.annepidem.2018.08.015
6. Kopelman PG. Obesity as a medical problem. Nature. (2000) 404:635–43. doi:10.1038/35007508
7. Giugliano G, Nicoletti G, Grella E, Giugliano F, Esposito K, Scuderi N, et al. Effect of liposuction on insulin resistance and vascular inflammatory markers in obese women. Br J Plastic Surg. (2004) 57:190–4. doi: 10.1016/j.bjps.2003.12.010
8. Westman EC, Yancy WS, Mavropoulos JC, Marquart M, McDuffie JR. The effect of a low-carbohydrate, ketogenic diet versus a low-glycemic index diet on glycemic control in type 2 diabetes mellitus. Nutr Metab. (2008) 5:36. doi: 10.1186/1743-7075-5-36
9. Bales CW, Kraus WE. Caloric restriction: implications for human cardiometabolic health. J Cardiopul Rehabil Prevention. (2013) 33:201–8. doi: 10.1097/HCR.0b013e318295019e
10. Mertens IL, Van Gaal LF. Overweight, obesity, and blood pressure: the effects of modest weight reduction. Obes Res. (2000)8:270–8. doi: 10.1038/oby.2000.32
11. Fothergill E,Guo J, Howard L, Kerns JC, Knuth ND, Brychta R, et al. Persistent metabolic adaptation 6 years after "The Biggest Loser" competition. Obesity. (2016) 24, 1612–1619. doi: 10.1002/oby.21538
12. Kirchner H, Hofmann SM, Fischer-Rosinský A, Hembree J, Abplanalp W, Ottaway N, et al. Caloric restriction chronically impairs metabolic programming in mice. Diabetes. (2012) 61:2734–42. doi: 10.2337/db11-1621
13. Hammer S, Snel M, Lamb HJ, Jazet IM, van der Meer RW, Pijl H, et al. Prolonged caloric restriction in obese patients with type 2 diabetes mellitus decreases myocardial triglyceride content and improves myocardial function. J Am Coll Cardiol. (2008) 52:1006–12. doi: 10.1016/j.jacc.2008.04.068
14. Keys A, Brozek J, Henschel A, Mickelsen O, Taylor HL. Experimental Starvation in Man. A Report from the Laboratory of Physiological Hygiene, University of Minnesota, Minneapolis, MN (1945). p. 1–48.
15. Xu S, Chen G, Chunrui L, Liu C. The Preventive and Therapeutic Effect of Caloric Restriction Therapy on Type 2 Diabetes Mellitus, Treatment of Type 2 Diabetes, Colleen Croniger. Nanjing: IntechOpen (2015). p. 185–194. doi: 10.5772/59281
16. Viscarra JA, Rodriguez R, Vazquez-Medina JP, Lee A, TiftMS, Tavoni SK, et al. Insulin and GLP-1 infusions demonstrate the onset of adipose-specific insulin resistance in a large fasting mammal: potential glucogenic role for GLP-1. Physiol Rep. (2013) 1:1–14. doi: 10.1002/phy2.23

17. Bouskila M, Pajvani UB, Scherer PE. Adiponectin: A relevant player in PPARg-agonist-mediated improvements in hepatic insulin sensitivity? Int J Obes. (2005) 29:S17–23. doi: 10.1038/sj.ijo.0802908
18. Havel PJ. Tissue TG and TC Protocol. Davis, CA: Mouse Metabolic Phenotyping Centers Protocols Version. Vol. 1 (2013). p. 1–3.
19. López-jaramillo P, Gómez-arbeláez D, López-lópez J, López-lópez C, Martínez-ortega J, Gómez-rodríguez A, et al. The role of leptin/adiponectin ratio in metabolic syndrome and diabetes. Hormone Mol Biol Clin Investig. (2014) 18:37–45. doi: 10.1515/hmbci-2013-0053
20. Tschritter O, Fritsche A, Thamer C, Haap M, Shirkavand F, Rahe S, et al. Plasma adiponectin concentrations predict insulin sensitivity of both glucose and lipid metabolism. Diabetes. (2003) 52:239–43. doi: 10.2337/diabetes.52.2.239
21. Havel PJ. Update on adipocyte hormones. Regulation of energy balance and carbohydrate/ lipid metabolism. Diabetes. (2014) 53(Suppl. 1): S143–51. doi:10.2337/diabetes.53.2007.S143
22. Linden MA, Fletcher JA, Meers GM, Thyfault JP, Laughlin MH, Rector RS. A return to ad libitum feeding following caloric restriction promotes hepatic steatosis in hyperphagic OLETF rats. Am J Physiol Gastrointest Liver Physiol. (2016) 311:G387–95. doi:10.1152/ajpgi.00089.2016
23. MacLean PS, Higgins JA, Jackman MR, Johnson GC, Fleming-Elder BK, Wyatt HR, et al. Peripheral metabolic responses to prolonged weight reduction that promote rapid, efficient regain in obesity-prone rats. Am J Physiol Regul Integr Comp Physiol. (2006) 290:R1577–88. doi: 10.1152/ajpregu.00810.2005
24. Kawano K, Hirashima T, Mori S, Natori T. OLETF (Otsuka Long-Evans Tokushima Fatty) rat: a newNIDDMrat strain. Diabetes Res Clin Pract. (1992) 24:S317–20. doi: 10.1016/0168-8227(94)90269-0
25. Kawano K, Hirashima T, Mori S, Saitoh Y, Kurosumi M, Natori T. Spontaneous long-term hyperglycemic rat with diabetic complications: Otsuka Long-Evans Tokushima Fatty (OLETF) strain. Diabetes. (1992) 41:1422–8. doi: 10.2337/diabetes.41.11.1422
26. Rodriguez R, Viscarra JA, Minas JN, Nakano D, Nishiyama A, Ortiz RM. Angiotensin receptor blockade increases pancreatic insulin secretion and decreases glucose intolerance during glucose supplementation in a model of metabolic syndrome. Endocrinology. (2012) 153:1684–95. doi: 10.1210/en.2011-1885
27. Vazquez-Medina JP, Popovich I, Thorwald MA, Viscarra JA, Rodriguez R, Sonanez-Organis JG, et al. Angiotensin receptor-mediated oxidative stress is associated with impaired cardiac redox signaling and mitochondrial function in insulin-resistant rats. Am J Physiol Circul Physiol. (2013) 305:599–607. doi: 10.1152/ajpheart.00101.2013
28. Rodriguez R, Minas JN, Vazquez-Medina JP, Nakano D, Parkes DG, Nishiyama A, et al. Chronic AT1 blockade improves glucose homeostasis in obese OLETF rats. J Endocrinol. (2018) 237:271–84. doi: 10.1530/JOE-17-0678
29. Manouze H, Ghestem A, Poillerat V, Bennis M, Ba-M'hamed S, Benoliel JJ, et al. Effects of single cage housing on stress, cognitive, and seizure parameters in the rat and mouse pilocarpine models of epilepsy. eNeuro. (2019) 6:1–23. doi: 10.1523/ENEURO.0179-18.2019
30. Thorwald MA, Godoy-Lugo JA, Rodriguez GJ, Rodriguez MA, Jamal M, Kinoshita H, et al. Nrf2-related gene expression is impaired during a glucose challenge in type II diabetic rat hearts. Free Radical BiolMed. (2019) 130:306–17. doi: 10.1016/j.freeradbiomed.2018.10.405
31. Vazquez-Anaya G, Martinez B, Soñanez-Organis JG, Nakano D, Nishiyama A, Ortiz RM. Exogenous thyroxine improves glucose intolerance in insulin resistant rats. J Endocrinol. (2017) 232:501–11. doi: 10.1530/JOE-16-0428

32. Folch J, LeesM, Sloane GH. A simple method for the isolation and purification of total lipides from animal tissues. J Biol Chem. (1957) 226:497–509.
33. Viscarra JA, Vázquez-Medina JP, Rodriguez R, Champagne CD, Adams SH, Crocker DE, et al. Decreased expression of adipose CD36 and FATP1 are associated with increased plasma non-esterified fatty acids during prolonged fasting in northern elephant seal pups (Mirounga angustirostris). J Exp Biol. (2012) 215:2455–64. doi: 10.1242/jeb.069070
34. Nakano D, Diah S, Kitada K, Hitomi H, Mori H, Masaki T, et al. Shortterm calorie restriction in early life attenuates the development of proteinuria but not glucose intolerance in type 2 diabetic OLETF rats. ISRN Endocrinol. 2011:768637. doi: 10.5402/2011/768637
35. Viscarra JA, Champagne CD, CrockerDE,Ortiz RM. 5'AMP-activated protein kinase activity is increased in adipose tissue of northern elephant seal pups during prolonged fasting-induced insulin resistance. J Endocrinol. (2011) 209:317–25. doi: 10.1530/JOE-11-0017
36. Mizuno A, Kuwajima M, Ishida K, Noma Y, Murakami T, Tateishi K, et al. Extrapancreatic action of truncated glucagon-like peptide-I in Otsuka Long-Evans Tokushima Fatty rats, an animal model for noninsulin-dependent diabetes mellitus. Metabol Clin Exp. (1997) 46:745–9. doi: 10.1016/S0026-0495(97)90117-7
37. Neschen S, Morino K, Hammond LE, Zhang D, Liu ZX, Romanelli AJ, et al. Prevention of hepatic steatosis and hepatic insulin resistance in mitochondrial acyl-CoA:glycerol-sn-3-phosphate acyltransferase 1 knockout mice. Cell Metab. (2005) 2:55–65. doi:10.1016/j.cmet.2005.06.006
38. KumashiroN, ErionDM, ZhangD, KahnM, Beddow SA, Chu X, et al. Cellular mechanism of insulin resistance in nonalcoholic fatty liver disease. Proc Natl Acad Sci USA. (2011) 108:16381–5. doi: 10.1073/pnas.1113359108
39. Baum N, Dichoso CC, Carlton CE. Blood urea nitrogen and serum creatinine. Physiol Interpret Urol. (1975) 5:583–8. doi: 10.1016/0090-4295(75)90105-3
40. Harp JB, Henry SA, DiGirolamo M. Dietary weight loss decreases serum angiotensin-converting enzyme activity in obese adults. Obes Res. (2002) 10:985–90. doi: 10.1038/oby.2002.134
41. Kelley DE, Wing R, Buonocore C, Sturis J, Polonsky K, Fitzsimmons M. Relative effects of calorie restriction and weight loss in noninsulindependent diabetes mellitus. J Clin Endocrinol Metab. (1993) 77:1287–93. doi: 10.1210/jcem.77.5.8077323
42. Bi S, Scott KA, Hyun J, Ladenheim EE, Moran TH. Running wheel activity prevents hyperphagia and obesity in otsuka long-evans tokushima fatty rats: role of hypothalamic signaling. Endocrinology. (2005) 146:1676–85. doi: 10.1210/en.2004-1441
43. Guillet C, Boirie Y. Insulin resistance: a contributing factor to age-related muscle mass loss? Diabetes Metabol. (2005) 31:5S20–6. doi: 10.1016/S1262-3636(05)73648-X
44. Barac-Nieto M, Spurr GB, Lotero H, Maksud MG. Body composition in chronic undernutrition. Am J Clin Nutr. (1978) 31:23–40. doi: 10.1093/ajcn/31.1.23
45. Corbett SW, Stern JS, Keesey RE. Energy expenditure in rats with diet-induced obesity. Am J Clin Nutr. (1986) 44:173–80. doi: 10.1093/ajcn/44.2.173
46. Hill JO,Wyatt HR, Peters JC. Energy balance and obesity. Circulation. (2012) 126:126–32. doi: 10.1161/CIRCULATIONAHA.111.087213
47. Yagi K, Kim S, Wanibuchi H, Yamashita T, Yamamura Y, Iwao H. Characteristics of diabetes, blood pressure, and cardiac and renal complications in otsuka long-evans tokushima fatty rats. Hypertension. (1997) 29:728–35. doi: 10.1161/01.HYP.29.3.728
48. Nicoll R, HeneinMY. Caloric restriction and its effect on blood pressure, heart rate variability and arterial stiffness and dilatation: a review of the evidence. Int J Mol Sci. (2018) 19:1–18. doi: 10.3390/ijms19030751

49. Kosegawa I, Katayama S, Kikuchi C, Kashiwabara H, Negishi K, Ishii J, et al. Metformin decreases blood pressure and obesity in OLETF rats via improvement of insulin resistance. Hypert Res Clin Exp. (1996) 19:37–41. doi: 10.1291/hypres.19.37
50. Rodriguez R, Moreno M, Lee AY, Godoy-Lugo JA, Nakano D, Nishiyama A, et al. Simultaneous GLP-1 receptor activation and angiotensin receptor blockade increase natriuresis independent of altered arterial pressure in obese OLETF rats. Hypertension Res. (2018) 41:798–808. doi: 10.1038/s41440-018-0070-0
51. Fujita Y, Kojima H, Hidaka H, Fujimiya M, Kashiwagi A, Kikkawa R. Increased intestinal glucose absorption and postprandial hyperglycaemia at the early step of glucose intolerance in Otsuka Long-Evans Tokushima Fatty rats. Diabetologia. (1998) 41:1459–66. doi: 10.1007/s001250051092
52. Ramnanan CJ, Edgerton DS, Cherrington AD. The role of insulin in the regulation of PEPCK and gluconeogenesis in vivo. US Endocrinol. (2009) 5:34–9. doi: 10.17925/USE.2009.05.1.34
53. McCurdy CE, Davidson RT, Cartee GD. Brief calorie restriction increases Akt2 phosphorylation in insulin- stimulated rat skeletal muscle. Am J Physiol Endocrinol Metab. (2003) 285:1–15. doi: 10.1152/ajpendo.00224.2003
54. Sequea DA, Sharma N, Arias EB, Cartee GD. Calorie restriction enhances insulin-stimulated glucose uptake and akt phosphorylation in both fast-twitch and slow-twitch skeletal muscle of 24-month-old rats. J Gerontol Ser A Biol Sci Med Sci. (2012) 67:1279–85. doi:10.1093/gerona/gls085
55. Combs TP, Berg AH, Obici S, Scherer PE, Rossetti L. Endogenous glucose production is inhibited by the adipose-derived protein Acrp30. J Clin Investig. (2001) 108:1875–81. doi:10.1172/JCI14120
56. Han Y, Joe Y, Seo E, Lee SR, Park MK, Lee HJ, et al. The hyperleptinemia and ObRb expression in hyperphagic obese rats. Biochem Biophys Res Commun. (2010) 394:70–4. doi:10.1016/j.bbrc.2010.02.104

Chapter 3:

1. Abbasi F, Brown BW, Lamendola C, McLaughlin T, Reaven GM. Relationship between obesity, insulin resistance, and coronary heart disease risk. *J Am Coll Cardiol.* 2002;40(5):937-943. doi:10.1016/S0735-1097(02)02051-X
2. Tai ES, Tan MLS, Stevens RD, Low YL, Muehlbauer MJ, Goh DLM et al. Insulin resistance is associated with a metabolic profile of altered protein metabolism in Chinese and Asian-Indian men. *Diabetologia.* 2010;53(4):757-767. doi:10.1007/s00125-009-1637-8
3. Koves TR, Ussher JR, Noland RC, Slentz D, Mosedale M, Ilkayeva O et al. Mitochondrial Overload and Incomplete Fatty Acid Oxidation Contribute to Skeletal Muscle Insulin Resistance. *Cell Metab.* 2008;7(1):45-56. doi:10.1016/j.cmet.2007.10.013
4. Gupte SA. Targeting the pentose phosphate pathway in syndrome X-related cardiovascular complications. *Drug Dev Res*. 2010;71(3):161-167. doi:10.1002/ddr.20359
5. Piccolo BD, Graham JL, Stanhope KL, Fiehn O, Havel PJ, Adams SH. Plasma amino acid and metabolite signatures tracking diabetes progression in the UCD-T2DM rat model. *Am J Physiol - Endocrinol Metab*. 2016;310:958-969. doi:10.1152/ajpendo.00052.2016
6. Yang MU, Van Itallie TB. Composition of weight lost during short term weight reduction. Metabolic responses of obese subjects to starvation and low calorie ketogenic and nonketogenic diets. *J Clin Invest*. 1976;58(3):722-730. doi:10.1172/JCI108519
7. Hall KD, Bemis T, Brychta R, Chen KY, Courville A, Crayner EJ et al. Calorie for Calorie, Dietary Fat Restriction Results in More Body Fat Loss than Carbohydrate Restriction in People with Obesity. *Cell Metab.* 2015;22:427-436.
8. Bales CW, Kraus WE. Caloric restriction: Implications for human cardiometabolic health. *J Cardiopulm Rehabil Prev.* 2013;33(4):201-208. doi:10.1097/HCR.0b013e318295019e
9. Selman C, Kerrison ND, Cooray A, Piper MDW, Lingard SJ, Barton RH et al. Coordinated multitissue transcriptional and plasma metabonomic profiles following acute caloric restriction in mice. *Physiol Genomics.* 2006;27(3):187-200. doi:10.1152/physiolgenomics.00084.2006
10. Collet TH, Sonoyama T, Henning E, et al. A metabolomic signature of acute caloric restriction. *J Clin Endocrinol Metab*. 2017;102(12):4486-4495. doi:10.1210/jc.2017-01020
11. Dror Y, Almashanu S, Lubart E, Sela BA, Shimoni L, Segal R. The impact of refeeding on blood fatty acids and amino acid profiles in elderly patients: A metabolomic analysis. *J Parenter Enter Nutr*. 2013;37(1):109-116. doi:10.1177/0148607112443260
12. Kawano K, Hirashima T, Mori S, Saitoh Y, Kurosumi M, Natori T. Spontaneous long-term hyperglycemic rat with diabetic complications: Otsuka Long-Evans Tokushima Fatty (OLETF) strain. *Diabetes*. 1992;41:1422-1428. doi:10.2337/diab.41.11.1422
13. Rodriguez R, Viscarra JA, Minas JN, Nakano D, Nishiyama A, Ortiz RM. Angiotensin receptor blockade increases pancreatic insulin secretion and decreases glucose intolerance during glucose supplementation in a model of metabolic syndrome. *Endocrinology*. 2012;153(4):1684–1695. doi:10.1210/en.2011-1885
14. Rodriguez R, Minas JN, Vazquez-Medina JP, Nakano D, Parkes DG, Nishiyama A et al. Chronic AT1 blockade improves glucose homeostasis in obese OLETF rats. *J Endocrinol*. 2018;237(3):271-284. doi:110.1016/j.bbi.2017.04.008
15. Vazquez-Medina JP, Popovich I, Thorwald MA, Viscarra JA, Rodriguez R, Sonanez-organis JG et al. Angiotensin receptor-mediated oxidative stress is associated with impaired cardiac redox signaling and mitochondrial function in insulin-resistant rats. *AJP Hear Circ Physiol*. 2013;305:599-607. doi:10.1152/ajpheart.00101.2013
16. Rector RS, Thyfault JP, Uptergrove GM, Morris EM, Naples SP, Borengasser SJ. et al. Mitochondrial dysfunction precedes insulin resistance and hepatic steatosis and contributes to

the natural history of non-alcoholic fatty liver disease in an obese rodent model. *J Hepatol.* 2010;52(5):727-736. doi:10.1016/j.jhep.2009.11.030

17. Yokoi N, Beppu M, Yoshida E, Hoshikawa R, Hidaka S, Matsubara T et al. Identification of putative biomarkers for prediabetes by metabolome analysis of rat models of type 2 diabetes. *Metabolomics.* 2015;11(5):1277-1286. doi:10.1007/s11306-015-0784-9

18. Cornejo MA, Nguyen J, Cazares J, Escobedo B, Nishiyama A, Nakano D et al. Partial Body Mass Recovery After Caloric Restriction Abolishes Improved Glucose Tolerance in Obese, Insulin Resistant Rats. *Front Endocrinol (Lausanne).* 2020;11(363):1-14. doi:10.3389/fendo.2020.00363
19. Fiehn O. Metabolomics by Gas Chromatography-Mass Spectrometry: the combination of targeted and untargeted profiling. *Curr Protoc Mol Biol*. 2016;114:30.4.1-30.4.32. doi:10.1002/0471142727.mb3004s114
20. Borrego SL, Fahrmann J, Datta R, Stringari C, Grapov D, Zeller M et al. Metabolic changes associated with methionine stress sensitivity in MDA-MB-468 breast cancer cells. *Cancer Metab.* 2016;4(1):1-17. doi:10.1186/s40170-016-0148-6
21. Dhillon J, Thorwald M, De La Cruz N, Vu E, Asghar SA, Kuse Q et al. Glucoregulatory and cardiometabolic profiles of almond vs. Cracker snacking for 8 weeks in young adults: A randomized controlled trial. *Nutrients.* 2018;10(8). doi:10.3390/nu10080960
22. Benjamini Y, Hochberg Y. Controlling The False Discovery Rate - A Practical And Powerful Approach To Multiple Testing Article. *J R Stat Soc*. 1995;57(1):289-300. doi:10.2307/2346101
23. Barupal DK, Haldiya PK, Wohlgemuth G, Kind T, Kothari SL, Pinkerton KE et al. MetaMapp: mapping and visualizing metabolomic data by integrating information from biochemical pathways and chemical and mass spectral similarity. *BMC Bioinformatics.* 2012;13(99):1-15. doi:10.1016/j.reprotox.2009.12.001
24. Kanehisa M, Sato Y, Kawashima M, Furumichi M, Tanabe M. KEGG as a reference resource for gene and protein annotation. *Nucleic Acids Res*. 2016;44(D1):D457-D462. doi:10.1093/nar/gkv1070
25. Goodpaster AM, Kennedy MA. Quantification and statistical significance analysis of group separation in NMR-based metabonomics studies. *Chemom Intell Lab Syst*. 2011;109(2):162-170. doi:10.1016/j.chemolab.2011.08.009.Quantification
26. Cahill JR GF. Starvation in Man. *Clin Endocrinol Metab*. 1976;5(2):397-415. doi:10.1056/NEJM197003192821209
27. Hagström-Toft E, Thörne A, Reynisdottir S, Moberg E, Rössner S, Bolinder J al. Evidence for a Major Role of Skeletal Muscle Lipolysis in the Regulation of Lipid Oxidation during Caloric Restriction in Vivo. Diabetes. 2001;50(7):1604-1611. doi:10.2337/diabetes.50.7.1604
28. Viscarra JA, Ortiz RM. Cellular mechanisms regulating fuel metabolism in mammals: Role of adipose tissue and lipids during prolonged food deprivation. Metabolism. 2013;62(7):889-897. doi:10.1016/j.metabol.2012.12.014
29. Goodman MN, Larsen R, Kaplan MM, Aoki TT, Young VR, Ruderman NB. Starvation in the rat. II. Effect of age and obesity on protein sparing and fuel metabolism. *Am J Physiol - Endocrinol Metab*. 1980;2(4):E277-E286. doi:10.1152/ajpendo.1980.239.4.e26
30. Casazza JP, Veech RL. The content of pentose-cycle intermediates in liver in starved, fed ad libitum and meal-fed rats. *Biochem J*. 1986;236(3):635-641. doi:10.1042/bj2360635
31. Gaster M. Reduced TCA flux in diabetic myotubes: A governing influence on the diabetic phenotype? *Biochem Biophys Res Commun*. 2009;387(4):651-655. doi:10.1016/j.bbrc.2009.07.064

32. Nelson JL, Harmon ME, Robergs RA. Identifying plasma glycerol concentration associated with urinary glycerol excretion in trained humans. *J Anal Toxicol*. 2011;35(9):617-623. doi:10.1093/anatox/35.9.617
33. Steinhauser ML, Olenchock BA, O'Keefe J, Lun M, Pierce KA, Lee H et al. The circulating metabolome of human starvation. *JCI insight*. 2018;3(16):1-16. doi:10.1172/jci.insight.121434
34. Bajaj M, DeFronzo RA. Metabolic and molecular basis of insulin resistance. *J Nucl Cardiol*. 2003;10(3):311-323. doi:10.1016/S1071-3581(03)00520-8
35. Bock G, Chittilapilly E, Basu R, Toffolo G, Cobelli C, Chandramouli V et al. Contribution of hepatic and extrahepatic insulin resistance to the pathogenesis of impaired fasting glucose: Role of increased rates of gluconeogenesis. *Diabetes*. 2007;56(6):1703-1711. doi:10.2337/db06-1776
36. Kubota T, Kubota N, Kumagai H, Yamaguchi S, Kozono H, Takahashi T et al. Impaired insulin signaling in endothelial cells reduces insulin-induced glucose uptake by skeletal muscle. *Cell Metab*. 2011;13(3):294-307. doi:10.1016/j.cmet.2011.01.018
37. Lee CG, Boyko EJ, Strotmeyer ES, Lewis CE, Cawthon PM, Hoffman AR et al. Association between insulin resistance and lean mass loss and fat mass gain in older men without diabetes mellitus. *J Am Geriatr Soc*. 2011;59(7):1217-1224. doi:10.1111/j.1532-5415.2011.03472.x
38. Nestel PJ, Straznicky N, Mellett NA, Wong G, De Souza DP, Tull DL et al. Specific plasma lipid classes and phospholipid fatty acids indicative of dairy food consumption associate with insulin sensitivity. *Am J Clin Nutr.* 2014;99(1):46-53. doi:10.3945/ajcn.113.071712
39. Mitch WE, Goldberg AL. Mechanisms of Muscle Wasting. *Mech Dis.* 1996;335(25):1897-1905
40. McCarty MF, DiNicolantonio JJ. An increased need for dietary cysteine in support of glutathione synthesis may underlie the increased risk for mortality associated with low protein intake in the elderly. *Age (Omaha).* 2015;37(96):1-12. doi:10.1007/s11357-015-9823-8
41. Saudek CD, Felig P. The metabolic events of starvation. *Am J Med*. 1976;60(1):117-126. doi:10.1016/0002-9343(76)90540-4

Chapter 4:

1. Markham A, Elkinson S. Luseogliflozin: First global approval. *Drugs.* 2014. doi:10.1007/s40265-014-0230-8
2. Yamada K, et al. Effects of a sodium glucose co-transporter 2 selective inhibitor , ipragliflozin , on the diurnal profile of plasma glucose in patients with type 2 diabetes : A study using continuous glucose monitoring. *J Diabetes Investig*. 2015;6(6):699-707. doi:10.1111/jdi.12370
3. Kalra S, et al. Newer antidiabetic drugs and calorie restriction mimicry. *Indian J Endocrinol Metab*. 2016. doi:10.4103/2230-8210.172242
4. Marton A, et al. Organ protection by SGLT2 inhibitors: role of metabolic energy and water conservation. *Nat Rev Nephrol*. 2020:1-13. doi:10.1038/s41581-020-00350-x
5. David-Silva A, et al. Dual SGLT1/SGLT2 inhibitor phlorizin ameliorates non-alcoholic fatty liver disease and hepatic glucose production in type 2 diabetic mice. *Diabetes, Metab Syndr Obes Targets Ther*. 2020;13:739-751. doi:10.2147/DMSO.S242282
6. Atageldiyeva K, et al. Sodium-glucose cotransporter 2 inhibitor and a low carbohydrate diet affect gluconeogenesis and glycogen content differently in the kidney and the liver of non-diabetic mice. *PLoS One*. 2016;11(6):1-17. doi:10.1371/journal.pone.0157672
7. Tanaka S, et al. Sodium–glucose cotransporter 2 inhibition normalizes glucose metabolism and suppresses oxidative stress in the kidneys of diabetic mice. *Kidney Int*. 2018;94(5):912-925. doi:10.1016/j.kint.2018.04.025
8. Xu L, et al. SGLT2 Inhibition by Empagliflozin Promotes Fat Utilization and Browning and Attenuates Inflammation and Insulin Resistance by Polarizing M2 Macrophages in Diet-induced Obese Mice. *EBioMedicine*. 2017;20:137-149. doi:10.1016/j.ebiom.2017.05.028
9. Ferrannini E, et al. Shift to fatty substrate utilization in response to sodium-glucose cotransporter 2 inhibition in subjects without diabetes and patients with type 2 diabetes. *Diabetes.* 2016;65(5):1190-1196. doi:10.2337/db15-1356
10. Mulder S, et al. A metabolomics-based molecular pathway analysis of how the sodium-glucose co-transporter-2 inhibitor dapagliflozin may slow kidney function decline in patients with diabetes. *Diabetes, Obes Metab.* 2020;22(7):1157-1166. doi:10.1111/dom.14018
11. Nakano D, et al. Short-Term Calorie Restriction in Early Life Attenuates the Development of Proteinuria but Not Glucose Intolerance in Type 2 Diabetic OLETF Rats. *ISRN Endocrinol*. 2011:1-7. doi:10.5402/2011/768637
12. Kojima N, et al. Effects of a New SGLT2 Inhibitor, Luseogliflozin, on Diabetic Nephropathy in T2DN Rats. *J Pharmacol Exp Ther*. 2013. doi:10.1124/jpet.113.203869
13. Manouze H, et al. Effects of Single Cage Housing on Stress, Cognitive, and Seizure Parameters in the Rat and Mouse Pilocarpine Models of Epilepsy. *eNeuro.* 2019;6(4):1-23. doi:10.1523/ENEURO.0179-18.2019
14. Rodriguez R, et al. Angiotensin receptor blockade increases pancreatic insulin secretion and decreases glucose intolerance during glucose supplementation in a model of metabolic syndrome. *Endocrinology.* 2012;153(4):1684-1695. doi:10.1210/en.2011-1885
15. Thorwald MA, et al. Nrf2-related gene expression is impaired during a glucose challenge in type II diabetic rat hearts. *Free Radic Biol Med.* 2019;130(July 2018):306-317. doi:10.1016/j.freeradbiomed.2018.10.405
16. Vazquez-Medina JP, et al. Angiotensin receptor-mediated oxidative stress is associated with impaired cardiac redox signaling and mitochondrial function in insulin-resistant rats. *AJP Hear Circ Physiol*. 2013;305:599-607. doi:10.1152/ajpheart.00101.2013
17. Bazzano T, et al. Renal biomarkers of male and female wistar rats (Rattus norvegicus) undergoing renal ischemia and reperfusion. *Acta Cir Bras.* 2015;30(4):277-288. doi:10.1590/S0102-865020150040000007

18. RRID:AB_2890623
19. RRID:AB_10883319
20. RRID:AB_2160031
21. RRID:AB_915794
22. RRID:AB_330330
23. RRID:AB_915783
24. RRID:AB_2315049
25. RRID:AB_2280448
26. RRID:AB_2191441
27. RRID:AB_2890624
28. RRID:AB_2210057
29. RRID:AB_1310695
30. Fiehn O. Metabolomics by Gas Chromatography-Mass Spectrometry: the combination of targeted and untargeted profiling. *Curr Protoc Mol Biol.* 2016;114:30.4.1-30.4.32. doi:10.1002/0471142727.mb3004s114
31. Borrego SL, et al. Metabolic changes associated with methionine stress sensitivity in MDA-MB-468 breast cancer cells. *Cancer Metab.* 2016;4(1):1-17. doi:10.1186/s40170-016-0148-6
32. Conover WJ, Iman RL. Rank transformations as a bridge between parametric and nonparametric statistics. *Am Stat.* 1981;35(3):124-128. doi:10.1080/00031305.1981.10479327
33. Dhillon J, et al. Glucoregulatory and cardiometabolic profiles of almond vs. Cracker snacking for 8 weeks in young adults: A randomized controlled trial. *Nutrients.* 2018;10(8). doi:10.3390/nu10080960
34. Benjamini Y, Hochberg Y. Controlling The False Discovery Rate - A Practical And Powerful Approach To Multiple Testing Article. *J R Stat Soc.* 1995;57(1):289-300. doi:10.2307/2346101
35. Barupal DK, et al. MetaMapp: mapping and visualizing metabolomic data by integrating information from biochemical pathways and chemical and mass spectral similarity. *BMC Bioinformatics.* 2012;13(99):1-15. doi:10.1016/j.reprotox.2009.12.001
36. Cornejo MA, et al. Partial Body Mass Recovery After Caloric Restriction Abolishes Improved Glucose Tolerance in Obese, Insulin Resistant Rats. *Front Endocrinol (Lausanne).* 2020;11(363):1-14. doi:10.3389/fendo.2020.00363
37. Washburn WN, Poucher SM. Differentiating sodium-glucose co-transporter-2 inhibitors in development for the treatment of type 2 diabetes mellitus. *Expert Opin Investig Drugs*. 2013;22(4):463-486. doi:10.1517/13543784.2013.774372
38. Liang Y, et al. Effect of canagliflozin on renal threshold for glucose, glycemia, and body weight in normal and diabetic animal models. *PLoS One*. 2012;7(2):2-8. doi:10.1371/journal.pone.0030555
39. Oliva RV, Bakris GL. Blood pressure effects of sodium-glucose co-transport 2 (SGLT2) inhibitors. *J Am Soc Hypertens*. 2014;8(5):330-339. doi:10.1016/j.jash.2014.02.003
40. Maciel AT, et al. Fractional excretion of potassium in the course of acute kidney injury in critically ill patients: potential monitoring tool? *Rev Bras Ter Intensiva.* 2014;26(2):143-147. doi:10.5935/0103-507X.20140021
41. Guthrie RM. Sodium-glucose co-transporter 2 inhibitors and the potential for cardiovascular risk reduction in patients with type 2 diabetes mellitus. *Postgrad Med.* 2013;125(3):21-32. doi:10.3810/pgm.2013.05.2654
42. Nakano D, et al. Short-term calorie restriction in early life attenuates the development of proteinuria but not glucose intolerance in type 2 diabetic OLETF rats. *ISRN Endocrinol*. 2011;2011:1-7. doi:10.5402/2011/768637

43. Nagai Y, et al. Temporary angiotensin II blockade at the prediabetic stage attenuates the development of renal injury in type 2 diabetic rats. *J Am Soc Nephrol*. 2005;16(3):703-711. doi:10.1681/ASN.2004080649
44. Fioretto P, et al. SGLT2 inhibitors and the diabetic kidney. *Diabetes Care*. 2016;39(August):S165-S171. doi:10.2337/dcS15-3006
45. Brenner BM. Hemodynamically mediated glomerular injury and the progressive nature of kidney disease. *Kidney Int.* 1983;23(4):647-655. doi:10.1038/ki.1983.72
46. Cherney DZI, et al. Renal hemodynamic effect of sodium-glucose cotransporter 2 inhibition in patients with type 1 diabetes mellitus. *Circulation.* 2014;129(5):587-597. doi:10.1161/CIRCULATIONAHA.113.005081
47. Škrtić M, et al. Characterisation of glomerular haemodynamic responses to SGLT2 inhibition in patients with type 1 diabetes and renal hyperfiltration. *Diabetologia.* 2014;57(12):2599-2602. doi:10.1007/s00125-014-3396-4
48. Choi JB, et al. Effect of the sodium-glucose cotransporter 2 inhibitor, dapagliflozin, on genitourinary infection in an animal model of type 2 diabetes. *Int Neurourol J*. 2020;24(1):21-28. doi:10.5213/inj.1938220.110
49. Komoroski B, et al. Dapagliflozin, a novel, selective SGLT2 inhibitor, improved glycemic control over 2 weeks in patients with type 2 diabetes mellitus. *Clin Pharmacol Ther*. 2009;85(5):513-519. doi:10.1038/clpt.2008.250
50. Vallon V, et al. SGLT2 mediates glucose reabsorption in the early proximal tubule. *J Am Soc Nephrol.* 2011;22(1):104-112. doi:10.1681/ASN.2010030246
51. Fujita Y, et al. Increased intestinal glucose absorption and postprandial hyperglycaemia at the early step of glucose intolerance in Otsuka Long-Evans Tokushima Fatty rats. *Diabetologia*. 1998;41:1459-1466. doi:10.1007/s001250051092
52. Coughlan KA, et al. Diabetes, metabolic syndrome and obesity: Targets and therapy dovepress AMPK activation: a therapeutic target for type 2 diabetes? *Diabetes, Metab Syndr Obes Targets Ther*. 2014;7:241-253. http://dx.doi.org/10.2147/DMSO.S43731.
53. Kubota T, et al. Impaired insulin signaling in endothelial cells reduces insulin-induced glucose uptake by skeletal muscle. *Cell Metab*. 2011;13(3):294-307. doi:10.1016/j.cmet.2011.01.018
54. Sequea DA, et al. Calorie restriction enhances insulin-stimulated glucose uptake and akt phosphorylation in both fast-twitch and slow-twitch skeletal muscle of 24-month-old rats. *Journals Gerontol - Ser A Biol Sci Med Sci.* 2012;67(12):1279-1285. doi:10.1093/gerona/gls085
55. Mccurdy CE, et al. Brief calorie restriction increases Akt2 phosphorylation in insulin-stimulated rat skeletal muscle. *Am J Physiol Endocrinol Metab*. 2003;285(4):1-15. doi:10.1152/ajpendo.00224.2003.Brief
56. Calera MR, et al. Insulin increases the association of Akt-2 with Glut4-containing vesicles. *J Biol Chem.* 1998;273(13):7201-7204. doi:10.1074/jbc.273.13.7201
57. Hajduch E, et al. Protein kinase B (PKB / Akt) - a key regulator of glucose transport? *FEBS Lett.* 2001;492:199-203.
58. Park SY, et al. Calorie restriction improves whole-body glucose disposal and insulin resistance in association with the increased adipocyte-specific GLUT4 expression in Otsuka Long-Evans Tokushima Fatty rats. *Arch Biochem Biophys*. 2005;436(2):276-284. doi:10.1016/j.abb.2005.01.010
59. Yang J, Holman GD. Comparison of GLUT4 and GLUT1 subcellular trafficking in basal and insulin-stimulated 3T3-L1 cells. *J Biol Chem*. 1993;268(7):4600-4603. doi:10.1016/s0021-9258(18)53438-4

Tables

Table 1. Mean ± SE relative (%) body composition at endpoint. Retro=Retroperitoneal fat depot; Epi= Epididymal fat depot; other = Accounts for the rest of the body mass. [a]*P* < 0.05 vs LETO. [b]*P* < 0.05 vs Control. [c]*P* < 0.05 vs CR.

Strain	Treatment	Retro (%)	Epi (%)	Heart (%)	Liver (%)	Kidney (%)	Other (%)
LETO	CR Control	1.3 ± 0.1	0.9 ± 0.1	0.4 ± 0	2.8 ± 0.1	1.5 ± 0.1	93.0 ± 0.3
	CR	0.8 ± 0.1	1.0 ± 0.1	0.3 ± 0	2.5 ± 0.1	1.4 ± 0.0	94.1 ± 0.1
	PR Control	1.3 ± 0.1	0.9 ± 0.1	0.3 ± 0	2.4 ± 0.2	1.1 ± 0.0	93.9 ± 0.3
	PR	1.3 ± 0.1	1.2 ± 0.1	0.3 ± 0	2.7 ± 0.1	1.3 ± 0.0	93.3 ± 0.1
OLETF	CR Control	3.4 ± 0.1 [a]	2.2 ± 0.1[a]	0.3 ± 0	2.8 ± 0.1	1.3 ± 0.0	89.9 ± 0.3 [a]
	CR	2.7 ± 0.2 [a, b]	1.8 ± 0.1[a]	0.3 ± 0	2.7 ± 0.2	1.4 ± 0.0	91.1 ± 0.3 [a, b]
	PR Control	3.2 ± 0.1 [a]	2.1 ± 0.2[a]	0.3 ± 0	2.8 ± 0.1	1.4 ± 0.1	90.2 ± 0.4 [a]
	PR	2.8 ± 0.2 [a]	1.8 ± 0.1[a]	0.3 ± 0	2.8 ± 0.1	1.2 ± 0.0	91.1 ± 0.2 [a]

Table 2. Mean ± SE plasma biochemical markers and electrolytes concentrations. Control. aP < 0.05 vs LETO. bP < 0.05 vs Control. cP < 0.05 vs CR.

Strain	Treatment	Urea (mmol/L)	Creatinine (µmol/L)	SI Urea: Creatinine ratio	Plasma Protein (µmol/L)	Plasma Aminoacids (% vs LETO CR Ctrl)
LETO	CR Control	9.0 ± 0.6	28.8 ± 2.9	357 ± 51	625 ± 32	100 ± 3
	CR	11.0 ± 0.5	50.3 ± 5.1 [b]	245 ± 19	602 ± 28	118 ± 9
	PR Control	9.8 ± 2.0 [b]	49.6 ± 2.1 [b]	244 ± 24	706 ± 25	126 ± 4
	PR	12.7 ± 0.2	41.8 ± 3.8	290 ± 19	674 ± 30	96 ± 4
OLETF	CR Control	9.6 ± 0.4	32.5 ± 2.9	312 ± 44	727 ± 47 [a]	91 ± 3
	CR	5.2 ± 1.0 [a, b]	31.9 ± 5.0 [a]	159 ± 22 [b]	655 ± 35	130 ± 14 [b]
	PR Control	9.9 ± 0.6 [c]	42.6 ± 2.0	243 ± 21	847 ± 41 [a]	96 ± 5 [c]
	PR	10.0 ± 0.4 [c]	40.5 ± 1.8	245 ± 13	765 ± 29 [c]	92 ± 5 [c]

Strain	Treatment	Aldosterone (pmol/L)	Cl^- (mmol/L)	K^+ (mmol/L)	Na^+ (mmol/L)
LETO	CR Control	4.8 ± 0.9	101 ± 2	7.4 ± 1.1	140 ± 2
	CR	7.4 ± 1.5	98 ± 1	5.7 ± 0.1	141 ± 1
	PR Control	7.4 ± 1.2	102 ± 2	6.1 ± 0.3	142 ± 2
	PR	15.2 ± 1.7	93 ± 4	6.8 ± 0.2	130 ± 5
OLETF	CR Control	10.4 ± 2.6	98 ± 2	5.8 ± 0.2	138 ± 3
	CR	5.0 ± 2.5	101 ± 0	5.5 ± 0.3	141 ± 1
	PR Control	10.1 ± 0.7	100 ± 1	7.9 ± 0.2 [a, c]	139 ± 1
	PR	9.1 ± 2.3 [b, c]	101 ± 1	7.1 ± 0.2	140 ± 1

Table 3. Fold changes were calculated as mean condition B / mean condition A, after mTIC normalization.

Condition A		Condition B		
Strain	**Treatment**	**Strain**	**Treatment**	**Comparison**
LETO	CR Ctrl	OLETF	CR Ctrl	A
LETO	PR Ctrl	OLETF	PR Ctrl	B
LETO	CR	OLETF	CR	C
LETO	PR	OLETF	PR	D
LETO	CR Ctrl	LETO	CR	E
LETO	PR Ctrl	LETO	PR	F
OLETF	CR Ctrl	OLETF	CR	G
OLETF	PR Ctrl	OLETF	PR	H
LETO	CR	LETO	PR	I
OLETF	CR	OLETF	PR	J

CR: Caloric Restriction; LETO: Long-Evans Tokushima Otsuka; OLETF: Otsuka Long-Evans Tokushima Fatty; PR: Partial Recovery

Table 4. Mean PC score ± SD for PC1 and PC2 for each group comparison and T-test P value for each comparison.

Comparison	Group	Mean PC1	*P* value	Mean PC2	*P* value
A	LETO CR Ctrl	5.16 ± 3.58	0.0019	-1.00 ± 3.76	0.3091
	OLETF CR Ctrl	-5.16 ± 1.15		1.00 ± 1.17	
B	LETO PR Ctrl	5.06 ± 1.50	<.0001	-0.38 ± 2.59	0.6400
	OLETF PR Ctrl	-5.06 ±1.13		0.38 ± 2.41	
C	LETO CR	-3.32 ± 0.76	0.0622	-1.72 ± 0.23	0.1093
	OLETF CR	3.32 ± 5.80		1.72 ± 3.74	
D	LETO PR	5.01 ±1.82	<.0001	-0.12 ± 3.39	0.8859
	OLETF PR	-5.01 ± 1.04		0.12 ± 1.52	
E	LETO CR Ctrl	-4.14 ± 0.47	0.0105	0.88 ± 3.42	0.3640
	LETO CR	4.14 ± 4.13		-0.88 ± 2.20	
F	LETO PR Ctrl	4.48 ± 1.85	<.0001	-0.31 ± 3.60	0.7775
	LETO PR	-4.48 ± 1.11		0.31 ± 3.09	
G	OLETF CR Ctrl	-4.65 ± 0.51	0.0158	-0.36 ± 0.32	0.7729
	OLETF CR	4.65 ± 5.20		0.36 ± 5.17	
H	OLETF PR Ctrl	3.58 ± 3.89	0.0139	1.42 ± 3.46	0.1457
	OLETF PR	-3.58 ± 0.57		-1.42 ± 1.33	
I	LETO CR	4.51 ± 2.36	0.0003	-0.40 ± 2.84	0.6334
	LETO PR	-4.51 ± 1.07		0.40 ± 2.16	
J	OLETF CR	4.28 ± 5.18	0.0207	0.22 ± 5.20	0.8595
	OLETF PR	-4.28 ± 0.44		-0.22 ± 0.46	

CR: Caloric Restriction; LETO: Long-Evans Tokushima Otsuka; OLETF: Otsuka Long-Evans Tokushima Fatty; PC: Principal Component; PR: Partial Recovery

Table 5. Metabolites with the top 5 positive and negative loadings (by absolute value) for PC1 and their respective pathway classification.

Comparison A: LETO CR Ctrl vs OLETF CR Ctrl

Metabolite	Pathway	PC1 Score
3-phosphoglycerate	Carbohydrate Metabolism	0.94
nicotinamide	Secondary Metabolism	0.93
threonic acid	Secondary Metabolism	0.92
isohexonic acid	Unknown/Variable	0.91
pseudo uridine	Nucleotide Metabolism	0.91
proline	Amino Acid Metabolism	-0.86
glucose	Carbohydrate Metabolism	-0.85
tocopherol alpha-	Secondary Metabolism	-0.83
ribitol	Carbohydrate Metabolism	-0.78
beta-sitosterol	Lipid Metabolism	-0.78

Comparison B: LETO PR Ctrl vs OLETF PR Ctrl

Metabolite	Pathway	PC1 Score
arachidonic acid	Lipid Metabolism	0.99
threonic acid	Secondary Metabolism	0.94
glycine	Amino Acid Metabolism	0.93
serine	Amino Acid Metabolism	0.93
N-acetylglycine	Unknown/Variable	0.92
taurine	Lipid Metabolism	-0.89
glucose	Carbohydrate Metabolism	-0.87
ribitol	Carbohydrate Metabolism	-0.83
hexitol	Carbohydrate Metabolism	-0.83
ribose	Carbohydrate Metabolism	-0.83

Comparison C: LETO CR vs OLETF CR

Metabolite	Pathway	PC1 Score
putrescine	Amino Acid Metabolism	0.99
2-deoxypentitol	Unknown/Variable	0.97
enolpyruvate	Unknown/Variable	0.97
pantothenic acid	Amino Acid Metabolism	0.96
beta-alanine	Nucleotide Metabolism	0.95
tryptophan	Amino Acid Metabolism	-0.75
lysine	Amino Acid Metabolism	-0.67
oxoproline	Amino Acid Metabolism	-0.66
arachidonic acid	Lipid Metabolism	-0.47
aminomalonate	Unknown/Variable	-0.43

Comparison D: LETO PR vs OLETF PR

Metabolite	Pathway	PC1 Score
glycerol-alpha-phosphate	Lipid Metabolism	0.95
threonic acid	Secondary Metabolism	0.94
isothreonic acid	Secondary Metabolism	0.94
3-phosphoglycerate	Carbohydrate Metabolism	0.92
pyrophosphate	Energy Metabolism	0.92
cholesterol	Lipid Metabolism	-0.91
2-hydroxybutanoic acid	Secondary Metabolism	-0.88
ribitol	Carbohydrate Metabolism	-0.88
beta-sitosterol	Lipid Metabolism	-0.84
ribose	Carbohydrate Metabolism	-0.81

Comparison E: LETO CR Ctrl vs LETO CR

Metabolite	Pathway	PC1 Score
xylitol	Carbohydrate Metabolism	0.97
tocopherol alpha-	Secondary Metabolism	0.95
pseudo uridine	Nucleotide Metabolism	0.93
myo-inositol	Carbohydrate Metabolism	0.92
aconitic acid	Energy Metabolism	0.90
glucose	Carbohydrate Metabolism	-0.70
3-hydroxybutyric acid	Energy Metabolism	-0.69
4-hydroxyphenylacetic acid	Amino Acid Metabolism	-0.62
palmitoleic acid	Lipid Metabolism	-0.59
isohexonic acid	Unknown/Variable	-0.55

Comparison F: LETO PR Ctrl vs LETO PR

Metabolite	Pathway	PC1 Score
phenylalanine	Amino Acid Metabolism	0.92
N-acetylglycine	Unknown/Variable	0.89
leucine	Amino Acid Metabolism	0.87
phenylethylamine	Amino Acid Metabolism	0.86
glycine	Amino Acid Metabolism	0.84
glucose	Carbohydrate Metabolism	-0.91
conduritol-beta-epoxide	Unknown/Variable	-0.84
indole-3-propionic acid	Unknown/Variable	-0.78
sulfuric acid	Nucleotide Metabolism	-0.77
sorbitol	Carbohydrate Metabolism	-0.74

Comparison G: OLETF CR Ctrl vs OLETF CR

Metabolite	Pathway	PC1 Score
citrulline	Amino Acid Metabolism	0.97
isoribose	Unknown/Variable	0.97
fumaric acid	Energy Metabolism	0.94
2,4-diaminobutyric acid	Amino Acid Metabolism	0.94
beta-alanine	Nucleotide Metabolism	0.93
glucose	Carbohydrate Metabolism	-0.94
tryptophan	Amino Acid Metabolism	-0.81
palmitoleic acid	Lipid Metabolism	-0.52
proline	Amino Acid Metabolism	-0.46
creatinine	Amino Acid Metabolism	-0.38

Comparison H: OLETF PR Ctrl vs OLETF PR

Metabolite	Pathway	PC1 Score
uric acid	Nucleotide Metabolism	0.93
glycerol	Carbohydrate Metabolism	0.92
malic acid	Energy Metabolism	0.88
ornithine	Amino Acid Metabolism	0.87
alpha-ketoglutarate	Energy Metabolism	0.87
conduritol-beta-epoxide	Unknown/Variable	-0.88
linoleic acid	Lipid Metabolism	-0.86
palmitic acid	Lipid Metabolism	-0.85
heptadecanoic acid	Unknown/Variable	-0.82
sucrose	Carbohydrate Metabolism	-0.78

Comparison I: LETO CR vs LETO PR

Metabolite	Pathway	PC1 Score
oxoproline	Amino Acid Metabolism	0.97
cholesterol	Lipid Metabolism	0.94
2,5-dihydroxypyrazine	Unknown/Variable	0.94
aminomalonate	Unknown/Variable	0.93
N-acetylglycine	Unknown/Variable	0.92
glucose	Carbohydrate Metabolism	-0.98
conduritol-beta-epoxide	Unknown/Variable	-0.74
sulfuric acid	Nucleotide Metabolism	-0.72
glycerol-alpha-phosphate	Lipid Metabolism	-0.68
palmitoleic acid	Lipid Metabolism	-0.54

Comparison J: OLETF CR vs OLETF PR

Metabolite	Pathway	PC1 Score
beta-alanine	Nucleotide Metabolism	0.97
isoribose	Unknown/Variable	0.96
fumaric acid	Energy Metabolism	0.95
putrescine	Amino Acid Metabolism	0.94
N-acetyl-5-hydroxytryptamine	Amino Acid Metabolism	0.94
glucose	Carbohydrate Metabolism	-0.96
tryptophan	Amino Acid Metabolism	-0.79
tocopherol alpha-	Secondary Metabolism	-0.74
lysine	Amino Acid Metabolism	-0.48
indole-3-propionic acid	Unknown/Variable	-0.38

Table 6. Main pathway changes after caloric restriction (CR) and partial recovery (PR) compared to ad libitum controls.

		Gluconeogenesis	Glycolysis	TCA Cycle	PPP	Lipogenesis	Lipolysis	Proteolysis	AA catabolism
LETO	After CR*	-	-	-	-	-	-	-	-
	After PR**	-	-	-	-	-	-	-	-
OLETF	After CR*	↑	-	↑	↑	-	↑	↑	↑
	After PR**	↑ †	-	-	-	-	↓	-	↓

AA: Amino acid; TCA: Tricarboxylic Acid; PPP: Pentose Phosphate Pathway; *CR vs CR Ctrl; **PR vs PR Ctrl; ↑ Increase; ↓ Decrease; - no detectable change; † shown by previous [18] univariate analysis but not by current metabolomics data

Table 7. Mean ± SE basal (T0) fasting blood glucose (mg/dl), fasting plasma insulin (ng/ml) concentrations, and glucose/insulin ratio (mg/ng)

	Glucose (mg/dl)	Insulin (ng/ml)	GI ratio (mg/ng)
LETO Control	69 ± 3	1.00 ± 0.06	0.71 ± 0.07
OLETF Control	93 ± 5[a]	1.19 ± 0.07	0.80 ± 0.06
OLETF SGLT2i Control	105 ± 3[a]	1.62 ± 0.19[a]	0.71 ± 0.09
LETO CR	74 ± 3	0.74 ± 0.12	1.18 ± 0.19[b]
OLETF CR	95 ± 3[a]	1.59 ± 0.16[a]	0.65 ± 0.07[a]
OLETF SGLT2i CR	93 ± 6[a]	0.93 ± 0.15[b,d]	0.89 ± 0.07

[a]$p < 0.05$ vs. LETO, [b]$p < 0.05$ vs. control, [c]$p < 0.05$ vs. SGLT2i, [d]$p < 0.05$ vs. OLETF CR

Table 8. Mean ± SE serum electrolyte concentration (mEq/L), 24 h urinary electrolyte excretion (mEq/d) and fractional excretion (FE) of electrolytes.

	LETO Control	OLETF Control	OLETF SGLT2i Control	LETO CR	OLETF CR	OLETF SGLT2i CR
Serum Na^+ (mEq/L)	134.9 ± 0.5	135.3 ± 3.1	132.3 ± 4.2	138.0 ± 0.4 [b,c]	132.0 ± 1.6 [a]	131.8 ± 1.0
Serum K^+ (mEq/L)	6.9 ± 0.9	6.4 ± 0.5	4.6 ± 0.7	4.9 ± 0.4	5.5 ± 1.2	5.4 ± 0.7
Serum Na^+/K^+ ratio	25.1 ± 3.3	21.4 ± 1.6	31.4 ± 4.9	30.4 ± 3.2	22.1 ± 3.5	26.6 ± 3.6
Urine Na^+ (mEq/d)	0.84 ± 0.09	0.63 ± 0.05	0.58 ± 0.08	0.55 ± 0.08	0.66 ± 0.06	0.61 ± 0.13
Urine K^+ (mEq/d)	2.27 ± 0.24	2.09 ± 0.06	2.14 ± 0.13	1.43 ± 0.17	1.31 ± 0.26	1.75 ± 0.38
Urine Na^+/K^+ ratio	0.38 ± 0.03	0.30 ± 0.03	0.27 ± 0.04	0.38 ± 0.02	0.57 ± 0.06 [a,b,c]	0.40 ± 0.06
FE Na^+ (%)	0.19 ± 0.03	0.12 ± 0.03	0.09 ± 0.02 [a]	0.13 ± 0.02	0.12 ± 0.01 [a]	0.06 ± 0.00 [a]
FE K^+ (%)	11.9 ± 1.8	8.4 ± 1.9	12.8 ± 2.9	10.1 ± 1.5	4.5 ± 0.9 [a,c]	5.4 ± 0.4 [a,c]

[a]$p < 0.05$ vs. LETO, [b]$p < 0.05$ vs. control, [c]$p < 0.05$ vs. SGLT2i.

Table 9. Comparisons between groups for metabolomics analysis. All fold-changes are calculated as mTIC normalized mean of Group B/ mean of Group A

Comparison	Group A	Group B
A	LETO Control	LETO CR
B	LETO Control	OLETF Control
C	LETO CR	OLETF CR
D	OLETF Control	OLETF CR
E	OLETF Control	OLETF SGLT2i
F	OLETF Control	OLETF SGLT2i + CR
G	OLETF CR	OLETF SGLT2i
H	OLETF CR	OLETF SGLT2i + CR
I	OLETF SGLT2i	OLETF SGLT2i + CR

Figures

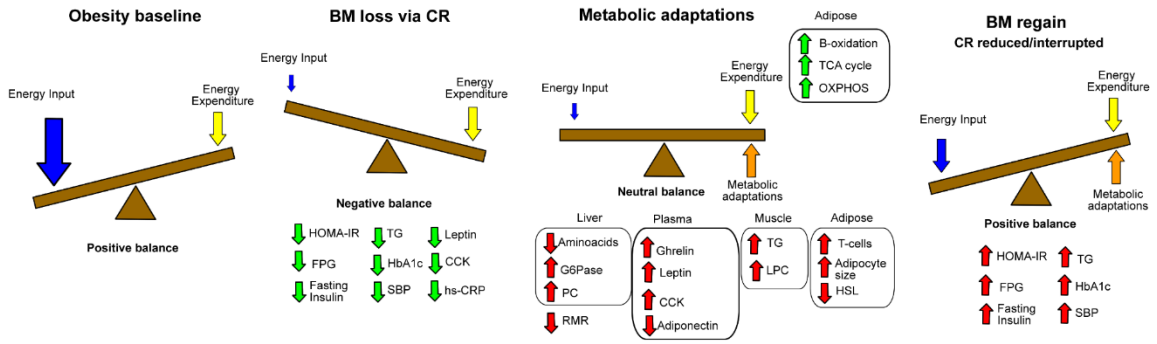

Figure 1. Progression of changes in energy balance from obesity baseline to body mass (BM) regain, and metabolic adaptations in response to caloric restriction (CR). Green arrows: Beneficial effects, red arrows: deleterious effects. CCK, cholecystokinin; FPG, fasting plasma glucose; G6Pase, Glucose 6-phosphatase; HbA1c, glycated hemoglobin; HOMA-IR, homeostatic model assessment of insulin resistance; hs-CRP, hormone sensitive C-reactive protein; HSL, hormone sensitive lipase; LPC, lysophosphatidic acid; OXPHOS, oxidative phosphorylation; RMR, resting metabolic rate; SBP, systolic blood pressure; TCA, tricarboxylic acid; TG, triglycerides

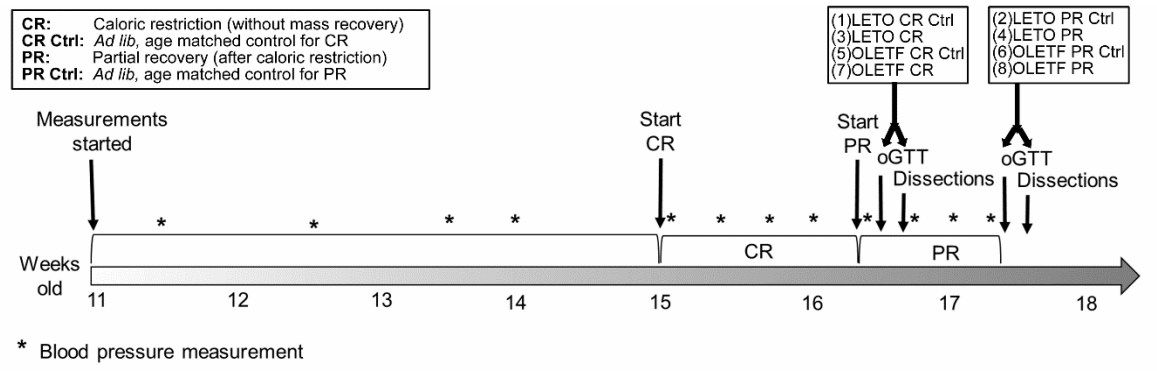

Figure 2. Study timeline. For both strains, first dissected groups were CR and CR control, and last dissected groups were PR and PR control.

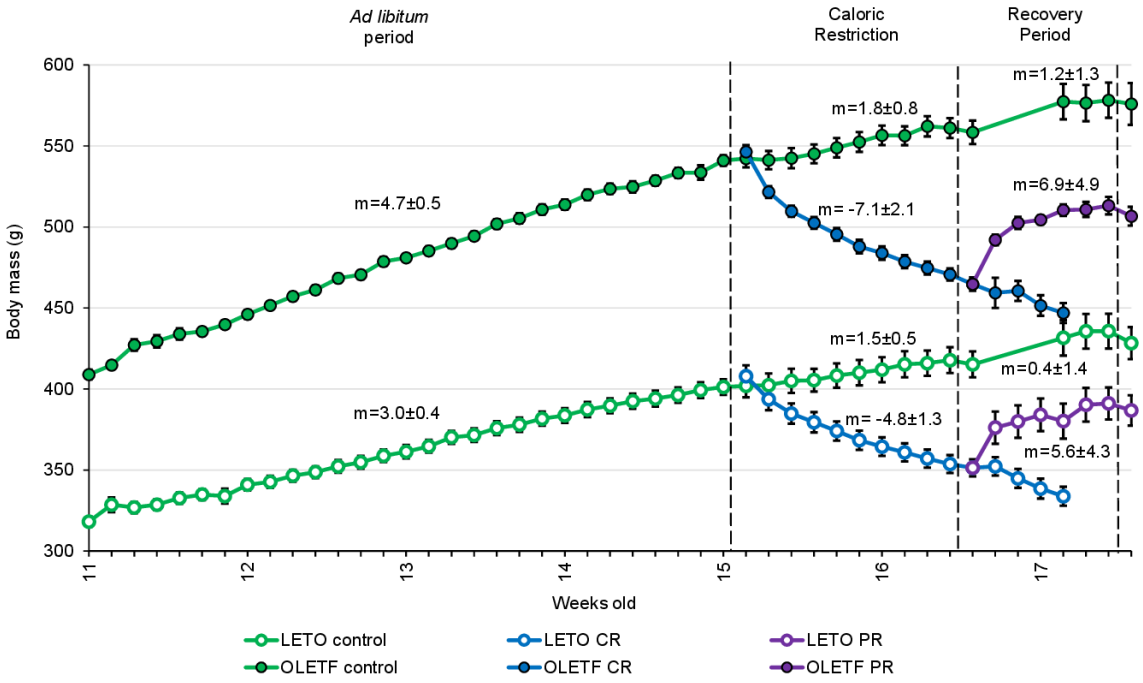

Figure 3. Mean ± SE animal body mass per week of age (n = 7, except for Controls before recovery period, where n = 14). m, mean slope of the line ± SE (body mass increase in g/day).

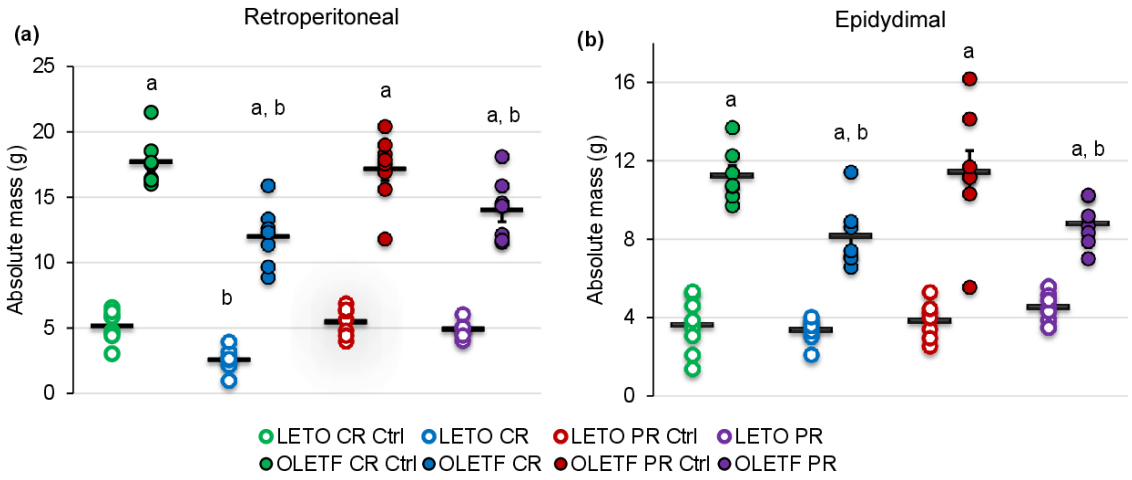

Figure 4. Mean ± SE absolute (g) (A) retroperitoneal and (B) epididymal adipose depots. aP < 0.05 vs. LETO. bP < 0.05 vs. Control.

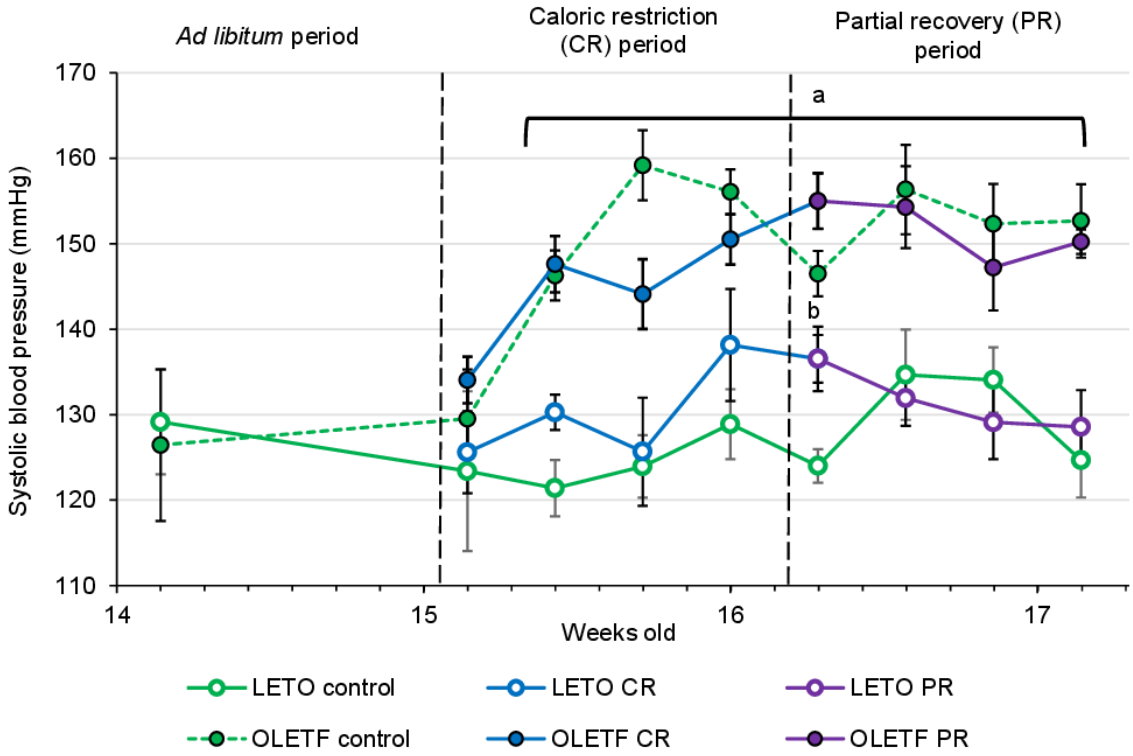

Figure 5. Mean ± SE values of systolic blood pressure (SBP) by weeks of age (n = 6). Solid lines represents CR and Recovery groups, whereas dashed lines represents Control groups. aP < 0.05 vs. LETO. bP < 0.05 vs. Control.

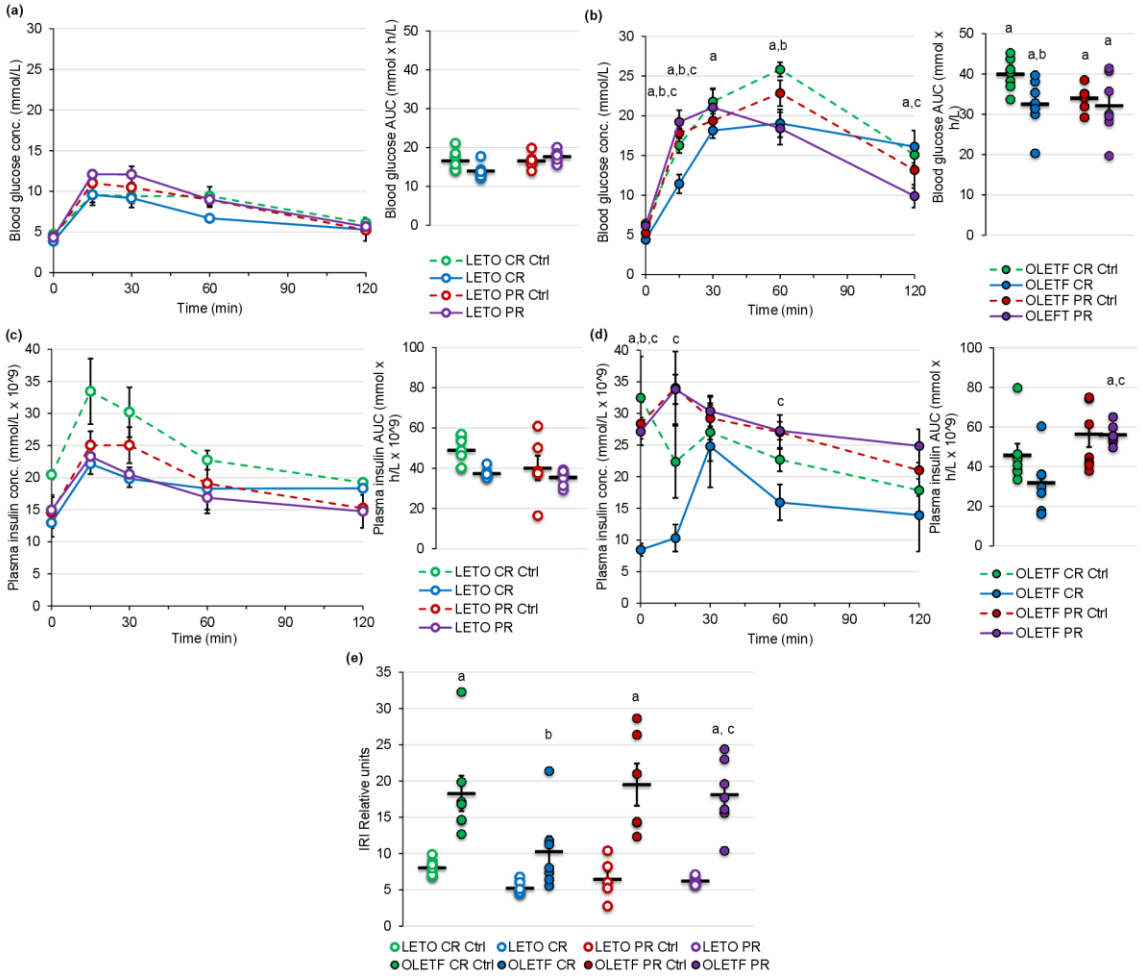

Figure 6. Mean ± SE blood glucose concentration (mmol/L) respect to time (min) and AUC (mmol × h/L) during oGTT for (A) LETO and (B) OLETF. Mean ± SE plasma insulin concentration (mmol/L × 10−9) with respect to time (min) and AUC calculations (mmol × h/L × 10−9) during oGTT for (C) LETO and (D) OLETF. Mean ± SE (E) insulin resistance index (IRI). aP < 0.05 vs. LETO. bP < 0.05 vs. Control. cP < 0.05 vs. CR.

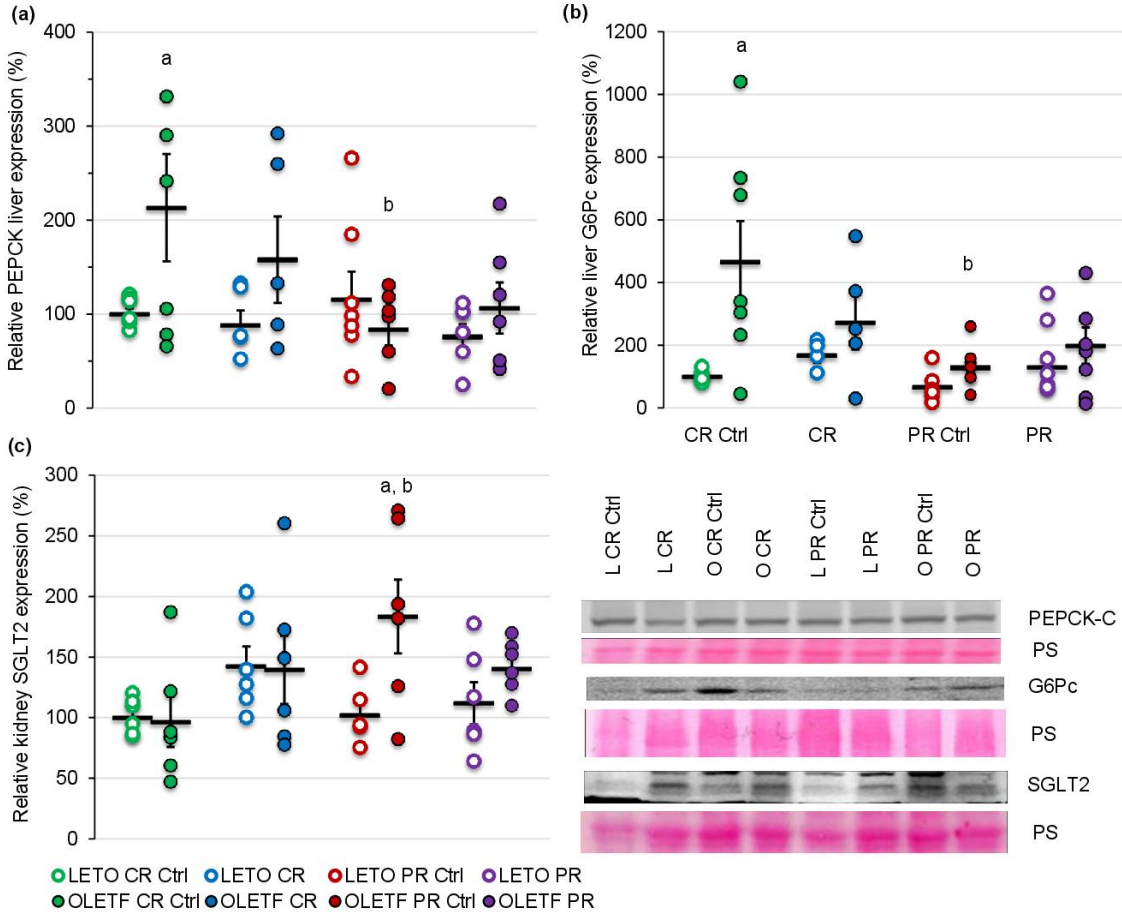

Figure 7. Mean ± SE relative expression of (A) liver PEPCK, (B) liver G6Pc, and (C) kidney SGLT2 expression. aP < 0.05 vs. LETO. bP < 0.05 vs. Control.

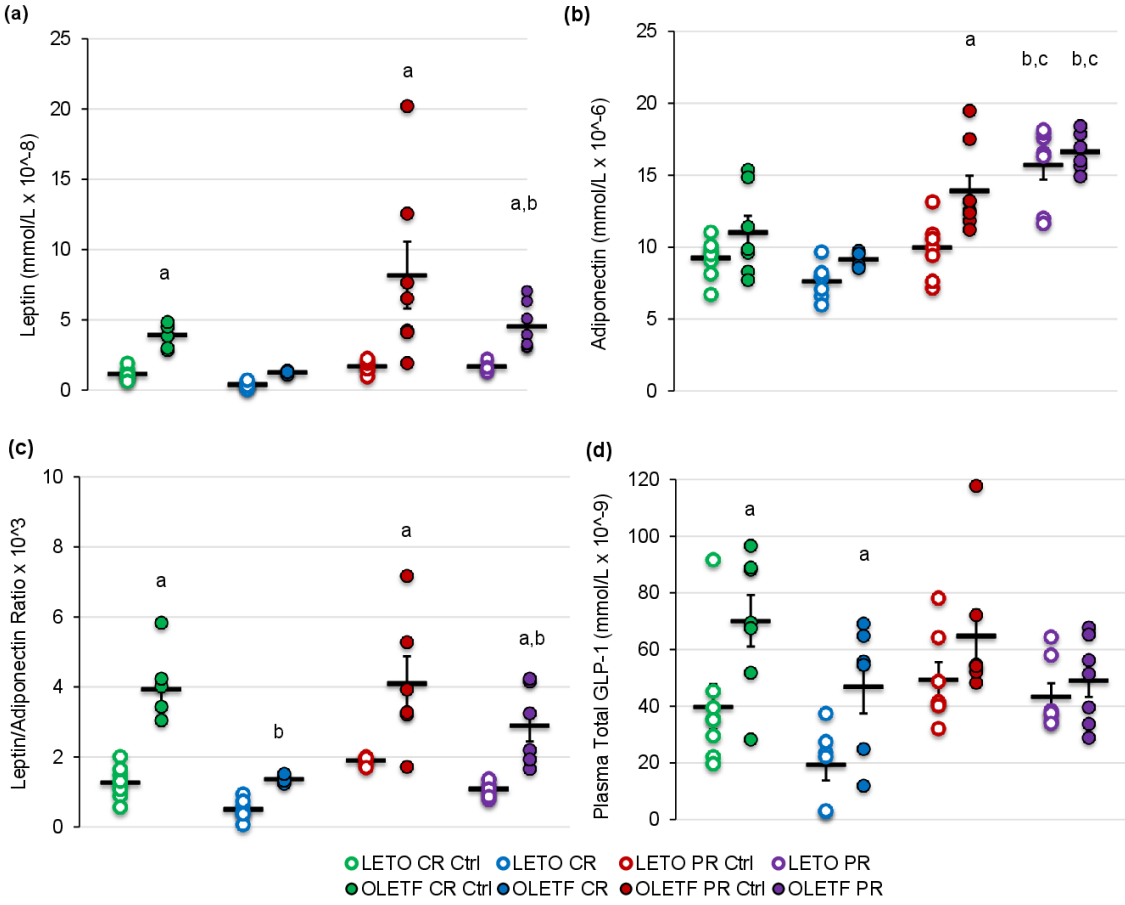

Figure 8. Mean ± SE (A) serum leptin (mmol/L × 10−8), (B) adiponectin (mmol/L × 10−6), (C) leptin/adiponectin ratio × 103, and (D) plasma total GLP-1 (mmol/L× 10−9). aP < 0.05 vs. LETO. bP < 0.05 vs. Control. cP < 0.05 vs. CR.

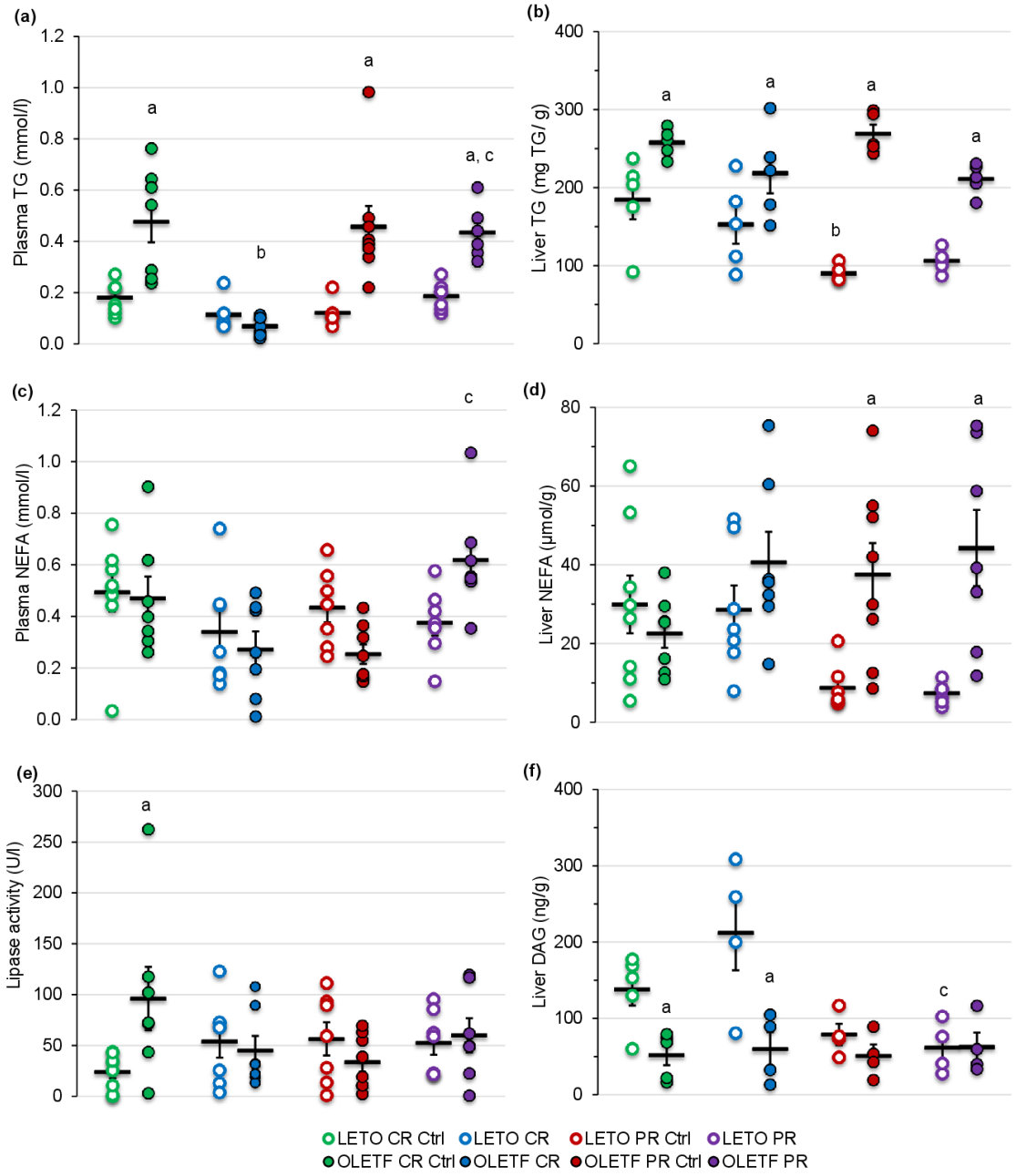

Figure 9. Mean ± SE (A) plasma TG (mmol/L), (B) liver TG (mg/g of tissue), (C) plasma NEFA (mmol/L), (D) liver NEFA (µmol/g of tissue), (E) plasma lipase activity (U/L), and (F) liver DAG (ng/g of tissue). aP < 0.05 vs. LETO. bP < 0.05 vs. Control. cP < 0.05 vs. CR.

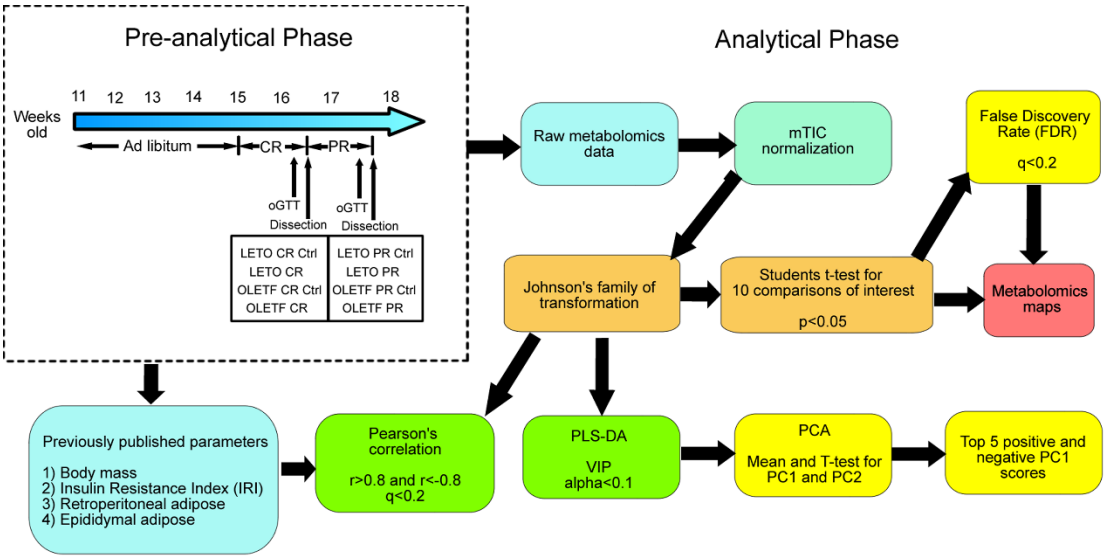

Figure 10. Project flowchart. CR: Caloric Restriction; LETO: Long-Evans Tokushima Otsuka; oGTT: oral Glucose Tolerance Test; OLETF: Otsuka Long-Evans Tokushima Fatty; PCA: Principal Component Analysis; PLS-DA: Partial Least Squares Discriminant Analysis; PR: Partial Recovery; VIP: Variable Importance in the Projection.

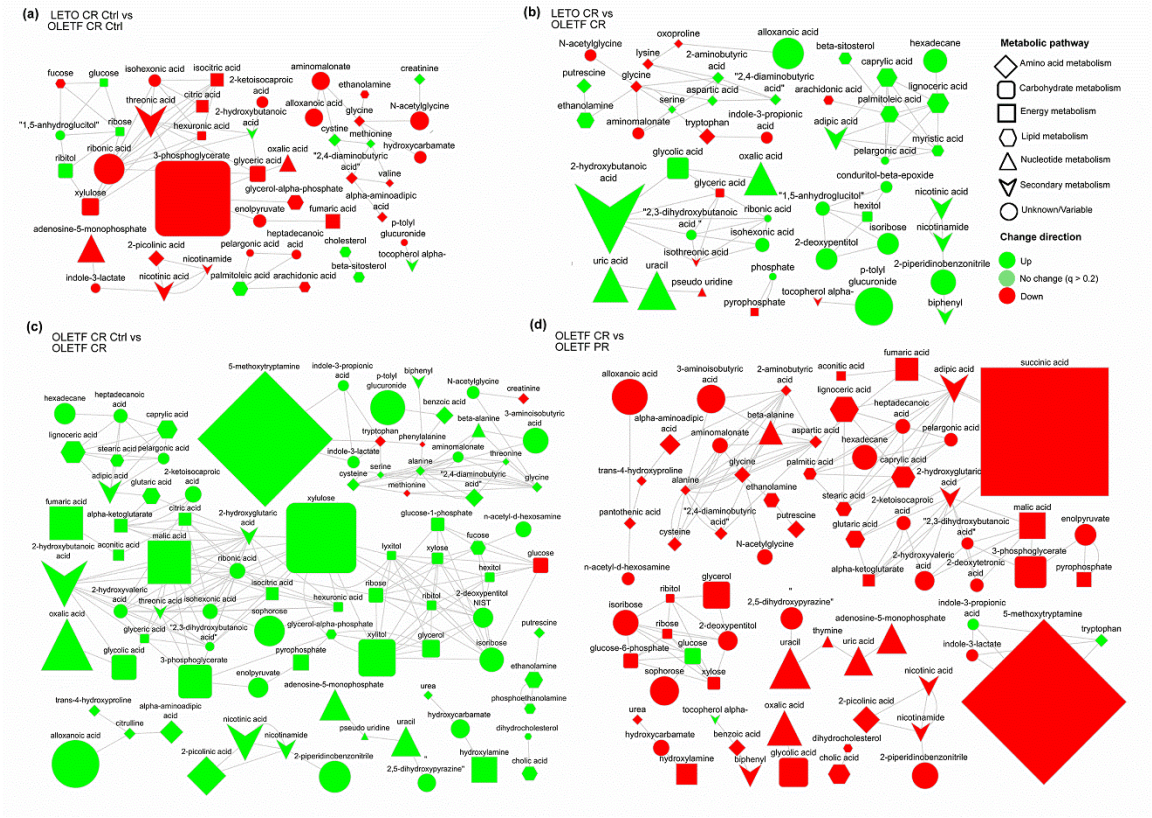

Figure 11. Metabolomics maps showing metabolites with p<0.05 after Student's t-test, representing mean plasma peak intensity fold-changes between groups in metabolites with q<0.2, for (a) LETO CR Ctrl vs OLETF CR Ctrl (Comparison A), (b) LETO CR vs OLETF CR (Comparison C), (c) OLETF CR Ctrl vs OLETF CR (Comparison G), (d) OLETF PR Ctrl vs OLETF PR (Comparison J).

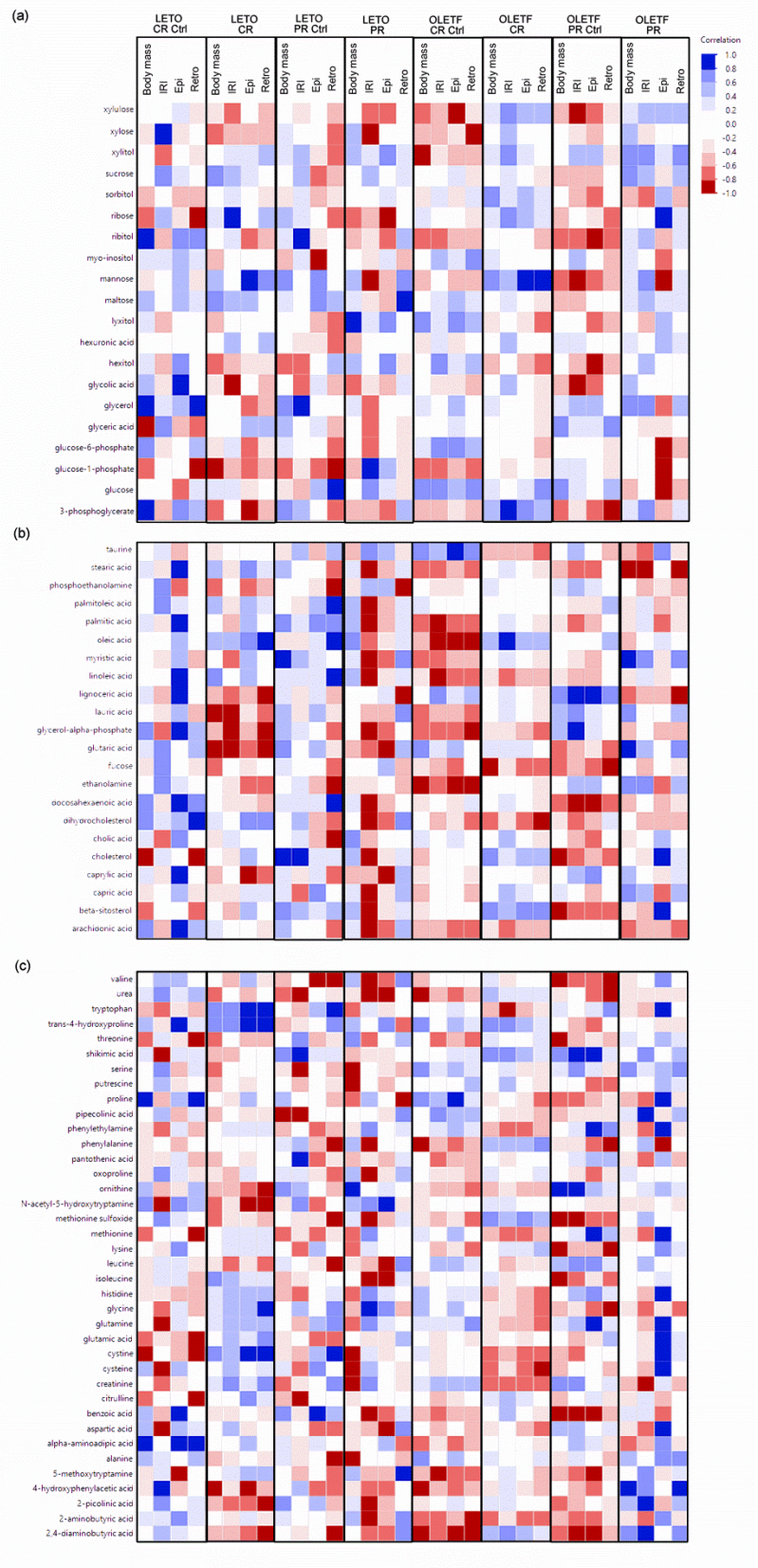
(a)
LETO CR Ctrl
LETO CR
LETO PR Ctrl
LETO PR
OLETF CR Ctrl
OLETF CR
OLETF PR Ctrl
OLETF PR
Body mass
IRI
Epi
Retro
Correlation
1.0
0.8
0.6
0.4
0.2
0.0
-0.2
-0.4
-0.6
-0.8
-1.0
xylulose
xylose
xylitol
sucrose
sorbitol
ribose
ribitol
myo-inositol
mannose
maltose
lyxitol
hexuronic acid
hexitol
glycolic acid
glycerol
glyceric acid
glucose-6-phosphate
glucose-1-phosphate
glucose
3-phosphoglycerate
(b)
taurine
stearic acid
phosphoethanolamine
palmitoleic acid
palmitic acid
oleic acid
myristic acid
linoleic acid
lignoceric acid
lauric acid
glycerol-alpha-phosphate
glutaric acid
fucose
ethanolamine
docosahexaenoic acid
dihydrocholesterol
cholic acid
cholesterol
caprylic acid
capric acid
beta-sitosterol
arachidonic acid
(c)
valine
urea
tryptophan
trans-4-hydroxyproline
threonine
shikimic acid
serine
putrescine
proline
pipecolinic acid
phenylethylamine
phenylalanine
pantothenic acid
oxoproline
ornithine
N-acetyl-5-hydroxytryptamine
methionine sulfoxide
methionine
lysine
leucine
isoleucine
histidine
glycine
glutamine
glutamic acid
cystine
cysteine
creatinine
citrulline
benzoic acid
aspartic acid
alpha-aminoadipic acid
alanine
5-methoxytryptamine
4-hydroxyphenylacetic acid
2-picolinic acid
2-aminobutyric acid
2,4-diaminobutyric acid

Figure 12. Pearson correlations (r) between Johnson transformed body mass (g), insulin resistance index (IRI) (relative units), retroperitoneal (retro) and epididymal (epi) adipose mass (g) vs Johnson transformed metabolites involved in (a) carbohydrate, (b) lipid and (c) amino acid metabolism.

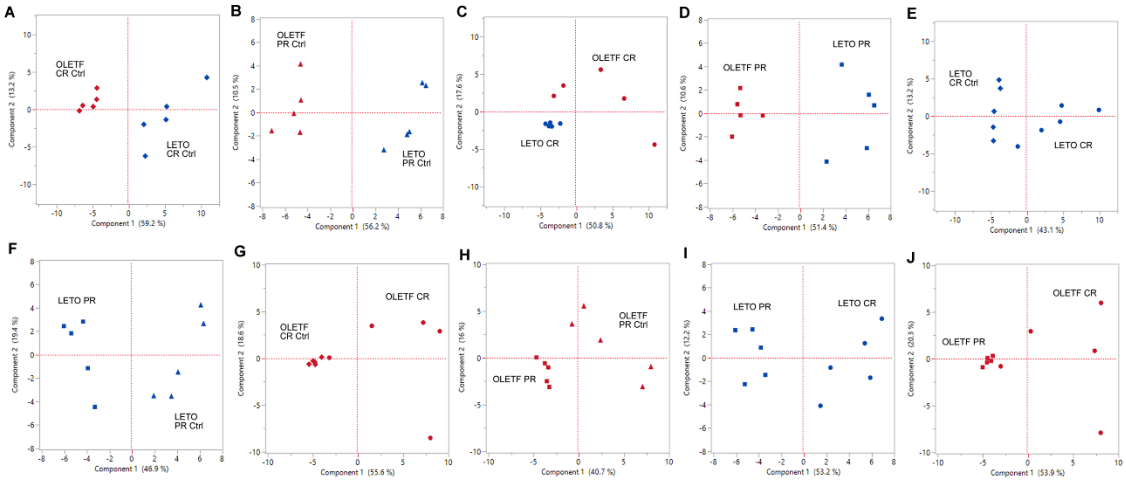

Figure 13. Principal component analysis (PCA) score plots of principal components 1 (x-axis) and 2 (y-axis) for (A) LETO CR Ctrl vs OLETF CR Ctrl, (B) LETO PR Ctrl vs OLETF PR Ctrl, (C) LETO CR vs OLETF CR, (D) LETO PR vs OLETF PR, (E) LETO CR Ctrl vs LETO CR, (F) LETO PR Ctrl vs LETO PR, (G) OLETF CR Ctrl vs OLETF CR, (H) OLETF PR Ctrl vs OLETF PR (I) LETO CR vs LETO PR, and (J) OLETF CR vs OLETF PR.

[Chapter 4 Figures]

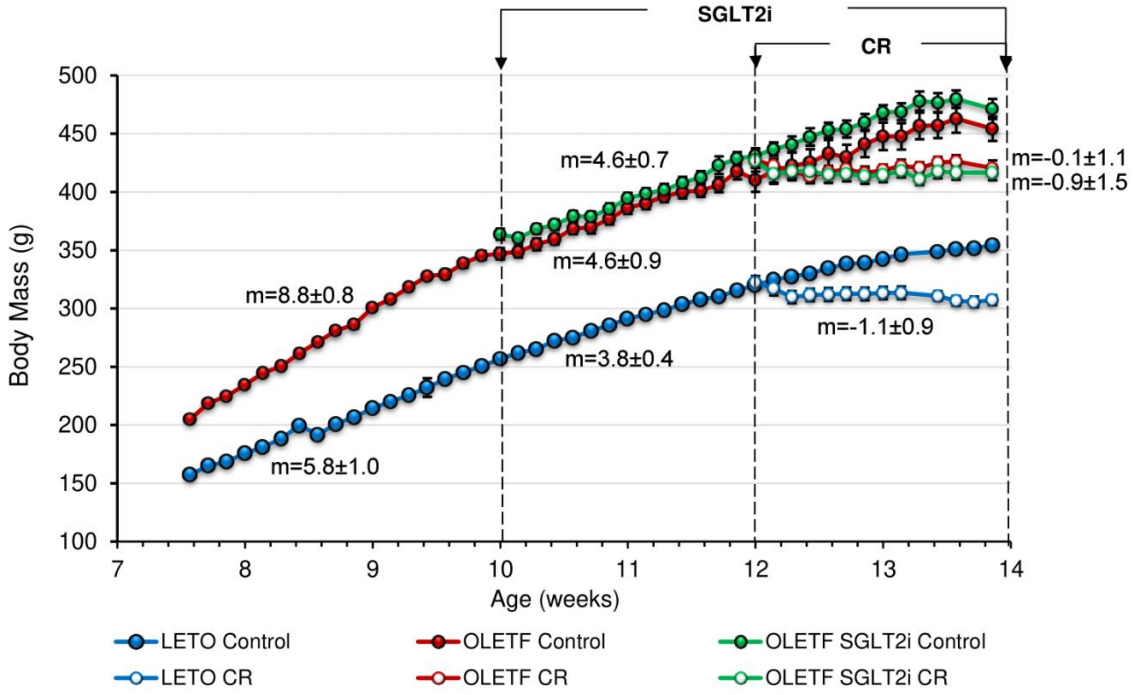

Figure 14. Mean ± SE incremental change in body mass per day (n=7). Data was not recorded during urine collection or after oGTTs and is denoted by gaps in data between one day to the next. m = mean slope of the line ± SE (g/d).

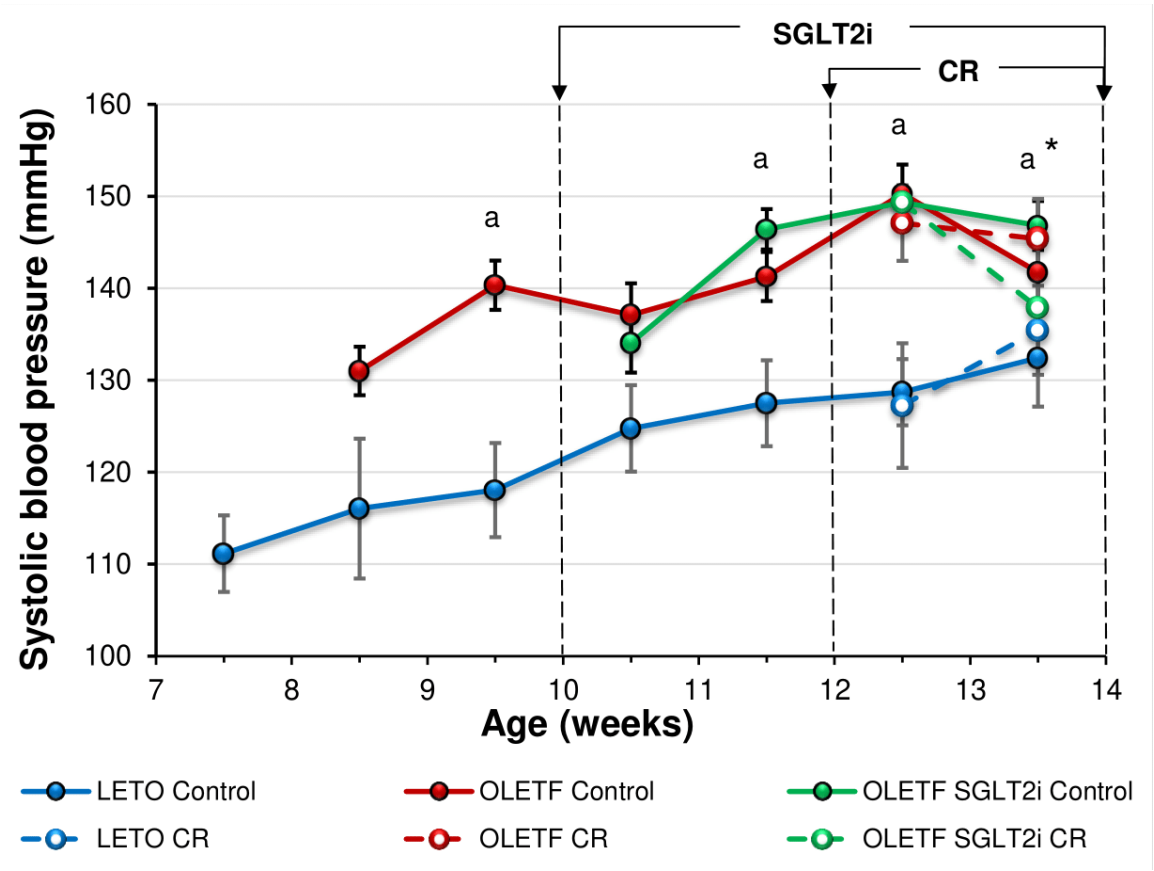

Figure 15. Mean ± SE systolic blood pressure (SBP) by weeks of age (n=6) ap < 0.05 vs LETO, *p < 0.05 vs OLETF SGLT2i CR (by t-test)

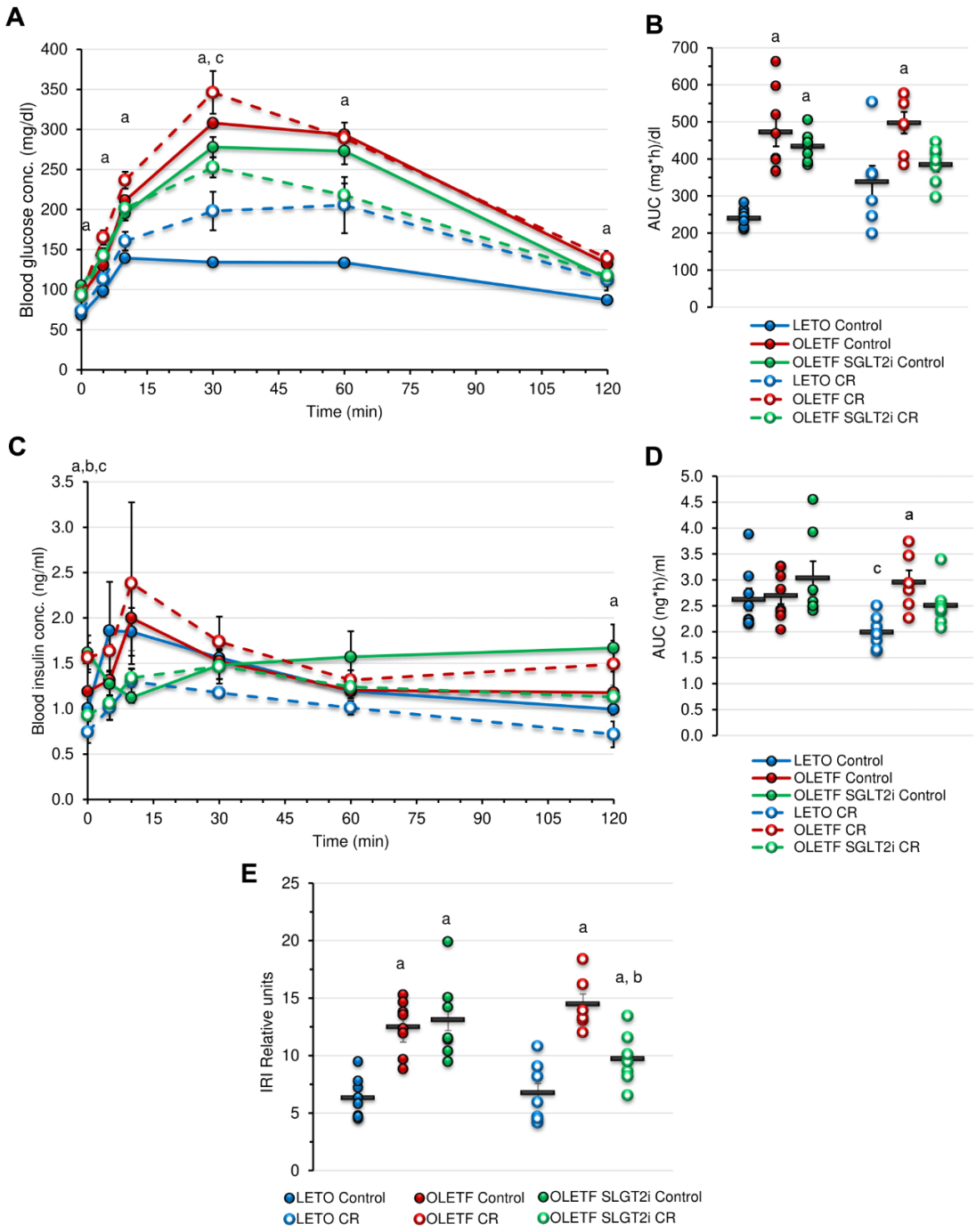

Figure 16. (A) Mean ± SE blood glucose concentration (mg/dL) over time (min) and (B) AUC glucose calculations (mg × h/dL) during oGTT. (C) Mean ± SE plasma insulin concentration (ng/mL) over time (min) and (D) AUCinsulin calculations (ng × h/mL) during oGTT. (E) Mean ± SE insulin resistance index (IRI) calculations.

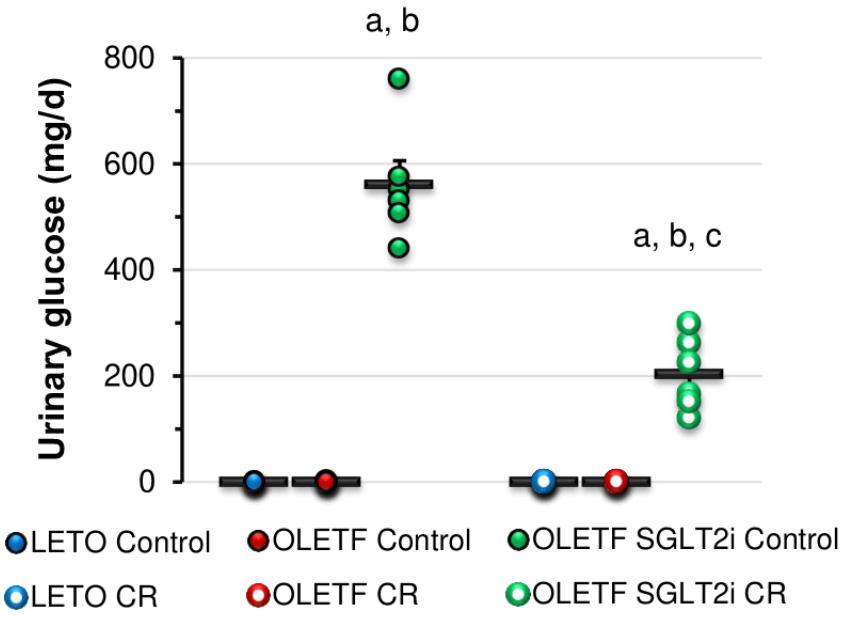

Figure 17. Mean ± SE 24 h urinary glucose excretion (mg/d). ap < 0.05 vs. LETO, bp< 0.05 vs. control, cp < 0.05 vs. SGLT2i

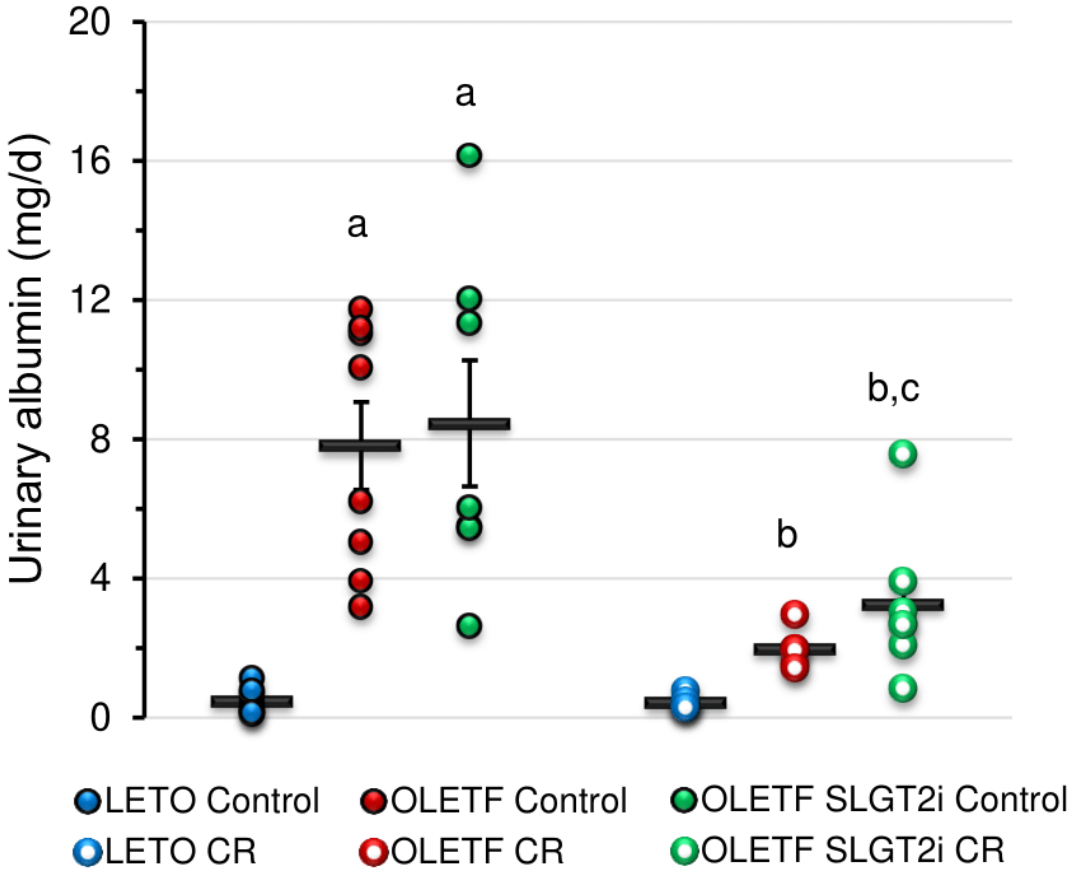

Figure 18. Mean ± SE urinary albumin excretion (mg/d). ap < 0.05 vs. LETO, bp < 0.05 vs. control, cp < 0.05 vs. SGLT2i

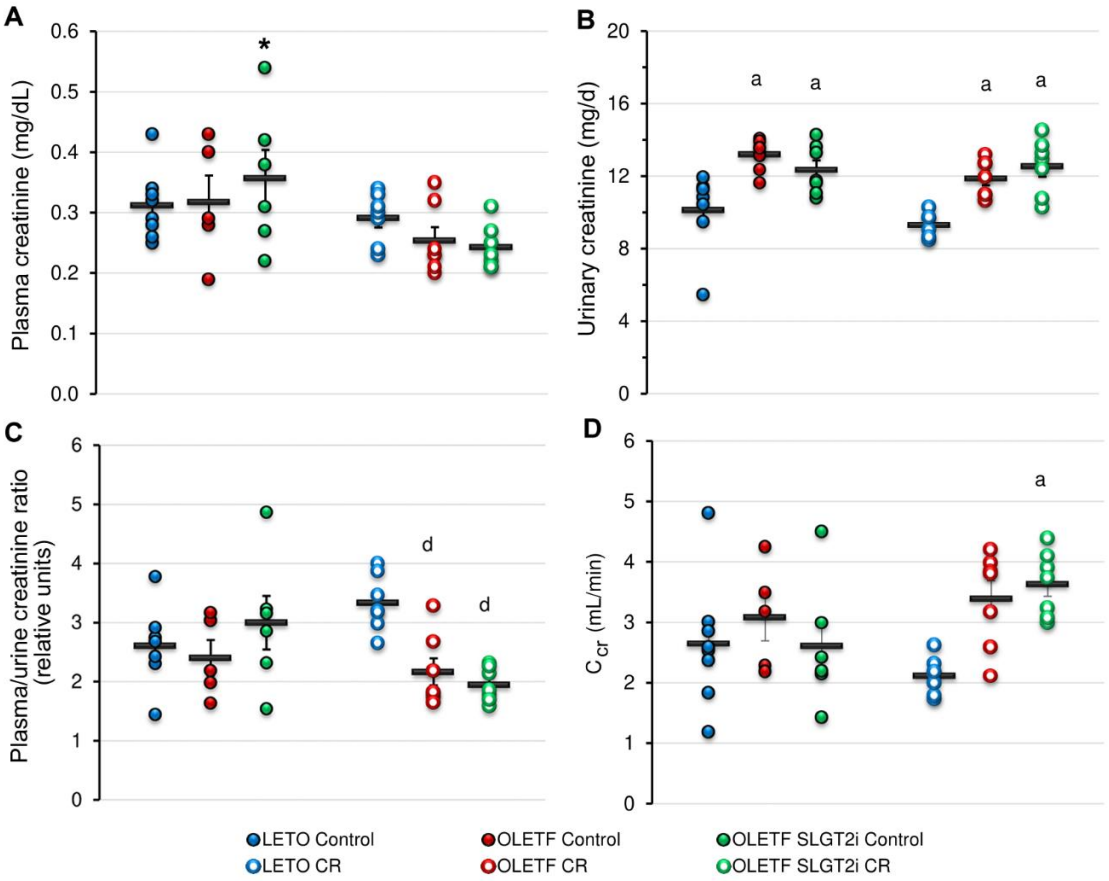

Figure 19. Mean ± SE **(A)** plasma creatinine (mg/dL), **(B)** urinary creatinine excretion (mg/d), **(C)** plasma/urine creatinine ratio (relative units), and **(D)** creatinine clearance (C_{cr}) (mL/min). $^{a}p < 0.05$ vs. LETO, $^{b}p < 0.05$ vs. control, $^{c}p < 0.05$ vs. SGLT2i, $^{d}p < 0.05$ vs. LETO CR. *$p < 0.05$ vs OLETF SGLT2i CR (by t-test)

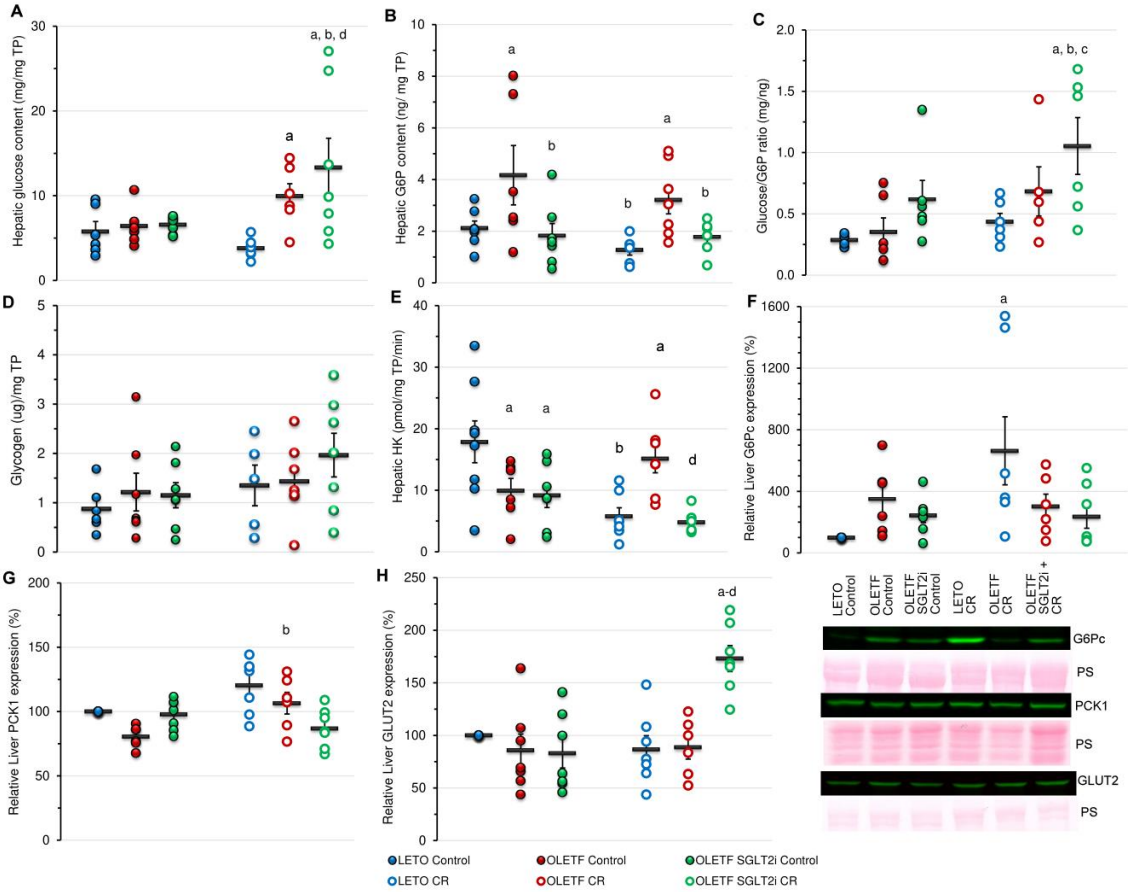

Figure 20. Mean ± SE **(A)** hepatic glucose content (mg glucose/mg TP), **(B)** glucose-6-phosphate (G6P) content (ng G6P/mg TP), **(C)** G6P:Glucose ratio (mg/ng), **(D)** glycogen content (µg glycogen/mg TP), **(E)** hexokinase activity (pmol/mg TP/min), and **(F)** relative cytosol PCK1, **(G)** cytosol G6Pc and **(H)** membrane GLUT2 expression. $^{a}P < 0.05$ vs. LETO. $^{b}P < 0.05$ vs. Control, $^{c}P < 0.05$ vs. SGLT2i, $^{d}P < 0.05$ vs. OLETF CR.

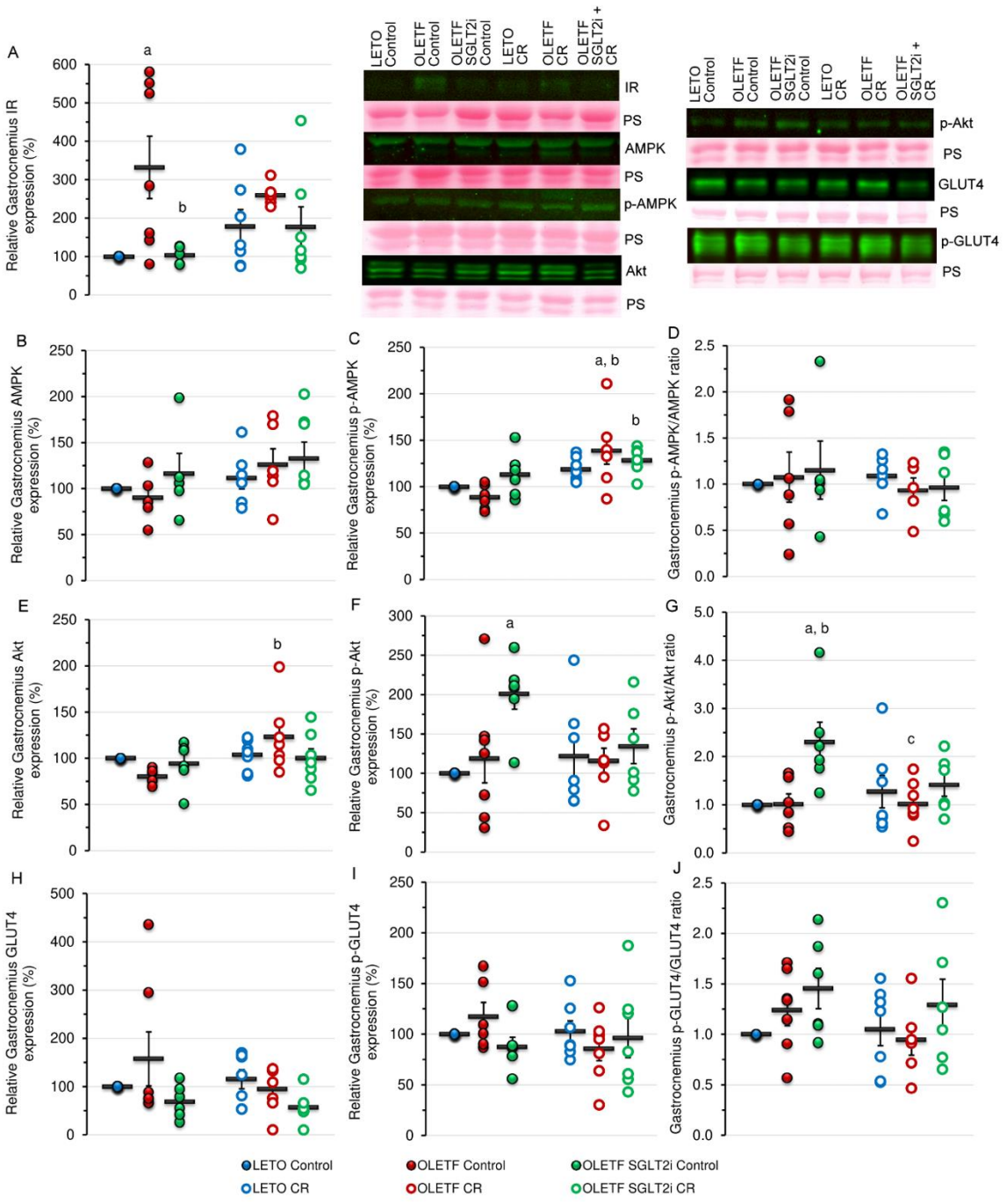

Figure 21. Mean ± SE relative expressions of **(A)** insulin receptor (IR), **(B)** AMPK, **(C)** p-AMPK, **(D)** p-AMPK/AMPK ratio, **(E)** Akt, **(F)** p-Akt, **(G)** p-Akt/Akt ratio, **(H)** GLUT4, **(I)** p-GLUT4, and **(J)** p-GLUT4/GLUT4 ratio in gastrocnemius muscle. $^{a}p < 0.05$ vs. LETO, $^{b}p < 0.05$ vs. control, $^{c}p < 0.05$ vs. SGLT2i, $^{d}p < 0.05$ vs. OLETF CR

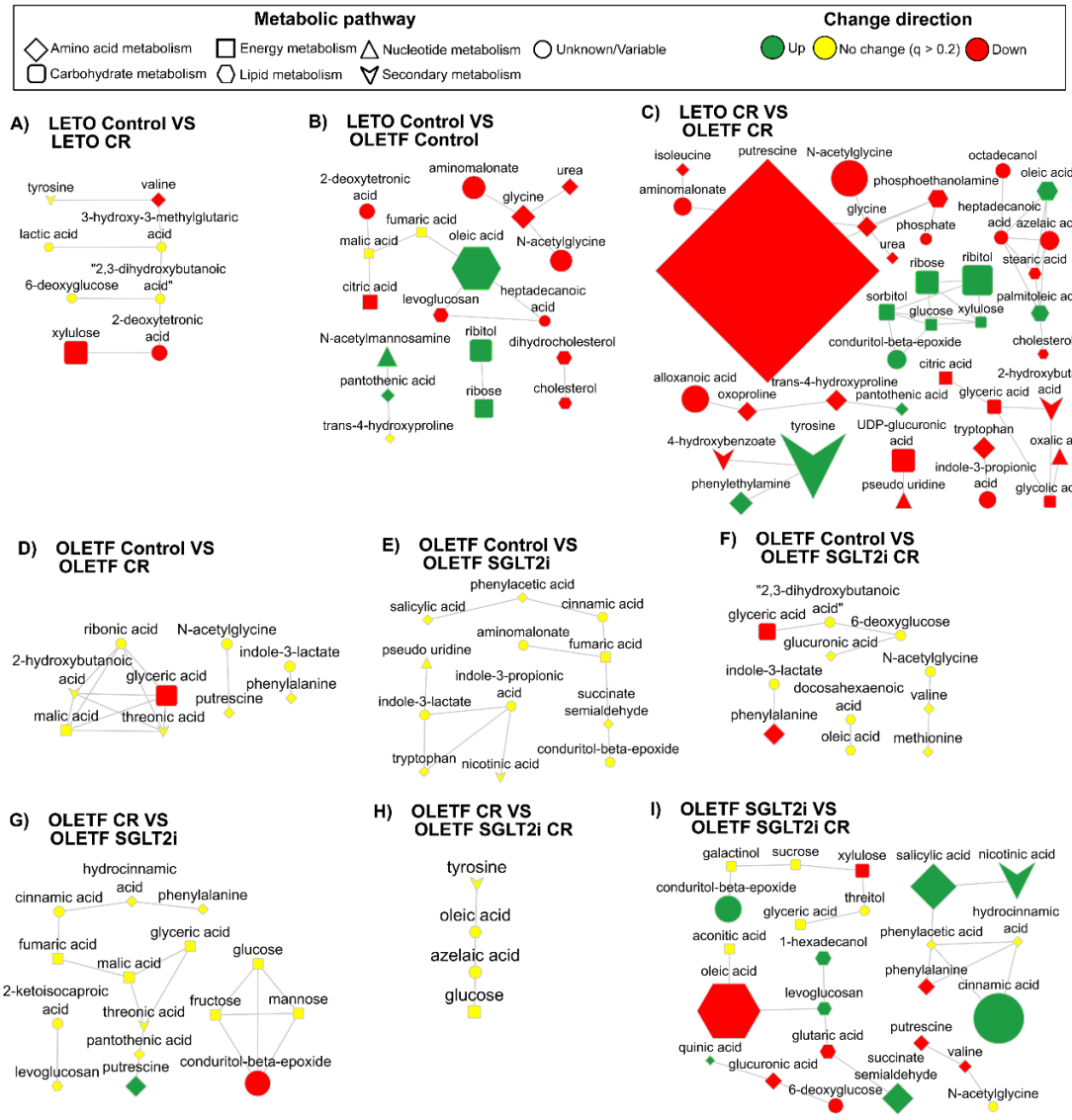

Figure 22. Metabolomic maps of 9 comparisons of interest, comparing fold-changes in mean plasma concentrations of detected metabolites. Only metabolites with $p < 0.05$ were mapped per comparison, and fold-changes are shown for metabolites with $q < 0.2$. Fold-changes are proportional to figure size.

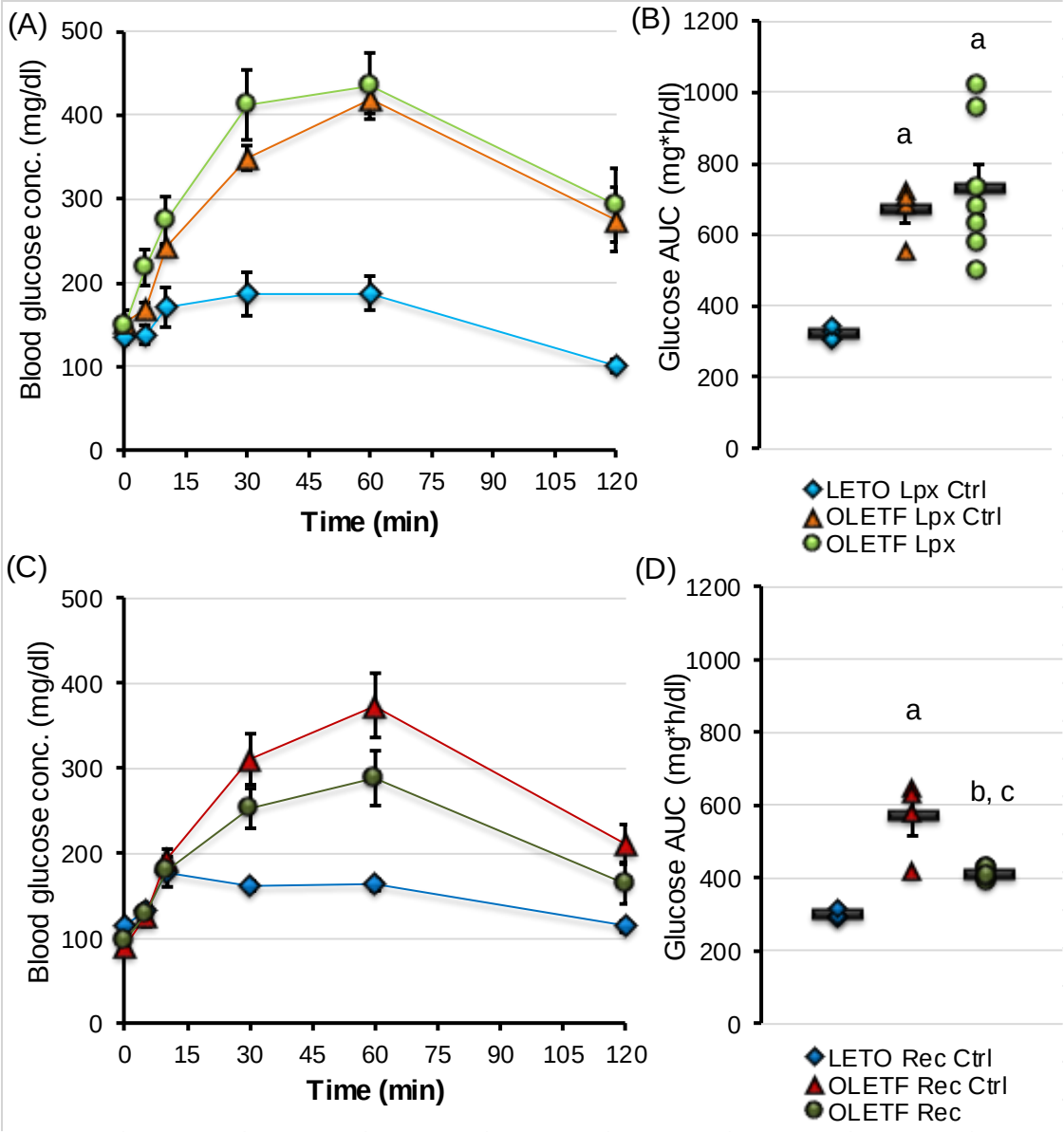

Figure 23. Mean ± SE of blood glucose concentration (mg/dl) VS time (min) after (A) lipectomy and (B) recovery. Mean ± SE glucose AUC (mg*h/dl) after (B) lipectomy and (D) recovery. aP<0.05 vs LETO, bP<0.05 vs Ctrl, cP<0.05 vs Lpx